Application of Holomorphic Embedding to the Power-Flow Problem

by

Muthu Kumar Subramanian

A Thesis Presented in Partial Fulfillment
of the Requirements for the Degree
Master of Science

Approved July 2014 by the
Graduate Supervisory Committee:

Daniel Tylavsky, Chair
John Undrill
Gerald Heydt

ARIZONA STATE UNIVERSITY

August 2014

ABSTRACT

With the power system being increasingly operated near its limits, there is an increasing need for a power-flow (PF) solution devoid of convergence issues. Traditional iterative methods are extremely initial-estimate dependent and not guaranteed to converge to the required solution. Holomorphic Embedding (HE) is a novel non-iterative procedure for solving the PF problem. While the theory behind a restricted version of the method is well rooted in complex analysis, holomorphic functions and algebraic curves, the practical implementation of the method requires going beyond the published details and involves numerical issues related to Taylor's series expansion, Padé approximants, convolution and solving linear matrix equations.

The HE power flow was developed by a non-electrical engineer with language that is foreign to most engineers. One purpose of this document to describe the approach using electric-power engineering parlance and provide an understanding rooted in electric power concepts. This understanding of the methodology is gained by applying the approach to a two-bus dc PF problem and then gradually from moving from this simple two-bus dc PF problem to the general ac PF case.

Software to implement the HE method was developed using MATLAB and numerical tests were carried out on small and medium sized systems to validate the approach. Implementation of different analytic continuation techniques is included and their relevance in applications such as evaluating the voltage solution and

estimating the bifurcation point (BP) is discussed. The ability of the HE method to

trace the PV curve of the system is identified.

ACKNOWLEDGEMENTS

First, I would like to express my sincere thanks to Dr. Tylavsky, my advisor for being a commendable source of knowledge and inspiration. From the beginning of my graduate career, he has inculcated a passion for the subject, guided me through several challenges in research and shaped my writing skills.

I express my sincere thanks to Yang Feng, doctoral student at ASU. Yang brought me up to speed on the work being done in the research group. The endless hours of discussion with him has molded my research. I consider it my privilege to have worked alongside such a wonderful person.

Dr. Antonio Trias, Gridquant Inc., deserves a special mention for the valuable inputs he gave to our research group. I would like to extend to my thanks to my graduate committee members Dr. Heydt and Dr. Undrill for their valuable feedback and suggestions to my thesis document. I am grateful to the all the faculty members of power engineering for the wonderful learning experience they provided for the last two years.

I would like to express my gratitude to the School of Electrical, Computer and Energy Engineering for providing me the opportunity to work as Teaching Assistant. Finally, my heart is with my family and friends who have kept me grounded during the entire period of my study.

TABLE OF CONTENTS

Page

LIST OF FIGURES

LIST OF TABLES

NOMENCLATURE

$|V_i|$ Voltage magnitude at bus i

a, b Scalars

$A_n(s)$ The nth order numerator term in three term recursive relation

B', B'' Approximations to Jacobian matrix in FDLF method

B_{ik} Line susceptance between bus i and bus k

$B_n(s)$ The nth order denominator term in three term recursive relation

BP   Bifurcation point

BPEE   Bus Power Equilibrium Equation

C Set of complex numbers

$c^{(i)}[n]$ n-th order term in the continued fraction

$c^l(s)$ Partial power series in the Viskovatov method

CPF   Continuation Power-flow

$f[n]$ Power series coefficient of degree n for function f

$f(s)$ Power series representation of function f using parameter s

FDLF   Fast Decoupled Power-flow

f_n Another notation for power series coefficient of degree n

G_{ik} Line conductance between bus i and bus k

GS   Gauss-Seidel

HE   Holomorphic Embedding

HV	High voltage
J_{ik}	Jacobian matrix entry in NR method
L	Degree of numerator polynomial in the Padé approximant
LHS	Left hand side
LV	Low voltage
M	Degree of denominator polynomial in the Padé approximant
m	Set of PQ buses
N	Number of buses in a power system
n	Used to indicate the degree of s in the power series
NR	Newton-Raphson
p	Set of PV buses
PBE	Power balance equation
PF	Power-flow
P_{Gi}	Real power generated at bus i
P_i	Real power injection at bus i
P_{Li}	Real power load at bus i
PV bus	Generator bus/ Voltage bus
PV curve	Power voltage curve
$Q(s)$	Reactive power represented as a power series in generator bus model I

Q_{Gi}	Reactive power generated at bus i
$Q_{Gi\,MAX}$	Maximum reactive power limit of generator at bus i
$Q_{Gi\,MIN}$	Minimum reactive power limit of generator at bus i
Q_i	Reactive power injection at bus i
Q_{Li}	Reactive power load at bus i
R	Transmission line resistance
RHS	Right hand side
Rhs_Known	Intermediate value in the calculation of the RHS vector in generator bus model I
s	Complex variable used in holomorphic embedding
S_i	Complex power injection at bus i
$slack$	Slack bus
V_i	Per unit voltage at bus i
$V_{i\,im}[n]$	Imaginary part of the voltage series coefficient of degree n
$V_{i\,re}[n]$	Real part of the voltage series coefficient of degree n
V_i^{sp}	Specified voltage at bus i
$V_i(0)$	Voltage function for bus i evaluated at $s=0$/ germ solution
$V_i(1)$	Voltage series for bus i evaluated at $s=1$.
$V_i(s)$	Voltage power series for bus i
$V_i[n]$	n-th order voltage series coefficients of bus i

VS	Voltage stability
V_{slack}	Slack bus voltage
$W_i(s)$	Inverse voltage series for bus i
$W_i[n]$	n-th order inverse voltage series coefficients of bus i
X	Transmission line reactance
Y	Bus admittance matrix
$Y_{i\,shunt}$	Shunt component of the bus admittance matrix at bus i
Y_{ik}	Admittance bus matrix entry between bus i and bus k
$Y_{ik\,trans}$	Series component of the bus admittance matrix between buses i and k
Z	Transmission line impedance
β_{ik}	Coefficient of iteration matrix corresponding to $V_{k\,re}[n]$ for generator bus i in generator bus model II
γ_{ik}	Coefficient of iteration matrix corresponding to $V_{k\,im}[n]$ for generator bus i in generator bus model II
$\epsilon_k^{\,j}$	Entry of kth column in the epsilon table. j measures the progression down the column
$\zeta_i[n\text{-}1]$	RHS element obtained from real power constraint in PV bus model II
θ_i	Voltage angle at bus i

$\kappa(A)$ Condition number of matrix A

λ Loading parameter

1 INTRODUCTION

1.1   POWER-FLOW PROBLEM

Power-flow (PF) studies are of primal importance in reliable operation of existing power system. Solving the PF problem constitutes an integral part of reliability studies such as contingency analysis, planning processes such as generation expansion planning and transmission expansion planning; also, the PF solution provides the initial point for dynamic simulation of power system components. The objective of the traditional PF problem is to find the static operating point of a balanced three-phase power system [1]. Given the network topology and its parameters, the complex power injections at load buses, the real power injection and voltage magnitude at generator buses, the primary results obtained from PF studies are bus voltage magnitudes and angles for load/PQ buses and bus voltage angles and reactive power for generator/PV buses. Secondary results such as flows across transmission lines, transformers, generator reactive power output, losses in the network can be calculated from the voltage solution.

Iterative methods such as Gauss-Seidel (GS), Newton-Raphson (NR), Fast Decoupled Load Flow (FDLF) and their many variants [2]-[6] are being used ubiquitously in the industry for solving the PF problem. While they appear to work well under normal loading conditions, as the loading increases, they can and do fail to converge [7], [8]. Furthermore, the trajectory that is taken by the iterative methods to approach the voltage solution is initial estimate dependent. For the power-flow problem,

which has multiple solutions, this means that these methods do not have a guarantee of convergence to the desired solution. All these problems have been addressed from time to time in the literature by proposing algorithmic enhancements to the existing methods [9]-[14]. However, a globally acceptable procedure to solve the convergence issues of iterative methods has yet to be developed.

1.2   VOLTAGE STABILITY PROBLEM

Voltage stability (VS) is defined as the ability of the power system to maintain steady-state voltages at all the buses after being subjected to a disturbance from a given initial operating condition [15]. The phenomenon of voltage instability (or voltage collapse) is responsible for major blackouts in the history of electric power industry; some of the major incidents reported worldwide are catalogued in [16], [17]. For a simple two-bus problem that has two solutions (high-voltage and low-voltage solutions) voltage collapse is said to occur when both the solutions coalesce. This idea can be easily extended to a general N-bus problem. Even an infinitesimal increase in loading beyond the voltage collapse point, also known as the bifurcation point (BP), results in no voltage solution to the PF problem. Traditional Newton-Raphson type methods fail to converge near the maximum loading point since the Jacobian matrix becomes ill-conditioned (approaches singularity), causing numerical errors in calculating the voltage solution. In the present voltage stability analysis practices, the PV curve obtained from some form of continuation power-flow (CPF) [18], [19] is a byproduct of

2

the process used to determine the saddle node bifurcation point of the system. Depending on the proportion by which load is incremented at different buses, different bifurcation points can be obtained. Knowledge of the loadability limit of the system before voltage collapse occurs is essential for system operators. This information becomes even more critical with the growing demand in electric power industry and the power system components being increasingly operated near their limits.

1.3   HOLOMORPHICALLY EMBEDDED PF FORMULATION

Holomorphic Embedding (HE) is a novel non-iterative way of solving the PF problem [20]. Unlike its counterpart iterative methods, the one implementation of HE, known as the Holomorphic Embedding Load-Flow Method (HELM), is guaranteed to find the operational high-voltage (HV) solution when it exists and unequivocally signal when such a solution does not exist [20]. The solution methodology involves embedding the originally non-holomorphic (or non-analytic) power-balance equations (PBE's) into a larger problem such that the resultant problem is holomorphic (analytic). While NR type methods can be viewed as a first order Taylor series approximation as a function of voltage, the HE method exploits the property of embedding, problem formulation and holomorphicity to express the voltage function as a Taylor series that is a function of (in essence) injected real and reactive power. The power series coefficients of the aforementioned series are calculated by establishing a recurrence relation from the embedded PBE's. Calculation of Jacobian matrix entries is not

involved in this solution procedure. Solving the PF problem using HE for a system of PQ buses (and one slack bus) is discussed in [21].

1.4 OBJECTIVE

The objective of this work is to apply the novel HE method to solve the general ac PF problem. This report covers the following topic areas.

1. Introduce the concept of analytic continuation and elucidate its relevance to the HE procedure.

2. Explore several techniques of analytic continuation and their numerical implementation.

3. Introduce the existing load-bus model and analyze the development of the two different generator bus models in detail.

4. Develop a solution procedure for solving the general case PF problem.

5. Compare the solution procedure of the HE method with NR method.

6. Develop a HE that can be used in estimating the saddle-node bifurcation point of the system with PQ buses.

1.5 ORGANIZATION

The report is organized into five additional chapters. The content of each chapter is discussed in brief below.

Chapter 2 is a review of the existing literature of PF methods and present practices in evaluating the BP of the system.

The concept of analytic continuation and its relevance to the solution methodology is presented in Chapter 3. Three different techniques of calculating analytic

continuation are explored with numerical examples, their merits and demerits in the context of solving the PF problem are explained.

In Chapter 4, the existing literature about the load bus model is introduced. The development of two different generator bus models using HE method and its incorporation in solving the general PF problem is discussed in detail. Test results from the IEEE 118 bus system are presented; the solution is validated against the results from commercial PF software.

Estimating the BP of a system with PQ buses using the HE procedure is discussed in Chapter 5. The estimate is compared against the actual value of BP obtained from existing CPF method.

Chapter 6 presents a summary of the reported work and scope for the future work.

2 LITERATURE REVIEW

The literature review will focus on the following: First, the developments in solving the PF problem are described. Next, the initial-estimate-dependency of iterative methods is illustrated. Finally, the literature on evaluating the BP of the system is discussed.

2.1 SOLUTION METHODOLOGIES TO THE POWER-FLOW PROBLEM

The power-flow problem involves solving the nonlinear system of PBE's. The numerical techniques employed to solve the PF problem have evolved over the years. Nevertheless, the quest for a single "best" method that caters to problems of all sizes and types with minimal computing requirements and desired convergence properties is still a work in progress.

The real and reactive power injections at every bus i, for an N-bus system can be related to the bus voltages, the system topology and the network parameters as follows:

$$P_i = |V_i| \sum_{k=0}^{N} |V_k| [G_{ik} \cos(\theta_i - \theta_k) + B_{ik} \sin(\theta_i - \theta_k)]$$

$$Q_i = |V_i| \sum_{k=0}^{N} |V_k| [G_{ik} \sin(\theta_i - \theta_k) + B_{ik} \cos(\theta_i - \theta_k)]$$

(2.1)

Equation (2.1) is referred to as the hybrid formulation where the bus admittance matrix (Y bus) entries are written in rectangular form and bus voltages are expressed in polar form. Equation (2.1) also constitutes the defining equations for a load bus, i, for a N-bus system whose complex power injections are known and complex voltages are unknown.

6

For a generator bus, the real power injection into the bus is known. The bus voltage magnitude is maintained to be constant by varying the quantity of VARS injected into the network. The defining equations for a generator bus, i, are:

$$P_i = |V_i| \sum_{k=0}^{N} |V_k| [G_{ik} \cos(\theta_i - \theta_k) + B_{ik} \sin(\theta_i - \theta_k)]$$

(2.2)

$$|V_i| = |V_i^{sp}|$$

A slack bus is necessary to compensate for the losses in the system. The voltage magnitude and angle are fixed for the slack bus. The real and reactive power injections are taken as free variables. Hence, for a slack bus,

$$|V_i| = |V_i^{sp}|$$

(2.3)

$$\theta_i = \theta_i^{sp}$$

Mathematically, for an N-bus system with one slack bus, there are up to 2^{N-1} voltage solutions. Of the possible solutions, only one solution corresponds to the operable solution also referred to as the HV solution. Iterative methods such as NR and FDLF with a "reasonable" estimate generally converge to the required HV solution. However, several factors such as poor initial estimate, high R/X ratio (typical of distribution systems) and operation near the maximum loading point can lead to ill-conditioned matrices [7] resulting in convergence issues.

2.1.1   GAUSS-SEIDEL METHOD

In the history of solving the ac PF problem, GS method was the first method to be implemented in digital computers. The nonlinear PBE for a load bus in (2.1) can be alternatively expressed as a "weakly linear" [22] system of equations as:

$$I_i = \sum_{k=1}^{N} Y_{ik} V_k = \frac{S_i^*}{V_i^*} \tag{2.4}$$

Equation (2.4) is still nonlinear because the bus voltages in the denominator and hence current injection into the bus are unknown. From (2.4), an iteration scheme is established to calculate the bus voltages [1].

$$V_i(n+1) = \frac{1}{Y_{ii}} \left[\frac{P_i - jQ_i}{V_i^*(n)} - \sum_{k=1}^{i-1} Y_{ik} V_k(n+1) - \sum_{k=i+1}^{N} Y_{ik} V_k(n) \right] \tag{2.5}$$

The coefficient n in equation (2.5) is the iteration index. The Gauss-Seidel method is a fixed point form with the bus voltages as variables. Starting with an initial estimate of bus voltages, using the complex power specified at each bus and the network parameters, a new vector of bus-voltage estimates $V_i(n+1)$ is obtained. The estimate of bus voltage for bus i, at iteration $n+1$, ($V_i(n+1)$) is expressed as a function of the most recently updated value of voltages up to bus i-1. For generator buses, the reactive power injection is unknown; it can be calculated from the updated value of bus voltages. The iteration process described in (2.5) is repeated until the difference between two successive voltage estimates is less than a pre-determined tolerance value. The GS method is easier to program; there is no need of factorizing a sparse matrix. The

8

memory requirements for the GS method are minimal; for an N-bus system, it is directly proportional to the system size N [23]. The Gauss-Seidel method has linear convergence characteristics [1].

In equation (2.5), only the buses connected to bus i are required to calculate the updated value of $V_i(n+1)$. The calculation of such bus voltages can be carried out independent of the remaining network. A larger problem can thus be split into a sequence of smaller problems based on the bus adjacency matrix and processed in parallel. Reference [24] presents a theoretical upper bound of speed up for different implementations of parallelized GS method. The computation time for the traditional GS method increases proportional to N^2[22].

2.1.2   NEWTON-RAPHSON METHOD

The NR method for solving nonlinear power-balance equations (PBE's) is a recursive method that solves a linear system of equations at each iteration; the linear equations are derived from a first order Taylor's series approximation of the function at the best estimate of the solution point. Since the PBE's are non-analytic, they cannot be differentiated in the complex form. Hence, the variables are broken down into real variables in either polar form or rectangular form. The first order partial derivatives of the PBE with respect to the bus voltage magnitude and angle (assuming polar form of the variables is used) constitute the entries of the Jacobian matrix. The Jacobian matrix evaluated at a particular point is representative of the slope of tangent vector to the PBE

at that point. Using this process, a linear system of equations that relates the Jacobian matrix and mismatches in the PBE's is obtained. A simplified version of the above mentioned linear relation is:

$$\begin{bmatrix} \Delta P \\ \Delta Q \end{bmatrix} = \begin{bmatrix} J_{11} & J_{12} \\ J_{21} & J_{22} \end{bmatrix} \begin{bmatrix} \Delta \theta \\ \Delta |V| \end{bmatrix} \tag{2.6}$$

where J_{11}, J_{12}, J_{21} and J_{22} are the entries of the Jacobian matrix defined in [1]. The entries ΔP, ΔQ are the mismatch in the PBE's and $\Delta \theta$, ΔV denote the update in bus voltage angle and magnitude respectively. In solving a N-bus system using the NR method, the equation corresponding to the slack bus in (2.6) can be eliminated. For a PV bus, the ΔQ equation is absent in (2.6). After, correcting for the slack buses and PV buses, the solution to the linear system of equations (2.6) for all buses, yields an update vector for system states ($\Delta \theta$, ΔV); the updates are added to the current estimate of voltage angle and magnitude (θ, V). The process is repeated iteratively until the maximum mismatch in the PBE's is less than a pre-determined value of tolerance. The NR method has quadratic convergence properties. Stott [22] claims that the full NR method converges in 2-5 iterations from a flat start initial estimate to the required solution irrespective of the problem size. A practical PF with discrete elements in the network such as on-load tap changing transformers (OLTC), phase shifters and FACTS devices is much more complicated and requires a few more iterations to converge.

2.1.3 ALGORITHMIC IMPROVEMENTS TO NEWTON'S METHOD

Since the advent of NR method in solving the PF problem, several enhancements have been proposed to improve its performance. A very trivial modification used to obtain faster convergence is to use a previously calculated voltage solution as the initial estimate instead of a flat start. Dishonest Newton methods use the same Jacobian matrix for the successive iterations [3], thereby saving the costs of computing the Jacobian and triangular matrix factorization for every iteration. Limits are sometimes imposed on the maximum permissible change in the estimates to deal with the non-smoothness in the function [25]. For a practical power system problem, the Jacobian matrix is extremely sparse with very few non-zero elements in every row. Hence, sparse matrix storage techniques and optimal ordering schemes to minimize the number of fill-ins that occur during the triangular matrix factorization are employed to reduce the computation time and storage requirements in NR method.

2.1.4 FAST DECOUPLED LOAD FLOW (FDLF) METHOD

Based on the typical characteristics of PF problems and through the experience gained via numerical experimentation, a series of approximations were made to the traditional NR method to produce what has become an industry standard known as the Fast Decoupled Load Flow. For PF problems, under nominal operating conditions, there is weak coupling between active power and voltage magnitudes; similarly, there is weak coupling between reactive power and voltage angle. Hence, in the FDLF

11

formulation the corresponding entries in the Jacobian matrix are neglected, leading to two decoupled system of equations that are solved independently [6]. Other assumptions used in deriving the FDLF Jacobian matrix are very small R/X ratio branches (typical of transmission systems) and small differences in voltage angle between adjacent buses. The Jacobian is thus reduced to constant matrix independent of the estimate of the system states, thereby saving the costs of updating and re-factorizing the matrix. The speed per iteration is approximately five times that of the full NR method [5]. The system of equations to be solved is reduced from (2.6) to:

$$\Delta P/V = B'\Delta\theta$$
$$\Delta Q/V = B''\Delta V$$
(2.7)

where B', B'' denote the constant approximations to the Jacobian matrix defined in [5]. One variation of the FDLF method is the X/B method. The elements of the B', B'' matrices are calculated in the X/B method [27] as:

$$B'_{ik} = \frac{-1}{X_{ik}}, \qquad B'_{ii} = \sum_{\substack{k=1 \\ k \neq i}}^{N} - B'_{ik}$$

$$B''_{ik} = \frac{-X_{ik}}{R_{ik}^2 + X_{ik}^2} \qquad B''_{ii} = \sum_{\substack{k=1 \\ k \neq i}}^{N} - B''_{ik}$$
(2.8)

The number of iterations required to converge using the FDLF increased over that needed with the NR method, but the computation time required per iteration drastically decreased [5]. Overall, the time taken to solve the PF problem decreased; as a result, the use of FDLF method has become more prevalent in the industry.

Reference [26] compares FDLF method with NR and GS methods based on memory requirements, CPU time, convergence properties, number of iterations and effects of low precision arithmetic on reliability of solution for medium and large sized systems. The FDLF method was found to be the fastest among the three methods on all the tested scenarios [26]. The convergence rate of FDLF method (assuming it converges) is between the NR (quadratic convergence) and GS (linear convergence) methods. One disadvantage of the FDLF method is it inherits the initial estimate dependency and convergence problems, especially near the BP, from its NR roots.

2.1.5 SERIES LOAD FLOW

A non-iterative approach to solve the PF problem has been proposed in [28] and tested on an eleven-bus system. Using a series reversion technique, the voltage variable is represented as an explicit series. The work is further extended in [30] by using a Taylor's series expansion in the neighbourhood of a feasible operating point. Sensitivity of voltages to the bus power injections could be directly determined using this technique. However, the existing series power-flow methods use an analytical representation of the iteration process rather than the original PBE's and it is impractical to obtain for large systems. In addition, they are initial estimate dependent in the sense that the initial operating point has to be obtained using an iterative approach.

2.2   NEED FOR A NON-ITERATIVE APPROACH

The PBE's constitute a nonlinear coupled system of equations with multiple solutions. When solving a nonlinear problem using an iterative approach, the convergence issues that arise are manifold. First off, there is no guarantee that the non-iterative approach will converge to a solution. If a PF case does not converge, there is no way to know if a solution does not exist or if the iterative method is to blame for the non-convergence. Also, there is little control over the solution to which the iterative method converges.

For a simple two-bus ac PF problem, there exist two solutions for a specified value of power injection: the HV solution and the LV solution. Typically, the HV solution is desired for practical purposes such as grid operation. However, the LV solution also finds some applications viz., in determining the unstable equilibrium points [39]. Depending on the initial estimate, NR method may converge to the HV solution or the LV solution or may not converge at all. These problems are inherent in all iterative methods applied to nonlinear problems and occur irrespective of the problem size. The initial estimate dependency of iterative methods can be illustrated with a simple two-bus example shown in Figure 2.1. The system has one slack bus and one load bus connected by a purely inductive transmission line. The system parameters are shown in per unit quantities in Figure 2.1.

$V_1 = 1 \angle 0°$

$|V_2| \angle \theta_2$

$R=0$
$X=j0.2$ p.u.

$P_2=1$ p.u.
$Q_2=1$ p.u.
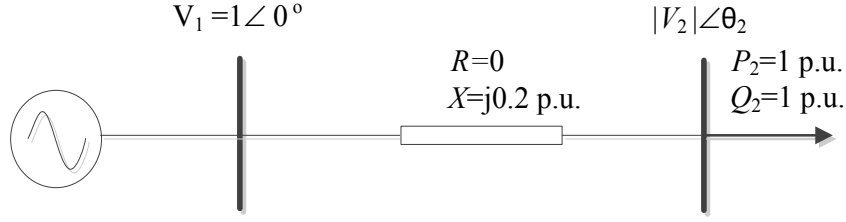
Figure 2.1 Convergence Problems in Iterative Methods: Two-bus Example

The voltage solutions for the two-bus system calculated in closed form are:

a) HV solution $= 0.6-j0.2=0.6324\angle-18.43°$

b) LV solution $= 0.4-j0.2=0.4472\angle-22.56°$.

In order to demonstrate the initial estimate dependency of NR method, a numerical experiment is conducted by solving the two-bus PF problem using NR method with different initial estimates and categorizing the initial estimate based on the solution to which the iterative method converges. The PBE's for bus 2 for this particular problem is derived from (2.1) are:

$$P_2 = \frac{|V_1||V_2|\sin\theta_2}{X} = 5|V_2|\sin\theta_2$$
$$Q_2 = \frac{|V_1||V_2|\cos\theta_2 - |V_2|^2}{X} = 5|V_2|\cos\theta_2 - 5|V_2|^2$$

(2.9)

The Jacobian matrix is obtained by taking the partial derivatives of the PBE expressed in (2.9) with respect to the bus voltage magnitude and angle.

$$\begin{bmatrix} \Delta\theta_2 \\ \Delta|V_2| \end{bmatrix} = \begin{bmatrix} 5|V_2|\cos\theta_2 & 5\sin\theta_2 \\ -5|V_2|\sin\theta_2 & 5\cos\theta_2 - 10V_2 \end{bmatrix}^{-1} \begin{bmatrix} \Delta P_2 \\ \Delta Q_2 \end{bmatrix}$$

(2.10)

Starting from an initial estimate for the voltage magnitude and angle, the Jacobian matrix and the mismatch in the PBE are evaluated from (2.9) and (2.10). By solving

15

the linear system of equations as described in (2.10), an update for bus voltage

magnitude and angle is found; Bus voltage magnitude and angle are updated and the

process is repeated until the mismatch in the PBE is less than 1e-04 p.u. The entire

procedure of solving the PF problem is repeated with different initial estimates for the

voltage. The initial estimate of the voltage magnitude is varied between 0.0 to 1.0 p.u.

in steps of 0.005 p.u. and the estimate of voltage angle is varied between $-\pi$ to $+\pi$

radians in steps of 0.01 radians.

Depending on the starting point, the NR method can converge to either the HV

solution or the LV solution or does not converge at all. For this simple problem, the

NR method is assumed not to converge at all if it fails to reach either the HV solution

or the LV solution within 15 iterations. Figure 2.2 shows the plot of initial estimates

classified based on the solution to which they converge.
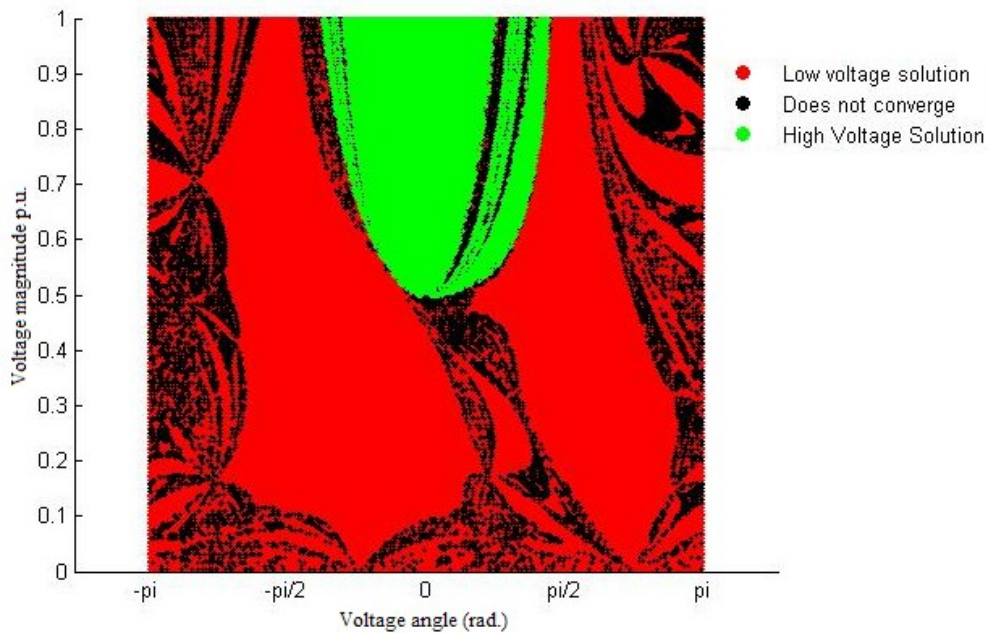
Figure 2.2 Initial Estimate Dependency of NR Method

In Figure 2.2, a red pixel indicates that, with that particular initial estimate of voltage, the NR method converges to the LV solution. Similarly, a green pixel and black pixel indicates convergence to HV solution and divergence respectively. The plot reveals that even for the simplest of problems, the NR method used here does not converge to the solution reliably.

Fast Decouple Power Flow (FDLF) method, being a variant of the NR method, also suffers from the problem of initial-estimate dependency. To demonstrate the same, the two-bus example shown in Figure 2.1 is solved using the *X/B* variation of the FDLF method. The *B'*, *B''* matrices constructed from (2.8) are:

$$B'_{22} = -\left(\frac{-1}{X_{12}}\right) = -\left(\frac{-1}{0.2}\right) = +5$$

$$B''_{22} = -\left(\frac{-X_{12}}{R_{12}^2 + X_{12}^2}\right) = -\left(\frac{-0.2}{0.2^2}\right) = +5$$

(2.11)

The iteration scheme for the two-bus problem (2.7) becomes:

$$\Delta\theta_2 = \frac{\Delta P_2/V_2}{B'} = 0.2(\Delta P_2/V_2)$$

$$\Delta V_2 = \frac{\Delta Q_2/V_2}{B''} = 0.2(\Delta Q_2/V_2)$$

(2.12)

The decoupled system of equations is solved by adopting a (1θ-$1V$) iteration. The two-bus problem is solved using FDLF with different initial estimates of the voltage (0 to 1 p.u. for voltage magnitude, $-\pi$ to $+\pi$ radians for voltage angle) at bus 2. The criterion for convergence is a mismatch of less than 1e-04 in the PBE's. The initial estimates are categorized based on the solution to which FDLF method converges and plotted in Figure 2.3.
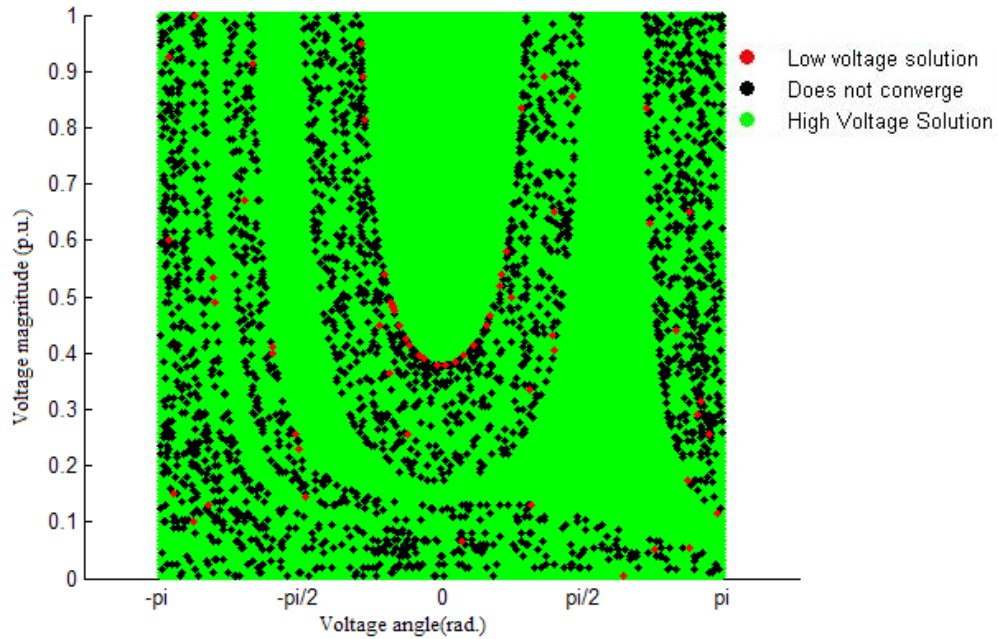
Figure 2.3 Initial Estimate Dependency of the FDLF Method

The convergence issues that can arise from iterative methods are evident from the above illustration. Also the when the system moves into extremis and the voltages move far from nominal, the iterative methods can and do fail to converge due to an ill-conditioned Jacobian matrix [29].

2.3   EVALUATING THE SADDLE NODE BIFURCATION POINT

In power system analysis, the BP (also known as the voltage collapse point), is representative of the maximum power transfer to a bus in the system. Methods for finding BP's can be broadly classified into three categories: continuation method, direct method and optimization method.

2.3.1   CONTINUATION METHOD

Continuation methods form a class of techniques in numerical methods that are capable of curve tracing around the critical points (turns or folds). The CPF [18] is one such method that can be used to trace the PV curve up to and including the loadability limit point of the system. The method of obtaining PV curves is extended from balanced positive sequence power systems to an unbalanced three-phase system in [32].

In the traditional form of CPF [18], the original PBE's are modified by inserting a load parameter λ. The CPF is a two-step process: a predictor step to evaluate the tangent vector to the function and a corrector step to correct the solution using a local parameterization technique. From a pre-solved HV solution, a series of predictor corrector steps are performed to trace the PV curve of the system. The continuation parameter is chosen to be the state variable that has the maximum tangent vector component [18].

For practical purposes, the maximum value up to which loading in a particular bus or a select few buses can be increased, before voltage collapse occurs, is required. Reference [31] presents an improved CPF that allows the power injections at each bus to vary according to multiple load variations and actual generation re-dispatch patterns. The BP of the system evaluated by uniformly increasing the power injection and the BP obtained by multiple power injection variations described above can differ by more than 28% [31]. The CPF gives the capability of increasing the loading at a particular

bus when the other loads remain constant; this is ensured by including a multiplier that designates the rate of change of load/generation, as the loading parameter λ is varied [18]. The CPF method finds wide practical applications in present day voltage stability assessment.

2.3.2 DIRECT METHOD FOR EVALUATING BIFURCATION POINT

As discussed earlier, the Jacobian matrix developed in NR method becomes singular at the BP. Reference [33] develops a method where the original PBE's are solved with the singularity of the Jacobian matrix imposed as an additional constraint to solve for the system states at the voltage collapse condition. The original system of equations is augmented such that for the enlarged system of equations, the modified Jacobian matrix at the BP is non-singular.

While the direct method allows for the direct evaluation of the BP, it is not possible to trace the locus of the PV curve. Also, the size of the matrix is doubled, thereby making the method computationally more expensive. The direct method is implemented to find the BP of a system with ac/dc interconnection, tested on a 2158 bus system in [19]. The direct method is extended from computing the static BP [33] to incorporate dynamic components such as Automatic Voltage Regulator (AVR) and Static VAR compensator (SVC) and determine the dynamic instabilities in [34].

2.3.3 OPTIMIZATION TECHNIQUES

Identifying the BP may be formulated as an optimization problem [35], [36], [37].The objective is to maximize loadability of the power system subject to the PBE's as the equality constraints and the generation capacity as inequality constraints. From a base case PF solution and a direction vector that dictates the load increment, the point at which bifurcation occurs can be determined [35]. This method however cannot be used to trace the low-voltage side of the PV curve. Reference [37] presents an optimization problem formulation to determine the BP, taking into account the excitation limits of generators. Such a bifurcation incorporating the dynamic components can occur before or after the static BP of the system.

An advantage of the optimization method is it allows the calculation of BP when the loading at one or a select few buses has to be increased with the other loads remaining constant. The primary drawback of optimization methods is that they involve solving a nonlinear optimization problem; hence, they are computationally intensive and practically infeasible. Also, non-smooth constraints such as tap-changing transformers, reactive power limits on generators are handled by solving a number of sub problems that are smooth. For medium to large size systems, the number of sub problems to be solved increases and the approach becomes unwieldy.

3 ANALYTIC CONTINUATION

3.1 INTRODUCTION

The PBE's in their present form (2.1) do not satisfy Cauchy-Riemann equations; hence, they are non-holomorphic. In HE method, the voltage function is embedded using a complex parameter, s, such that the resultant system of equations is holomorphic. This allows the voltage function to be expressed as a Taylor's series whose radius of convergence is unknown. Analytic continuation techniques need to be employed to find the converged value of this voltage function (i.e. the voltage solution).

Analytic continuation, a field of study in complex analysis, is defined as the technique of extending the domain of a given analytic function. In the context of solving the PF problem using HE, analytic continuation is used to represent the voltage function outside the radius of convergence of the voltage power series. The concept of analytic continuation can be demonstrated using a simple example involving the geometric series [39].

Consider the series $f_1(s)$ given by

$$f_1(s) = 1 + s + s^2 + s^3 + \cdots \tag{3.1}$$

The infinite series expression in (3.1) converges only for values of s that satisfy the relation $|s| < 1$. It is straightforward to show that for $|s| < 1$, the series $f_1(s)$ can be equivalently represented as:

$$f_1(s) = 1 + s + s^2 + s^3 + \cdots = \frac{1}{1-s} \tag{3.2}$$

22

$$\sum_{n=0}^{\infty} s^n$$

R=1

s=1

Im(s)

Re(s)
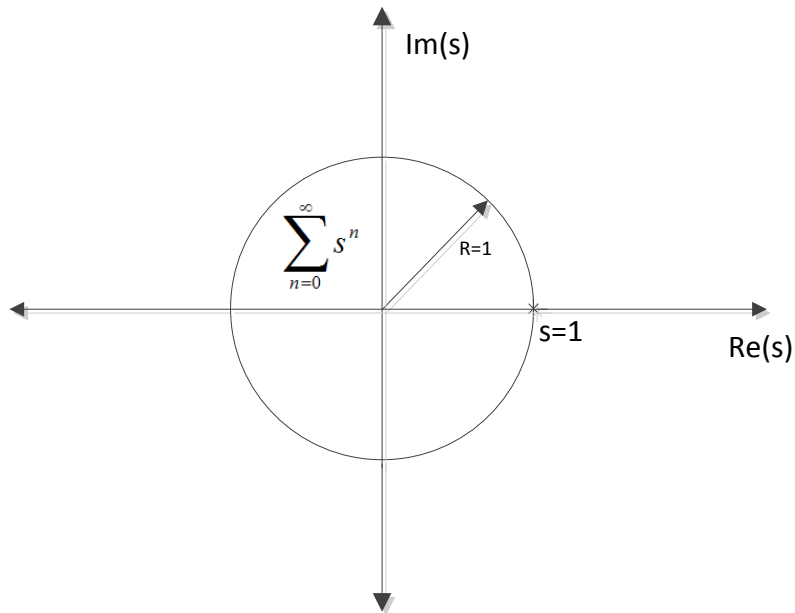
Figure 3.1 Radius of Convergence of Power Series $f_1(s)$

Figure 3.1 shows the region of convergence of the infinite series $f_1(s)$ in the complex s plane. By exploiting the property of analytic continuation, it is possible to construct a different function that

a) Coincides with the original function within its radius of convergence

b) Extends the domain of convergence of the original function.

Consider an integral function $f_2(s)$ given by

$$f_2(s) = \int_0^\infty e^{-(1-s)x} dx \tag{3.3}$$

The integral can be explicitly evaluated as:

$$f_2(s) = \int_0^\infty e^{-(1-s)x} dx = \lim_{A \to \infty} \int_0^A e^{-(1-s)x} dx = \lim_{A \to \infty} \frac{1 - e^{-(1-s)A}}{1-s} = \frac{1}{1-s} \tag{3.4}$$

IFF $\mathrm{Re}(s) < 1$

23

The function $f_2(s)$ represents the original geometric series accurately when $|s|<1$. In addition, $f_2(s)$ is valid over a larger domain ($Real(s) < 1$) in the complex plane. Thus, $f_2(s)$ is an analytic continuation of the original series $f_1(s)$.

Furthermore, consider the function $f_3(s)$ defined below:

$$f_3(s) = \frac{1}{1-s} \qquad\qquad (3.5)$$

The function $f_3(s)$ represents the functions $f_1(s), f_2(s)$ accurately in their respective domains. Also, $f_3(s)$ is valid for all values of $s \in C$, except at $s=1$. The function $f_3(s)$ represents what is known as the maximal analytic continuation (more about this below) of the original function $f_1(s)$. The region of convergence of the functions $f_1(s), f_2(s)$ and $f_3(s)$ is shown in Figure 3.2.
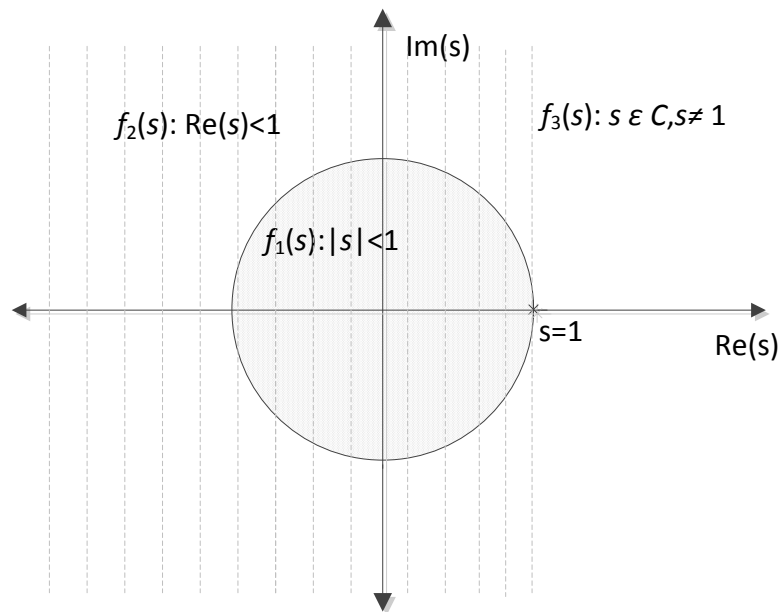
Figure 3.2 Domain of Convergence of $f_1(s), f_2(s)$ and $f_3(s)$

As shown in the illustration above, there are different approaches for finding a function that is the analytic continuation of another function. The problem of interest is

24

to find the analytic continuation that extends the analytic function f to the largest domain in the complex plane, i.e. the maximal analytic continuation. Stahl's Padé convergence theory [42], [43] shows that, "For an analytic function f with finite singularities, the close to diagonal sequence of diagonal Padé approximants converge in minimal logarithmic capacity to the original function in the extremal domain." In other words, Padé approximants can be used to evaluate the maximal analytic continuation.

This chapter examines the calculation of the Padé approximants using three different approaches:

a) Direct method (or matrix method)

b) Continued fractions (Viskovatov approach)

c) Epsilon algorithm

Numerical issues and computational trade-offs associated with evaluating the Padé approximants are discussed. The calculation procedures of the different methods are demonstrated with numerical examples.

3.2   DIRECT METHOD (OR MATRIX METHOD)

The technique of finding a rational interpolant for the power series of interest using the direct method was developed by Henri Padé in 1890, hence the name Padé approximants [44]. The Padé approximants calculated with increasing number of coefficients in the series and differing degrees of numerator and denominator

polynomial are listed in a tabular format known as the Padé table [44]. Consider the

power series representation of an analytic function $c(s)$:

$$c(s) = c_0 + c_1 s + c_2 s^2 + c_3 s^3 + \ldots = \sum_{n=0}^{\infty} c[n] s^n \tag{3.6}$$

The coefficient of the power series of degree n is denoted using the notation $c[n]$

or c_n. For a power series given by (3.6), the Padé approximant is a rational fraction of

the following form:

$$[L/M]\text{Padé} = \frac{a_0 + a_1 s + a_2 s^2 + \ldots + a_L s^L}{b_0 + b_1 s + b_2 s^2 + \ldots + b_M s^M} \tag{3.7}$$

In equation (3.7) L is the degree of the numerator polynomial and M is the degree of

the denominator polynomial. It is convention to refer such approximants as $[L/M]$ Padé

(approximants.) The procedure to evaluate the $[L/M]$ Padé approximant from the

truncated power series expression of (3.6) is shown below:

$$c(s) = c_0 + c_1 s + c_2 s^2 + \ldots c_{L+M} s^{L+M} + O(s^{L+M+1})$$
$$= \frac{a_0 + a_1 s + a_2 s^2 + \ldots + a_L s^L}{b_0 + b_1 s + b_2 s^2 + \ldots + b_M s^M} = \frac{a(s)}{b(s)} \tag{3.8}$$

where the coefficients c_0 through c_{L+M} are known. In (3.8) $O(s^{L+M+1})$ indicates the

truncation error for the $[L/M]$ Padé. In (3.8), there are $L+M+1$ known coefficients in the

power series while there are $L+M+2$ unknowns in the Padé approximant. Hence, one of

the coefficients in the Padé approximant can be chosen as a free variable to scale the

entire equation. The constant term in the denominator polynomial b_0 is chosen to be 1

here. Multiplying (3.8) by $b(s)$ on both sides:

$$\left(b_0 + b_1 s + b_2 s^2 + \ldots + b_M s^M \right)\left(c_0 + c_1 s + c_2 s^2 + \ldots c_{L+M} s^{L+M} \right)$$
$$= a_0 + a_1 s + a_2 s^2 + \ldots + a_L s^L \tag{3.9}$$

Equating the coefficients of s^{L+1} to s^{L+M} on LHS to 0:

$$
\begin{aligned}
b_M c_{L-M+1} + b_{M-1} c_{L-M+2} + \cdots b_0 c_{L+1} &= 0 \\
b_M c_{L-M+2} + b_{M-1} c_{L-M+3} + \cdots b_0 c_{L+2} &= 0 \\
&\vdots \\
b_M c_L + b_{M-1} c_{L+1} + \cdots b_0 c_{L+M} &= 0
\end{aligned}
\tag{3.10}
$$

This is a system of M linear equations; it can be expressed in a matrix form as shown in (3.11). Equation (3.11) can be solved using traditional LU factorization techniques to obtain the denominator polynomial coefficients.

$$
\begin{bmatrix}
c_{L-M+1} & c_{L-M+2} & c_{L-M+3} & \cdots & c_L \\
c_{L-M+2} & c_{L-M+3} & c_{L-M+4} & \cdots & c_{L+1} \\
c_{L-M+3} & c_{L-M+4} & c_{L-M+5} & \cdots & c_{L+2} \\
\vdots & \vdots & \vdots & \ddots & \vdots \\
c_L & c_{L+1} & c_{L+2} & \cdots & c_{L+M-1}
\end{bmatrix}
\begin{bmatrix}
b_M \\
b_{M-1} \\
b_{M-2} \\
\vdots \\
b_1
\end{bmatrix}
= -
\begin{bmatrix}
c_{L+1} \\
c_{L+2} \\
c_{L+3} \\
\vdots \\
c_{L+M}
\end{bmatrix}
\tag{3.11}
$$

By equating the coefficients of like powers of s on both sides from s^0 to s^L in (3.8), the numerator polynomial coefficients can be evaluated.

$$
\begin{aligned}
c_0 &= a_0 \\
b_0 c_1 + b_1 c_0 &= a_1 \\
b_0 c_2 + b_1 c_1 + b_2 c_0 &= a_2 \\
&\vdots \\
\sum_{k=0}^{L} c_k b_{L-k} &= a_L
\end{aligned}
\tag{3.12}
$$

The coefficients of the c series are known; the b series coefficients are evaluated from (3.11). Thus from equation (3.12) the numerator polynomial coefficients can be evaluated.

The matrix method described in [44] allows the calculation of rational approximant of any arbitrary degree. However, from the discussion of Stahl's Padé convergence theory in section (3.1), the diagonal/near-diagonal Padé approximant is of interest since it yields the maximal analytic continuation. A diagonal Padé approximant is a rational

approximant whose numerator and denominator polynomial degrees are equal (i.e. *L=M*). If the difference between the degree of the numerator and denominator polynomial is 1, (i.e. |*L-M*|=1), it is said to be a near-diagonal Padé approximant.

Using the above mentioned calculation procedure, a near-diagonal [0/1] Padé approximant is calculated for the geometric series given in (3.1). For constructing a [*L/M*] Padé approximant, *L+M+*1 terms (or, coefficients up to s^{L+M}) are required in the series. Hence, the series (3.1) truncated at two terms (truncated up to s^1) for evaluating the [0/1] Padé. The Padé approximant evaluated using (3.6)-(3.12) is found to be $\dfrac{1}{1-s}$. The [0/1] Padé coincides with $f_3(s)$ shown in (3.5). This example can be used to demonstrate fact the Padé approximant is indeed the maximal analytic continuation for this series, hence the best possible representation of the power series.

3.3   VISKOVATOV METHOD

The Viskovatov method may be thought of as a two step approach. The first step it to take the original power series and convert it to a continued fraction. The second step is to convert the continued fraction to a rational function. The first step relies on recursively inverting partial series (shown below). It requires that all the inverses of the partial series that are required exist.

For the Taylor's series representation of an analytic function $c(s)$ as shown in (3.6), evaluating a continued fraction using the Viskovatov method is discussed in reference [44]. The procedure is explained in equations (3.13)-(3.19).

28

$$
\begin{aligned}
c(s) &= c[0] + c[1]s + c[2]s^2 + \ldots + c[n]s^n + \ldots \\
&= c[0] + s(c[1] + c[2]s + \ldots + c[n]s^{n-1} + \ldots) \\
&= c[0] + \cfrac{s}{\cfrac{1}{c[1] + c[2]s + \ldots + c[n]s^{n-1} + \ldots}} \\
&= c[0] + \frac{s}{c^{(1)}(s)}
\end{aligned}
\tag{3.13}
$$

The quantity $c^{(1)}(s)$ in (3.13) is the reciprocal of another power series given by:

$$
\begin{aligned}
c^{(1)}(s) &= \frac{1}{(c[1] + c[2]s + c[3]s^2 + \ldots + c[n]s^{n-1} + \ldots)} \\
&= c^{(1)}[0] + c^{(1)}[1]s + \ldots + c^{(1)}[n-1]s^{n-1} + \ldots
\end{aligned}
\tag{3.14}
$$

The coefficient of $c^{(1)}(s)$ is evaluated using the fact that the product of the two power series should yield 1.0. In other words, the product of a series and its inverse should equal 1.0 for the constant term and zero for the remaining powers of s.

$$
\begin{aligned}
&(c^{(1)}[0] + c^{(1)}[1]s + \ldots + c^{(1)}[n-1]s^{n-1} + \ldots) \\
&(c[1] + c[2]s + \ldots + c[n]s^{n-1} + \ldots) = 1
\end{aligned}
\tag{3.15}
$$

Equation (3.15) is a product of two power series on the LHS. Since this product must equal 1.0 for the constant term, it must be the case that

$$
c^{(1)}[0] = \frac{1}{c[1]}
\tag{3.16}
$$

The coefficients of the remaining powers of s in (3.15) should be zero. Hence the coefficients, $c^{(1)}[n]$, $\forall n = 1, 2, 3, \cdots$ can be calculated using the relation,

$$
c^{(1)}[n] = -\frac{\displaystyle\sum_{k=0}^{n-1} c^{(1)}[k]c[n+1-k]}{c[1]}
\tag{3.17}
$$

Applying the technique described above recursively, equation (3.13) becomes:

$$
c(s) = c[0] + \cfrac{s}{c^{(1)}[0] + \cfrac{s}{\cfrac{1}{c^{(1)}[1] + \ldots + c^{(1)}[n-1]s^{n-2} + \ldots}}}
\tag{3.18}
$$

$$c(s) = c[0] + \cfrac{s}{c^{(1)}[0] + \cfrac{s}{c^{(2)}[0] + \cfrac{s}{c^{(3)}[0] + \dots}}} \tag{3.19}$$

Depending upon where the continued fraction in (3.19) is truncated, a three-term recursion relationship can be used to find a rational function which is equivalent to either a diagonal or near-diagonal Padé approximant (i.e., a [1/0], [1/1], [2/1] … Padé approximant) depending upon the number of terms in the continued fraction. This is proved by the principle of mathematical induction in [44] and the iterative re-expansion of the continued fraction in [45].

For a power series truncated at finite number of terms, say n, the continued fraction can be evaluated directly by replacing $s=1$ in (3.19) and then calculating from the last element $c^{(n)}[0]$ progressing upward. It can also be evaluated in a rational form A_n/B_n as a function of s using the three-term recursion relation [44].

$$
\begin{aligned}
&A_0(s) = c[0], \, A_1(s) = c[0]c^{(1)}[0] + s \\
&A_i(s) = c^{(i)}[0]A_{i-1}(s) + sA_{i-2}(s), \, i = 2,\, 3,\dots \\
&B_0(s) = 1, \, B_1(s) = c^{(1)}[0] \\
&B_i(s) = c^{(i)}[0]B_{i-1}(s) + sB_{i-2}(s), \, i = 2,\, 3,\dots
\end{aligned}
\tag{3.20}
$$

The three-term recursion relation is preferred since it gives flexibility in choosing the number of terms in the continued fraction. In other words, when using the three-term recursion relation, an *a posteriori* increase in the length of the power series involves fewer calculations compared to direct evaluation of the continued fraction.

3.4 EPSILON ALGORITHM

In the previous two approaches, the power series is approximated with a rational approximant as a function of s. This rational approximant may then be evaluated for any value of s. If the interest is only in the value of the approximant, for instance at $s=1.0$, a more economical algorithm, the epsilon algorithm, can be used instead. The epsilon algorithm developed in [47] involves the transformation of the sequences into a two dimensional array called the epsilon table (ϵ table). Wynn's identity [48] establishes a relationship between the entries of the ϵ table and the Padé table. The epsilon algorithm is a faster way of evaluating the Padé approximant for a specified value of s. The calculation procedure in constructing the ϵ table is presented in [44].

The notation $\epsilon_k^{(j)}$ is used to indicate the entries of the epsilon table. The subscript k denotes the column and the superscript j indicates the progression down the column. The first column is $\epsilon_{-1}^{(j)}$ is defined to be zeros. The second column is defined as the series (sum of the sequence terms) which is to be evaluated. The remaining elements are calculated from the epsilon algorithm, which connects the elements in a rhombus pattern as shown in Table 3.2.

Table 3.1 Structure of the ϵ Table

$$\varepsilon_{-1}^{(0)}$$

$$\varepsilon_0^{(0)}$$

$$\varepsilon_{-1}^{(1)} \qquad\qquad \varepsilon_1^{(0)}$$

$$\varepsilon_0^{(1)} \qquad\qquad \varepsilon_2^{(0)}$$

$$\varepsilon_{-1}^{(2)} \qquad\qquad \varepsilon_1^{(1)} \qquad \vdots$$

$$\varepsilon_0^{(2)} \qquad \vdots$$

$$\varepsilon_{-1}^{(3)} \qquad \vdots$$

$$\vdots$$

Table 3.2 Rhombus Pattern to Evaluate Entries of the ϵ Table

$$\varepsilon_k^{(j)}$$

$$\varepsilon_{k-1}^{(j+1)} \qquad\qquad \varepsilon_{k+1}^{(j)}$$

$$\varepsilon_k^{(j+1)}$$

The entries of Table 3.1 are calculated using the relation shown in (3.21).

$$\varepsilon_{k+1}^{(j)} = \varepsilon_{k-1}^{(j+1)} + \left[\varepsilon_k^{(j+1)} - \varepsilon_k^{(j)}\right]^{-1} \qquad\qquad (3.21)$$

It is assumed that all the entries of the table exist. Since the epsilon algorithm uses the reciprocal differences of the power series coefficients, the trailing digits of the coefficients are more critical in accurately representing the function. It can be

observed that when two successive elements of a column $\epsilon_k^{(j+1)}, \epsilon_k^{(j)}$ are equal, from (3.21) $\epsilon_{k+1}^{(j)}$ is not defined. Such cases are said to be degenerate. It is shown in [48] that the Padé approximant calculated with a fixed number of terms in the series and evaluated at a particular value of s is numerically equivalent to the value obtained from the even column of the epsilon table constructed with the same number of terms in the series. For the above statement to hold true, the Padé has to exist and the epsilon table should be non-degenerate [48]. The epsilon algorithm is computationally appealing in calculating Padé approximants since it does not involve solving a matrix equation.

3.5 NUMERICAL ILLUSTRATION OF ANALYTIC CONTINUATION

This section demonstrates the numerical implementation of the different analytic continuation techniques discussed in Sections 3.2-3.4. The context in which analytic continuation is used in this research is to evaluate the maximal analytic continuation of the holomorphic voltage function. However, the analytic continuation finds other practical applications such as summing a divergent series and the acceleration of convergence of slow convergent series. For the illustration of analytic continuation techniques, one such application is considered. The irrational constant π is evaluated from a slowly converging series.

Consider the Gregory series for π [49] shown in (3.22).

$$\pi = \sum_{k=0}^{\infty} \frac{(-1)^k 4}{2k+1} \tag{3.22}$$

33

It can be observed from (3.22) that as variable k increases, the terms in the sequence become small. Also, the sign in the series is alternating because of the $(-1)^k$ term. When two consecutive terms of the series are taken together, they tend to cancel each other leaving a small residual; these residuals add up with increasing number of terms in the series resulting in the value of π. Hence, the Gregory's series is extremely slow to converge.

Equation (3.23) shows the Gregory's series truncated up to seven terms.

$$\pi(s) = 4 - \frac{4}{3}s + \frac{4}{5}s^2 - \frac{4}{7}s^3 + \frac{4}{9}s^4 - \frac{4}{11}s^5 + \frac{4}{13}s^6 \tag{3.23}$$

Evaluating (3.23) at $s=1$, equation (3.22) with a truncation error of order $O(s^7)$ can be recovered.

The analytic continuation of this power series is evaluated from the truncated series using the matrix method, the Viskovatov method and the epsilon algorithm and the results are tabulated below. All calculations were completed with double precision using MATLAB. The intermediate results are shown with only four digits of precision for brevity.

3.5.1 PADÉ APPROXIMANTS USING MATRIX METHOD

Given coefficients up to s^6 of Gregory's series in (3.23), the [3/3] diagonal Padé can be evaluated. The constant coefficient in the denominator polynomial is chosen to be 1.0. Using (3.11), the denominator polynomial coefficients b_1 through b_3 can be expressed using a matrix equation. The coefficients of the power series from (3.23) are

substituted in the matrix equation and the denominator polynomial coefficients are calculated.

$$\begin{bmatrix} c_1 & c_2 & c_3 \\ c_2 & c_3 & c_4 \\ c_4 & c_5 & c_6 \end{bmatrix}\begin{bmatrix} b_3 \\ b_2 \\ b_1 \end{bmatrix} = -\begin{bmatrix} c_4 \\ c_5 \\ c_6 \end{bmatrix}$$

$$\begin{bmatrix} -4/3 & 4/5 & -4/7 \\ 4/5 & -4/7 & 4/9 \\ -4/7 & 4/9 & -4/11 \end{bmatrix}\begin{bmatrix} b_3 \\ b_2 \\ b_1 \end{bmatrix} = -\begin{bmatrix} 4/9 \\ -4/11 \\ 4/13 \end{bmatrix} \tag{3.24}$$

$$\begin{bmatrix} b_3 \\ b_2 \\ b_1 \end{bmatrix} = \begin{bmatrix} 0.0816 \\ 0.7343 \\ 1.6154 \end{bmatrix}$$

Calculating the numerator polynomial coefficients from (3.12)

$$\sum_{k=0}^{L} c_k b_{L-k} = a_L$$

$$a_0 = c_0 = 4$$
$$a_1 = b_0 c_1 + b_1 c_0 = 1 \cdot (-4/3) + 1.6154(4) = 5.1283 \tag{3.25}$$
$$a_2 = b_0 c_2 + b_1 c_1 + b_2 c_0 = 1 \cdot (4/5) + 1.6154(-4/3) + 0.7343(4) = 1.5833$$
Similarly,
$$a_3 = 1 \cdot (-4/7) + 1.6154(4/5) + 0.7343(-4/3) + 0.0816(4) = 0.0682$$

The [3/3] Padé approximant evaluated using the matrix method is shown in (3.26).

$$\pi(s) = \frac{4 + 5.1283\,s + 1.5833\,s^2 + 0.0682\,s^3}{1 + 1.6154\,s + 0.7343\,s^2 + 0.0816\,s^3} \tag{3.26}$$

$$\pi(1) = 3.141614906832299$$

Evaluating (3.26) at *s*=1 yields the required numerical value of π. The error in the estimated value of π using the [3/3] Padé is 7.0834*e*-04%.

3.5.2   CONTINUED FRACTION

From the power series approximation of π in (3.23), a continued fraction is constructed using the Viskovatov approach (equations (3.13)-(3.19)).

$$\pi(s) = 4 + \cfrac{s}{\cfrac{1}{-\cfrac{4}{3} + \cfrac{4}{5}s - \cfrac{4}{7}s^2 + \cfrac{4}{9}s^3 - \cfrac{4}{11}s^4 + \cfrac{4}{13}s^5}}}$$

$$= 4 + \cfrac{s}{-0.7500 - 0.4500s + 0.0514s^2 - 0.0263s^3 + 0.0167s^4 - 0.0119s^5}$$

$$= 4 + \cfrac{s}{-0.7500 + s(0.4500 + 0.0514s - 0.0263s^2 + 0.0167s^3 - 0.0119s^4)}$$

$$= 4 + \cfrac{s}{-0.75 + \cfrac{s}{-2.2222 - 0.2540s + 0.1008s^2 - 0.0563s^3 + 0.0370s^4}}$$

$$\vdots$$

(3.27)

Repeating the procedure the continued fraction expansion is obtained in (3.28)

$$\pi(s) = 4 + \cfrac{s}{-0.75 + \cfrac{s}{-2.2222 + \cfrac{s}{-3.9375 + \cfrac{s}{-0.6400 + \cfrac{s}{-9.6680 + \cfrac{s}{-0.3019}}}}}}$$

(3.28)

Evaluated at $s=1$, the value of π evaluated with 16 digits of precision from (3.28) is

$$\pi(1) = 3.141614906832298$$

(3.29)

The percentage error in the value of π evaluated from the continued fraction with seven terms in the original series is 7.0834e-04%.

3.5.3   EPSILON ALGORITHM

The epsilon table is constructed as shown in Section 3.4 above. The entries of the first column (denoted by ϵ_{-1} in Table 3.1) are all zeros. The second column (denoted by ϵ_0) is the sum of the power series coefficients; in other words, the entry of the second

column is the series from (3.23) rather than the sequence elements. Evaluating (3.23)

at $s=1$, the entries of the second column are calculated as:

$$
\begin{aligned}
\varepsilon_0^{(0)} &= c_0 = 4 \\
\varepsilon_0^{(1)} &= c_0 + c_1 s = 4 - \frac{4}{3} = 2.6667 \\
\varepsilon_0^{(2)} &= c_0 + c_1 s + c_2 s^2 = 4 - \frac{4}{3} + \frac{4}{5} = 3.4667 \\
&\vdots
\end{aligned}
\tag{3.30}
$$

The remaining entries of the epsilon table are constructed using (3.21) as follows:

$$
\begin{aligned}
\varepsilon_1^{(0)} &= \varepsilon_{-1}^{(1)} + \left[\varepsilon_0^{(1)} - \varepsilon_0^{(0)}\right]^{-1} = 0 + (2.6667 - 4)^{-1} = -0.75 \\
\varepsilon_1^{(1)} &= \varepsilon_{-1}^{(2)} + \left[\varepsilon_0^{(2)} - \varepsilon_0^{(1)}\right]^{-1} = 0 + (3.4667 - 2.6667)^{-1} = 1.25 \\
&\vdots \\
\varepsilon_2^{(0)} &= \varepsilon_0^{(1)} + \left[\varepsilon_1^{(1)} - \varepsilon_1^{(0)}\right]^{-1} = 2.6667 + (1.25 - (-0.75))^{-1} = 3.1667 \\
&\vdots
\end{aligned}
\tag{3.31}
$$

Table 3.3 shows the entries of the of the epsilon table. The odd columns do not

carry any meaningful information except that they are required in constructing the

subsequent columns in the epsilon table. The epsilon algorithm is computationally

less expensive when the analytic continuation has to be evaluated at one particular

value. In this case, at $s=1$ for the Gregory's series.

Table 3.3 Epsilon Table for Gregory's π Series

ε_{-1}	ε_0	ε_1	ε_2	ε_3	ε_4	ε_5	ε_6
0							
	4						
0		-0.75					
	2.6667		3.1667				
0		1.25		-28.75			
	3.4667		3.1333		3.1423		
0		-1.75		82.25		-969.938	
	2.8952		3.1452		3.1413		3.1416
0		2.25		-177.75		3515.062	
	3.3397		3.1397		3.1416		
0		-2.75		327.25			
	2.9760		3.1427				
0		3.25					
	3.2837						

The approximate value of π evaluated using the epsilon algorithm is the element in the furthest even column. With 16 digits of precision, the value of π is evaluated as 3.141614906832299. The percent error in the value of π is 7.0834e-04%.

The percentage error in value of π obtained using different analytical continuation techniques is found to be the same. Moreover, the value of π calculated using the different procedures was numerically verified to be the exact up to 15 decimal places.

3.5.4   ACCELERATION OF CONVERGENCE OF π SERIES

The acceleration in the convergence of the series is best shown by comparing the value of π obtained by directly summing the series against the value of obtained from the Padé approximant (using the matrix method) with the same number of terms in the

series. It has been already established that the continued fraction and epsilon algorithm are equivalent to the evaluating the Padé approximant. In

Table 3.4, the first column indicates the number of terms in the series. The diagonal Padé approximant is evaluated using the matrix method and listed in the second column. Columns 3 and 4 indicate the value of π obtained by evaluating the Padé approximants and the power series respectively. The results are tabulated in

Table 3.4 with eight digits of precision. The numbers showed in bold are the correct digits of π.

Table 3.4 Evaluating π using Padé Approximants with Matrix Method

Number of terms in series	Diagonal Padé approximant	Diagonal Padé evaluated at s=1	Truncated power series approximation
3	$\dfrac{4+1.07s}{1+0.6s}$	**3.16**666667	3.46666667
5	$\dfrac{4+3.11s+0.27s^2}{1+1.11s+0.24s^2}$	**3.14**234234	3.33968253
7	$\dfrac{4+5.13s+1.58s^2+0.07s^3}{1+1.16s+0.73s^2+0.08s^3}$	**3.141**61490	3.28373848
9	$\dfrac{4+7.13s+3.90s^2+0.67s^3+0.02s^4}{1+2.12s+1.48s^2+0.38s^3 0.03s^4}$	**3.14159**331	3.25236593

Graphically, the acceleration of convergence using the analytic continuation techniques is shown in Figure 3.3. The value of π estimated by the power series and Padé approximant is plotted against the number of terms in the series and compared with the actual value of π.
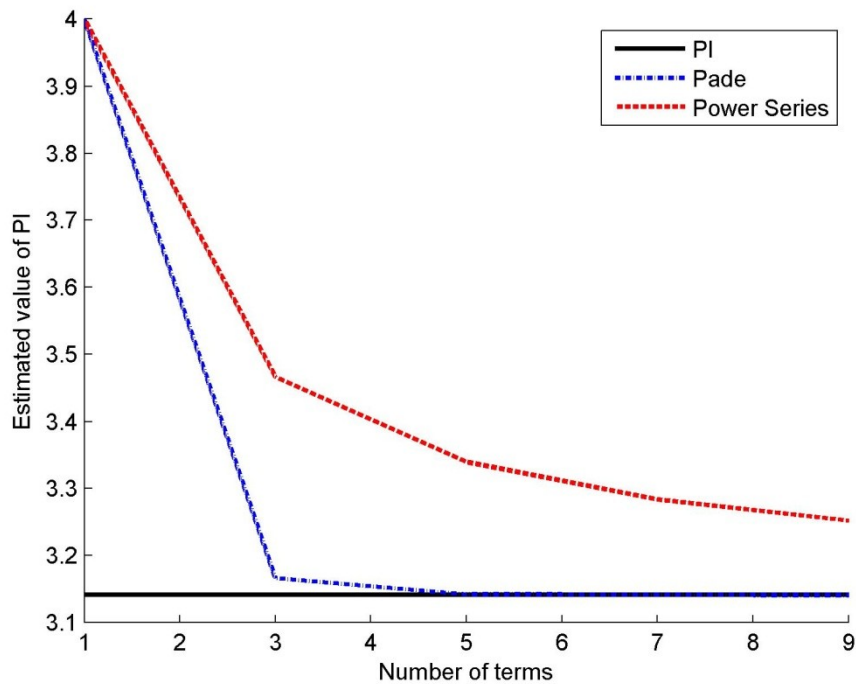
Figure 3.3 Convergence of Power Series vs. Padé Approximant

From Figure 3.3, it is clearly seen that the convergence of the series can be accelerated by the use of Padé approximants. For the same degree of accuracy as a [3/3] Padé (calculated with 7 terms in the series), 31831 terms are required in the power series approximation. While this example uses an extremely slowly converging power series and while most gains are not this dramatic, this example gives a sense of what can be achieved using Padé approximants.

The illustration of evaluating π shows that Padé approximants can be used to accelerate slow converging series. It can also be used to evaluate certain ostensibly diverging power series. More importantly, it can be used to evaluate the maximal analytic continuation of the function as proved in Stahl's theory [42], [43].

3.6   NUMERICAL ISSUES IN EVALUATING THE ANALYTIC

CONTINUATION

Numerical issues in evaluating an analytic function occur in

a) Calculation of power series coefficients of an analytic function.

b) Evaluating the analytic continuation of the power series.

The description of errors belonging to category a) can be subcategorized into the following

i.   Round-off errors: The calculation of power series coefficients in the PF problem typically involves some form of convolution (as will be discussed in Chapter 4). Round-off errors that occur during the calculation of one coefficient compound in the calculation of the next coefficient and so on. Reference [20] suggests that calculation of 40-60 terms in the series can exhaust the double precision arithmetic due to round-off errors.

ii.   Truncation errors: The power series approximation must be truncated to a finite number of terms in order to calculate its analytic continuation. If sufficient terms are not included in the series, the analytic continuation might not be an accurate representation of the original function. The solution to this problem is to add more terms in the series with appropriate consideration of the occurrence of round-off errors and to the possibility that a solution might not exist to the original equations.

The errors belonging to category b) are more relevant in this context and will be discussed in detail with numerical examples later. The illustration of the numerical issues is done using the matrix method of evaluating the Padé approximants. The other methods of evaluating analytic continuation are also equally prone to such errors. While implementing the different algorithms, their numerical performance should be taken into account.

3.6.1   DEGENERATE POWER SERIES

The power series representation of an analytic function is said to be degenerate if it leads to a singular matrix in calculation of the Padé approximants. Calculating the denominator polynomial coefficients of the Padé approximant requires solving a linear system of equations (3.11). The elements of the matrix in (3.11) depend on the calculated coefficients of the power series. A degenerate series results in a singular matrix with no solution. It is critical to be able to determine degenerate cases in the numerical implementation of the Padé approximants to obtain reliable results.

A specific example of degeneracy occurs in the geometric series where the [$L/2$] Padé approximants are degenerate for any value of L. A geometric series can arise out of solving a simple scalar equation devoid of any complexities (viz. nonlinearity, complex conjugate operation) using the holomorphic embedding procedure. Such degeneracy can be illustrated using the following simple scalar linear equation,

$$(1 + a)x = b \qquad\qquad (3.32)$$

where a, b are scalars. While the solution to the problem is trivial, solving this problem in a manner that will be used for the nonlinear problem will help in understand the numerical issues that can occur in the solution procedure.

To solve this problem, the variable x is expressed as a function of a complex parameter s.

$$x(s) = x[0] + x[1]s + x[2]s^2 + \dots \qquad (3.33)$$

From (3.32) a fixed-point form is established.

$$x(s) = b - ax(s) \qquad (3.34)$$

The equation is embedded with the complex parameter s such that at s=0 the solution is known.

$$x(s) = b - asx(s) \qquad (3.35)$$

The function $x(s)$ is expanded and coefficients of like powers of s on both sides of the equation are equated.

$$x[0] + x[1]s + x[2]s^2 = b - as\left(x[0] + x[1]s + x[2]s^2\right) \qquad (3.36)$$

$$\begin{aligned}
x[0] &= b \\
x[1] &= -ax[0] = -ab \\
x[2] &= -ax[1] = a^2 b \\
&\vdots
\end{aligned} \qquad (3.37)$$

In general, the power series coefficients of the series $x(s)$ can be expressed as:

$$x[0] = b \qquad (3.38)$$

$$x[n] = -ax[n-1] = (-a)^n b, n \geq 1$$

where $x[n]$ denotes the coefficient of s^n in the power series.

The series $x(s)$ to be evaluated for any arbitrary scalar a, b is

$$x(s) = b - abs + a^2bs^2 \ldots \tag{3.39}$$

From the calculated series coefficients, the evaluation of [L/2] Padé approximant

for an arbitrary value of L follows from (3.11) and (3.12).

$$\begin{bmatrix} x[L-1] & x[L] \\ x[L] & x[L+1] \end{bmatrix} \begin{bmatrix} b_2 \\ b_1 \end{bmatrix} = -\begin{bmatrix} x[L+1] \\ x[L+2] \end{bmatrix} \tag{3.40}$$

Substituting (3.38) in the above equation,

$$\begin{bmatrix} (-a)^{L-1}b & (-a)^L b \\ (-a)^L b & (-a)^{L+1}b \end{bmatrix} \begin{bmatrix} b_2 \\ b_1 \end{bmatrix} = -\begin{bmatrix} (-a)^{L+1}b \\ (-a)^{L+2}b \end{bmatrix} \tag{3.41}$$

The determinant of the LHS matrix is zero as shown in (3.42)

$$\begin{vmatrix} (-a)^{L-1}b & (-a)^L b \\ (-a)^L b & (-a)^{L+1}b \end{vmatrix} = \left((-a)^{L-1}b\right)^2 \begin{vmatrix} 1 & -a \\ -a & a^2 \end{vmatrix} \tag{3.42}$$

$$= \left((-a)^{L-1}b\right)^2 \left(a^2 - a^2\right) = 0$$

Equation (3.42) shows that the Padé matrix for an [L/2] approximant turns out to be

singular for a geometric series resulting in no possible solution for the b coefficients. If

the coefficients are floating point numbers, the round-off error may prevent the matrix

from being exactly singular. However, the condition number of the Padé matrix will be

very high and the results obtained from any such calculation may be erroneous.

For this specific problem, it can be shown that the [0/1] Padé, $x(s) = \dfrac{b}{1+as}$ is an

exact representation of the solution. Evaluating the [L/2] Padé can be associated with

solving an over determined system of equations. It occurs due to specifying one too

many coefficients when it is not required. Hence, it becomes essential in the numerical

algorithm to recognize the cases where a smaller degree Padé approximant is sufficient to accurately represent the power series.

3.6.2 ILL-CONDITIONED PADÉ MATRIX IN EVALUATING A CONVERGENT SERIES

The power series coefficients of a convergent series, in most practical applications do not become exactly zero for higher order terms. Due to floating point arithmetic truncation and round-off errors in the calculation, the coefficients decrease monotonically until they become small enough to be considered numerical zeros. In such scenarios, evaluating a higher degree Padé means adding rows of numerical zeros, that are nearly linearly dependent on each other to the Padé matrix (3.11), leading to a very high condition number of the Padé matrix.

The following example of solving a two-bus dc PF problem from [46] results in a convergent series and stands to illustrate the numerical issues associated with the Padé matrix. Solving the quadratic equation that arises from the two-bus dc PF using HE is demonstrated; it is then extended to the general ac PF problem in the next chapter.
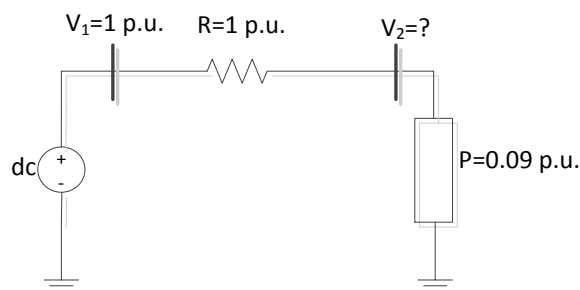
Figure 3.4 Solving a dc PF problem using the HE procedure

The real power delivered at bus 2, P_2, is related to the system voltages V_1, V_2 and the

line resistance R as follows:

$$P_2 = V_2 I_2 = V_2 \frac{(V_1 - V_2)}{R}$$

$$V_2 = V_1 - \frac{RP}{V_2} (or)$$

$$V_2{}^2 - V_2 V_1 + RP = 0$$

(3.43)

For the system parameters in Figure 3.4, the expression is $V_2{}^2 - V_2 + 0.09 = 0$. The

solution for this quadratic can be explicitly calculated as V_2=0.9, 0.1 which are the HV

and LV solutions respectively. Now consider solving the simple quadratic using the

holomorphic embedding procedure. The receiving end voltage V_2 is expressed as a

function of a complex parameter s. One possible embedding to calculate the HV

solution is:

$$V_2(s) = 1 - \frac{s0.09}{V_2(s)}$$

$$where, V_2(s) = V_2[0] + V_2[1]s + V_2[2]s^2 + \ldots$$

(3.44)

From the embedding it can be observed that the solution at s=0, $V_2(0)$ =1, is indeed

an operating solution under no-load conditions. This solution at s=0 is known as the

germ solution or, in short, germ; the HV solution is an analytic continuation of the germ

solution.

In calculating the voltage power-series coefficients from (3.44) a new series $W_2(s)$

is defined as the reciprocal of the voltage series.

$$W_2(s) = \frac{1}{V_2(s)} = \left(W_2[0] + W_2[1]s + W_2[2]s^2 + \ldots \right)$$

(3.45)

The coefficients of the reciprocal series can be calculated using the relation that the product of the two power series should yield 1.0. Thus, for the constant term, $W_2[0] = \dfrac{1}{V_2[0]}$. It can be shown that, for a general value of n expanding (3.45) and equating the coefficients of s^n on LHS to zero yields:

$$W_2[n] = -\frac{\displaystyle\sum_{k=0}^{n-1} W_2[k]V_2[n-k]}{V_2[0]}, n \geq 1 \qquad (3.46)$$

From (3.44), substituting for $1/V_2(s)$ with the reciprocal power series $W_2(s)$ yields:

$$\begin{aligned}
&V_2[0] + V_2[1]s + V_2[2]s^2 + \ldots \\
&= 1 - s0.09\big(W_2[0] + W_2[1]s + W_2[2]s^2 + \ldots\big)
\end{aligned} \qquad (3.47)$$

Equating the coefficients of s on both sides of (3.47) the power series coefficients $V_2[n]$ can be calculated as:

$$\begin{aligned}
V_2[0] &= 1 \\
V_2[n] &= -0.09 W_2[n-1], \forall n \geq 1
\end{aligned} \qquad (3.48)$$

The power series evaluated using (3.46) and (3.48) is a convergent series whose coefficients decrease monotonically.

$$V_2(s) = 1 - .09s - 0.0081s^2 - 0.0015s^3 + \ldots \qquad (3.49)$$

When evaluating a diagonal [M/M] Padé, coefficients up to s^{2M} are required in the series. As the degree of the Padé approximant needed in evaluating the series (3.49) increases, the condition number of the matrix that arises from (3.24) for this particular problem becomes larger. Recall that in solving the $Ax=b$ problem, if the condition number $\kappa(A)=10^k$, up to k digits of precision could be lost [50]. While evaluating a

lower degree approximant may appear to be a potential solution to the problem, it may lead to large truncation error in the solution.

Table 3.5 shows that for this particular convergent series, the condition number of the Padé matrix increases up to the order of 10^{19} as the degree of the Padé approximant increases. Thus, choosing an appropriate degree of the Padé approximant can involve a tradeoff between the desired numerical stability properties as indicated by the condition number and the allowable error tolerance in the solution. Also, the computational complexity that is involved in obtaining a higher degree approximant should be taken into consideration for practical applications.

Table 3.5 Condition Number of the Padé matrix used in Calculating the Padé Approximant

Degree of Padé approximant	Condition number of Padé matrix
[2/2]	$1.2548e+02$
[4/4]	$2.2891e+06$
[6/6]	$4.9530e+10$
[8/8]	$1.1808e+15$
[10/10]	$2.9682e+19$

To summarize, this chapter discusses the relevance of analytic continuation in solving the PF problem, illustrates different methods of evaluating the analytic continuation with numerical examples and highlights the numerical issues that should be taken into consideration.

4 SOLVING A GENERAL CASE POWER-FLOW PROBLEM WITH

HOLOMORPHIC EMBEDDING

4.1 INTRODUCTION TO HOLOMORPHIC EMBEDDING

Holomorphic functions form a branch of study in complex analysis. A brief introduction about holomorphic functions followed by the development of load bus model available in existing literature is presented in this section 4.1.

4.1.1 HOLOMORPHIC FUNCTIONS

Functions of complex variables that are complex differentiable everywhere in a neighborhood around a point are said to be holomorphic about that point. Holomorphic functions can be uniquely expressed using a convergent Taylor series in the neighborhood of the point. The term 'analytic' is often used interchangeably with 'holomorphic'. Analytic refers to a broader class of functions (real, complex or more generic) that satisfy certain conditions whereas holomorphic refers to only complex valued functions.

In real analysis, differentiability in a neighborhood does not guarantee analyticity; however, in complex functions, differentiability in a neighborhood guarantees analyticity. Analytic functions can be entire or non-entire. Functions whose Taylor series expansion coincides with the actual function in the whole of the complex plane are termed as entire. Examples of entire functions include trigonometric functions such as sine, cosine and exponential function (e^x). Entire functions have infinite radii of

convergence. For non-entire functions, the function can be expressed with a convergent Taylor series only within an open disc of finite radius, centered about the point at which the derivatives are calculated [38]. Analytic continuation techniques are employed to extend the domain of convergence of such non-entire functions.

Holomorphic embedding (HE) as it is to be used here is the technique of embedding the non-analytic PBE's within a large problem with complex variables ensuring that the resultant problem is holomorphic. For the PBE's, the non-analyticity (non-holomorphicity) is due to the complex conjugate operator. The solution procedure for the load bus model using a particular embedding is shown in [21].

4.1.2 LOAD BUS MODELING USING HE

Consider the PBE of a load bus whose complex power injection S_i is known. If m were the set of PQ buses, the Power Balance Equation (PBE) for bus i, could be expressed as,

$$\sum_{k=1}^{N} Y_{ik} V_k = \frac{S_i^*}{V_i^*} , i \in m \tag{4.1}$$

where Y_{ik} is the (i, k) element of the bus admittance matrix, S_i and V_i are the complex power injection and voltage at bus i, respectively. The shunt elements in (4.1) are moved to the RHS and the equation is embedded with a complex parameter s as follows [21]:

$$\sum_{k=1}^{N} Y_{ik\,trans} V_k(s) = \frac{s S_i^*}{V_i^*(s^*)} - s Y_{i\,shunt} V_i(s) , i \in m \tag{4.2}$$

At *s*=1, the original PBE's (4.1) are recovered from the embedded system of equations, thereby retrieving the HV solution. In (4.2) $Y_{ik\ trans}$ corresponds to the "series branch" part of the admittance matrix. Consequently, the entries of each row of the $Y_{ik\ trans}$ matrix add up to zero; an exception is the row associated with nodes adjacent to the slack bus. (Note that the embedded PBE for the slack bus is to be introduced later and not included in (4.2).) The shunt admittance matrix, $Y_{i\ shunt}$ entries model the shunt admittance components of the transmission line, off-nominal transformer tap model, shunt capacitors/ reactors in the network.

With the parameter *s* as a variable, the notation $V(s)$ is used to emphasize that the voltage has become a holomorphic function of the complex parameter *s*. The complex conjugate of the voltage, V^* that appears in the PBE is replaced by, $V^*(s^*)$ and not $V^*(s)$. The presence of s^* rather than *s* in this term retains the property of holomorphism and therefore analyticity. (More about this below.)

4.1.3 GERM SOLUTION FOR LOAD BUS MODEL

For solving the PF problem, a slack bus whose voltage magnitude and angle are known is required. The defining equation for a slack bus is $V_i=V_i^{sp}\angle 0^{\rm o}$ (*i*∈ *slack*) where V_i^{sp} is the specified voltage magnitude at bus *i*. The complex power injection at the slack bus is a free variable.

In (4.2), since the shunt elements are moved to the RHS and multiplied by *s* and the complex power injections are also multiplied by *s*, the solution of (4.2) at *s*=0

corresponds to a network with no loads and no shunt element; hence all voltages are identical to the slack bus voltage at $s=0$. It will be shown that it is convenient to use the following model for the slack bus so that at $s=0$ the slack bus voltage is 1.0.

$$V_i(s) = 1 + (V_i^{sp} - 1)s, i \in slack \tag{4.3}$$

In summary, for a system with only PQ buses, at $s=0$, all the shunt terms ($Y_{i\,shunt}$) and power injection (S_i) in the PF equation (4.2) vanishes. This represents the reference case where there is no generation and no load. In this case, (4.2) and (4.3) reduce to

$$\sum_{k=1}^{N} Y_{ik\,trans}V_k(0) = 0 \, , \, i \in m \tag{4.4}$$

$$V_i(0) = 1, i \in slack$$

Equation (4.4) is a linear system of equations that could be solved to obtain the germ solution. Since the entries of each row of the $Y_{ik\,trans}$ matrix sum up to zero and the slack bus voltage is 1.0, equation (4.4) holds good when all the bus voltages are equal to $1\angle 0^o$, which is called the germ solution. This is analogous to the flat start for voltages in NR method.

In equation (4.4), if the slack bus equation were not included, the resulting $Y_{ik\,trans}$ matrix would be singular, leading to no possible solution for the germ. However, in order to account for the slack bus, the entire row i, ($\forall \, i$=slack bus) in the $Y_{ik\,trans}$ matrix is zeroed, except the coefficient corresponding to V_{slack}. Hence the $Y_{ik\,trans}$ matrix is non-singular, resulting in a unique solution for the germ.

53

Since the voltage function as defined above is holomorphic (analytic), one possible methodology of solving the problem (and the one used here) is to express voltage as a power series, evaluate the coefficients of the power series and then generate an analytic continuation of the series.

4.1.4 POWER SERIES EXPANSION

Embedding the PF equations such that the resulting equation is holomorphic allows the voltage function to be represented by an equivalent power series. The voltage function $V(s)$ in (4.2) can be expressed as a Maclaurin series with s as the expansion parameter.

$$V(s) = \sum_{n=0}^{\infty} V[n](s)^n \tag{4.5}$$

where the coefficients $V[n]$ are complex numbers.

What follows is a proof of holomorphicity of the chosen embedding in (4.2) when $V(s)$ is expressed as a Maclaurin's series. In particular, this justifies the usage of $V^*(s^*)$ as opposed to $V^*(s)$ in the embedding.

In order to be holomorphic, a function must satisfy the Cauchy-Riemann equations. An equivalent condition known as Wirtinger's derivative requires that $\partial V/\partial s^* = 0$ [40]. i.e. The function $V(s)$ should be independent of s^* in order to be holomorphic. The Maclaurin series expansion of the $V^*(s)$ (if it were to exist) and $V^*(s^*)$, truncated at n terms are shown below:

54

$$V^*(s) = V^*[0] + V^*[1]s^* + \ldots + V^*[n]\left(s^*\right)^n$$
$$V^*(s^*) = V^*[0] + V^*[1]s + \ldots + V^*[n]s^n \qquad (4.6)$$

In (4.6), the function $V^*(s)$ upon expansion has s^* terms on the RHS and Wirtinger's condition will not be satisfied. However, the expansion of $V^*(s^*)$ independent of s^* such that $\partial V^*(s^*)/\partial s^* = 0$. Thus the embedding (4.2) is holomorphic only when the denominator in the RHS of (4.2) is chosen to be $V^*(s^*)$.

Assuming that we can represent the bus voltages as a Maclaurin series function of s, that is $V_i(s)$ and $V_i^*(s^*)$, we can substitute the series, (4.5) and (4.6), into (4.2) to yield:

$$\sum_{k=1}^{N} Y_{ik\,trans}\left(V_k[0] + V_k[1]s + V_k[2]s^2 + \ldots\right)$$
$$= \frac{sS_i^*}{\left(V_i^*[0] + V_i^*[1]s + V_i^*[2]s^2 + \ldots\right)} - sY_{i\,shunt}\left(V_i[0] + V_i[1]s + V_i[2]s^2 + \ldots\right) \qquad (4.7)$$

Our problem now is reduced to finding the series coefficients that satisfy (4.7). As the first task it is recognized that in (4.7), the inverse of the voltage power series has to be calculated. For every voltage function $V(s)$, let $W(s)$ be the new inverse power series defined as $W(s) = W[0] + W[1]s + W[2]s^2 + \ldots$. Since $W(s)$ is the inverse of the $V(s)$,

$$W(s) = \frac{1}{V(s)} = W[0] + W[1]s + W[2]s^2 + \ldots \qquad (4.8)$$

In order to calculate the coefficients of the inverse power series, (4.8) is multiplied by $V(s)$ on both sides.

$$W(s) \times V(s) = 1$$
$$\left(W[0] + W[1]s + W[2]s^2 + \ldots\right)\left(V[0] + V[1]s + V[2]s^2 + \ldots\right) = 1 \qquad (4.9)$$

By equating the coefficients of powers of s on both sides of the equation,

$$W[0]V[0] = 1 \qquad\qquad \Rightarrow W[0] = \frac{1}{V[0]}$$

$$W[0]V[1] + W[1]V[0] = 0 \qquad \Rightarrow W[1] = -\frac{W[0]V[1]}{V[0]} \qquad (4.10)$$

$$W[0]V[2] + W[1]V[1] + W[2]V[0] = 0 \quad \Rightarrow W[2] = -\frac{W[0]V[2] + W[1]V[1]}{V[0]}$$

$$\vdots$$

In general, it can be written as:

$$W[0] = \frac{1}{V[0]}$$

$$W[n] = -\frac{\sum_{k=0}^{n-1} W[k]V[n-k]}{V[0]}, n \geq 1 \qquad (4.11)$$

It is to be remembered that in solving (4.7), for every series $V_i(s)$, the inverse series $W_i(s)$ has to be calculated. Substituting equation (4.8) in (4.7):

$$\sum_{k=1}^{N} Y_{ik\,trans}\left(V_k[0] + V_k[1]s + V_k[2]s^2 + \ldots\right)$$
$$= sS_i^*(W_i^*[0] + W_i^*[1]s + W_i^*[2]s^2 + \ldots) \qquad (4.12)$$
$$- sY_{i\,shunt}\left(V_i[0] + V_i[1]s + V_i[2]s^2 + \ldots\right)$$

Equating the coefficients of s, s^2, s^3 … on both sides of (4.12) a recurrence relation can be developed to solve for the power series coefficients. The general expression for calculating the power series coefficients $V_i[n]$ for $n>0$ can be obtained as:

$$\sum_{k=1}^{N} Y_{ik\,trans}V_k[n] = S_i^* W_i^*[n-1] - Y_{i\,shunt}V_i[n-1] \qquad (4.13)$$

Equation (4.13) can be used to evaluate the coefficients of the voltage series for load bus. In order to define a similar equation for slack bus, a special notation δ_{ni} has to be introduced.

$$\delta_{ni} = \begin{cases} 1, if\ n=i \\ 0, otherwise \end{cases} \qquad (4.14)$$

The term δ_{ni} is associated with parameters that occur only for the powers of s raised to i and vanish for the remaining powers of s. Thus, from the slack bus equation defined in (4.3), an expression for the power series coefficients can be written as:

$$V_i[n] = \delta_{n0} + \delta_{n1}(V_i^{sp} - 1), i \in slack \qquad (4.15)$$

Remember that the solution for $n=0$ is the germ solution, where all bus voltages are $1\angle 0^o$. By knowing the V and W series up to $(n-1)$ coefficients, the nth coefficient of the voltage power series can be calculated from (4.13) and (4.15) by solving a linear matrix equation. The coefficients of inverse series W_i up to n coefficients can be obtained from the voltage series up to n coefficients from (4.11). Thus by evaluating the appropriate germ solution at $s=0$, the entire voltage power series up to the desired number of terms can be constructed from (4.13). The power series obtained thus, evaluated at $s=1$, will give the required voltage solution. If the radius of convergence of the any of the voltage series is less than 1.0, the power series will not converge by itself to the desired solution. The radius of convergence is generally unknown; hence, the property of analytic continuation is employed to represent the powers series within and beyond its radius of convergence and evaluate the voltage solution.

4.2   GENERATOR BUS MODEL I USING HOLOMORPHIC EMBEDDING

Current literature does not contain a holomorphically embedded equation for modeling the generator bus. In PF studies, generator / PV / voltage bus refers to a bus

in which the voltage is to be held at a constant value. The reactive power capability of

the generator is a limiting factor in maintaining a constant bus voltage magnitude.

Therefore, for a generator bus, the voltage magnitude and real power output are

known quantities while voltage angle and reactive power are unknown.

The traditional defining equations for a PV bus i, are:

$$P_i = \text{Re}(V_i \sum_{k=1}^{N} Y_{ik}{}^* V_k{}^*), \forall i \in p \qquad (4.16)$$

$$|V_i| = V_i^{sp}, \forall i \in p \qquad (4.17)$$

where P_i denotes the real power injection and V_i^{sp} the voltage magnitude at bus i.

The reactive power being a variable is a significant difference between the

generator bus and the load bus models. Two different approaches for handling the

reactive power term in the PBE's are studied. In the first approach, the reactive power

term is made a free variable, represented as a function of the complex s parameter. A

second approach is to eliminate the reactive power term by summing the complex

power and it's conjugate. Both approaches are developed in detail and used in solving

the general case PF problem. Described in this section is the first PV bus model.

Generator bus model I involves modeling the unknown reactive power injection as

a holomorphic function in the s parameter [52]. The voltage magnitude constraint of

the generator bus is also embedded, with the bus voltage defined as a holomorphic

function. This section presents the PV bus formulation for a N-bus system and

demonstrates the calculation of the power series coefficients. The numerical

implementation of the formulation requires breaking the equation into real and imaginary parts.

For the N-bus system, let p denote the set of PV buses. The complex PBE's for a generator bus $i \epsilon p$, with the reactive power, Q, represented as a holomorphic function is:

$$\sum_{k=1}^{N} Y_{ik\,trans} V_k(s) = \frac{sP_i - jQ_i(s)}{V_i^*(s^*)} - Y_{i\,shunt} V_i(s) \, , \, i \in p \qquad (4.18)$$

In (4.18), an additional free variable $Q_i(s)$ is introduced. It is important to note that unlike the voltage power series that can have complex coefficients, the reactive power series has only real coefficients.

Inclusion of a free variable in the generator bus model requires an additional constraint. For the generator bus, we have the voltage magnitude constraint (4.17). Equation (4.17) can be embedded in the complex parameter s as shown below:

$$V_i(s) * V_i^*(s^*) = 1 + s\left(\left|V_i^{sp}\right|^2 - 1\right), i \in p \qquad (4.19)$$

Evaluating (4.19) at $s=1$, the voltage magnitude constraint of the generator bus can be retrieved. Equations (4.18) and (4.19) represent the HE formulation for the generator bus model.

For a problem with N buses, the HE system of equations that describe the different bus types are shown in equations (4.2), (4.3), (4.18) and (4.19). The original PBE's and their counterpart holomorphically embedded equations for each type of bus are summarized from the above listed equations in Table 4.1.

Table 4.1 Non Holomorphic PBE's and the Corresponding HE Formulation

Bus type of bus i	Original Power Balance Equation	Holomorphically Embedded Equation
Slack	$V_{slack} = V_i^{sp}$	$V_{slack}(s) = 1 + (V_i^{sp} - 1)s$
Load bus	$\sum_{k=1}^{N} Y_{ik} V_k = \dfrac{S_i^*}{V_i^*}$	$\sum_{k=1}^{N} Y_{ik\,trans} V_k(s) = \dfrac{sS_i^*}{V_i^*(s^*)} - sY_{i\,shunt} V_i(s)$
Generator bus	$P_i = \mathrm{Re}(V_i \sum_{k=1}^{N} Y_{ik}^* V_k^*)$	$\sum_{k=1}^{N} Y_{ik\,trans} V_k(s) = \dfrac{sP_i - jQ_i(s)}{V_i^*(s^*)} - sY_{i\,shunt} V_i(s)$
	$|V_i| = V_i^{sp}$	$V_i(s) * V_i^*(s^*) = 1 + \left(\left| V_i^{sp} \right|^2 - 1 \right)s$

Solving the embedded equations representing the generator bus, along with the HE formulation of the load bus and slack bus (refer Table 4.1) at $s=0$ gives the germ solution. The process for evaluating the germ solution for the generator bus model I is shown in section 4.2.1. To calculate the coefficients of the voltage and reactive power series from generator bus model I, a recurrence relation has to be established similar to the load bus model. The calculation procedure is more involved and is explained in detail as follows.

Expressing voltage and reactive power as a full power series in (4.18) for a PV bus $i\epsilon p$:

$$
\begin{aligned}
&\sum_{k=1}^{N} Y_{ik\,trans}\left(V_k[0] + V_k[1]s + V_k[2]s^2 + \ldots \right) \\
&= \frac{sP_i - j\left(Q_i[0] + Q_i[1]s + Q_i[2]s^2 + \ldots \right)}{\left(V_i^*[0] + V_i^*[1]s + V_i^*[2]s^2 + \ldots \right)} - Y_{i\,shunt}\left(V_i[0] + V_i[1]s + \ldots \right)
\end{aligned}
\tag{4.20}
$$

An inverse function $W_i(s)$ is defined to be reciprocal of the voltage power series for bus i. The definition of the inverse series, calculation of its coefficients is identical to the load bus model described by the equations (4.8) - (4.11). Thus (4.20) becomes

$$
\begin{aligned}
&\sum_{k=1}^{N} Y_{ik\,trans}\left(V_k[0] + V_k[1]s + V_k[2]s^2 + \ldots\right) \\
&= \left(sP_i - j\left(Q_i[0] + Q_i[1]s + Q_i[2]s^2 + \ldots\right)\right)\left(W_i^*[0] + W_i^*[1]s + W_i^*[2]s^2 + \ldots\right) \\
&\quad - Y_{i\,shunt}\left(V_i[0] + V_i[1]s + \ldots\right)
\end{aligned}
\tag{4.21}
$$

Equating the coefficients of s, s^2 and so on up to s^n,

$$
\sum_{k=1}^{N} Y_{ik} V_k[1] = P_i W_i^*[0] - j\left(Q_i[0]W_i^*[1] + Q_i[1]W_i^*[0]\right) - Y_{i\,shunt} V_i[0]
$$

$$
\sum_{k=1}^{N} Y_{ik} V_k[2] = P_i W_i^*[1] - j\left(Q_i[0]W_i^*[2] + Q_i[1]W_i^*[1] + Q_i[2]W_i^*[0]\right) - Y_{i\,shunt} V_i[1] \tag{4.22}
$$

$$
\vdots
$$

$$
\sum_{k=1}^{N} Y_{ik} V_k[n] = P_i W_i^*[n-1] - j\left(\sum_{k=0}^{n} Q_i[k]W_i^*[n-k]\right) - Y_{i\,shunt} V_i[n-1]
$$

In (4.22), the calculation of the voltage series coefficients $V_i[n]$ involves the sum of product of two power series coefficients Q_i, W_i (the $\sum_{k=0}^{n} Q_i[k]W_i^*[n-k]$ term) which can be expanded as:

$$
\begin{aligned}
&\sum_{k=0}^{n} Q_i[k]W_i^*[n-k] \\
&= Q_i[0]W_i^*[n] + Q_i[1]W_i^*[n-1] + Q_i[2]W_i^*[n-2] + \ldots Q_i[n]W_i^*[0]
\end{aligned}
\tag{4.23}
$$

Observe from (4.22) and (4.23) that in calculating of the nth order coefficient of the voltage power series (i.e. $V_i[n]$), both the nth order coefficients of the W series and the Q series ($W_i[n]$, $Q_i[n]$) are required. Recall, the calculation of $W_i[n]$ requires the $V_i[n]$ term from (4.11) whereas calculating $V_i[n]$ was the objective to begin with. This scenario is

unlike the load bus model where the nth coefficient of the power series could be expressed in terms of coefficients up to the degree n-1.

From (4.23), a linear recurrence relationship to calculate the power series coefficients has to be developed. A two-part solution is devised to achieve this.

    i.   The germ solution of the voltage and reactive power series is determined and used to simplify (4.22).

    ii.   The voltage power series is broken down into real and imaginary coefficients when enforcing the voltage magnitude constraint and real power constraint of the generator bus model.

The implementation details of the above-suggestions in determining the germ solution and power series coefficients of the generator bus model are shown in the following sections.

4.2.1   GERM SOLUTION FOR THE GENERATOR BUS MODEL I

To obtain the germ solution of the PV bus model in a general PF problem, the HE equations corresponding to load bus (equation (4.2)), generator bus (equations (4.18) and (4.19)) and slack bus (equation (4.3)) have to be solved simultaneously at s=0. At s=0, the system of equations listed above becomes:

$$\sum_{k=1}^{N} Y_{ik\,trans} V_k(0) = 0 \; , \; i \in m$$

$$\sum_{k=1}^{N} Y_{ik\,trans} V_k(0) = \frac{-jQ_i(0)}{V_i^*(0)} \; , \; i \in p \tag{4.24}$$

$$V_i(0) * V_i^*(0) = 1, i \in p$$

$$V_i(0) = 1, i \in slack$$

In (4.24), the slack bus voltage is known to be 1.0. If the germ solution for the remaining bus voltages were chosen to be 1.0, the load bus equation in (4.24) would be satisfied (refer discussion in Section 4.1.3); the generator voltage magnitude constraint in (4.24) will also be met, since the product $V_i(0)\ V_i^*(0)$ would equal 1.0. The embedded generator power balance constraint (4.24), however, has a variable $Q_i(0)$ on the RHS of (4.24). Substituting the assumed germ voltage solution of 1.0 for all buses in (4.24), the embedded generator bus PBE becomes:

$$\sum_{k=1}^{N} Y_{ik\,trans}\, V_k(s) = \frac{-jQ_i(0)}{V_i^*(0)}, i \in p$$
$$\Rightarrow 0 = \frac{-jQ_i(0)}{1}, i \in p$$
$$Q_i(0) = 0, i \in p$$

(4.25)

If the reactive power germ, $Q_i(0)$ ($\forall\ i\epsilon p$) were chosen to be 0.0 (from (4.25)) and all bus voltages were equal to 1.0, the embedded system of equations for all bus types at $s=0$; (equation (4.24)) are satisfied. Hence, $V_i(0)=1$, $Q_i(0)=0$ is chosen to be the germ solution to the embedded system of equations presented in (4.2), (4.3), (4.18) and (4.19). It is also the physical solution for the no-load, no-generation case for a general PF problem when there are no shunts and the generator bus voltages are maintained at 1.0. The calculated germ solution, $V_i(0)$ and $Q_i(0)$ also represent the constant term (coefficient of s^0 term) in the power series, $V_i[0]$ and $Q_i[0]$, respectively, for generator bus model I.

4.2.2 EVALUATING POWER SERIES COEFFICIENTS FOR GENERATOR BUS MODEL I

With the particular choice of embedding for the generator bus model as shown in (4.18) and (4.19), the calculation of the germ solution was demonstrated in Section 4.2.1. This subsection shows the procedure of calculating the remaining power series coefficients.

Rewriting (4.22) derived from the power balance constraint of the generator bus model, with the new evaluated germ $Q_i[0]=0$, $W_i[0]=1/V_i[0]=1$ yields.

$$
\begin{aligned}
&\sum_{k=1}^{N} Y_{ik\,trans} V_k[n] \\
&= P_i W_i^*[n-1] - j\left(\sum_{k=1}^{n-1} Q_i[k]W_i^*[n-k] + Q_i[n]\right) - Y_{ishunt}V_i[n-1]
\end{aligned}
\tag{4.26}
$$

A new quantity $Rhs\_Known[n\text{-}1]$ is introduced to make the equation succinct in the subsequent steps. $Rhs\_Known[n\text{-}1]$ denotes the quantities in the RHS of (4.26) with coefficients up to degree n-1.

$$
\begin{aligned}
&Rhs\_Known[n-1] \\
&= P_i W_i^*[n-1] - j\left(\sum_{k=1}^{n-1} Q_i[k]W_i^*[n-k]\right) - Y_{ishunt}V_i[n-1]
\end{aligned}
\tag{4.27}
$$

Substituting(4.27), equation (4.26)becomes,

$$
\sum_{k=1}^{N} Y_{ik\,trans} V_k[n] = Rhs\_Known\,[n-1] - jQ_i[n]
\tag{4.28}
$$

Equation (4.28), which was derived from the embedded PBE of the generator bus, (4.18), defines a recurrence relation that is used in calculating the voltage series coefficients and reactive power series coefficients. A similar equation needs to be

derived from the voltage magnitude constraint of the generator bus, (4.19). Expressing

the voltage function $V_i(s)$ as power series in equation (4.19) yields:

$$\left(V_i[0]+V_i[1]s+V_i[2]s^2+...\right)*\left(V_i^*[0]+V_i^*[1]s+V_i^*[2]s^2+...\right)$$
$$=1+\left(\left|V_i^{sp}\right|^2-1\right)s \tag{4.29}$$

Equating the coefficients of powers of s on both sides yields,

$$V_i[0]V_i^*[0]=1$$
$$\Rightarrow V_i[0]=1 \quad (germ\ solution)$$

$$V_i[0]V_i^*[1]+V_i[1]V_i^*[0]=\left|V_i^{sp}\right|^2-1$$
$$\Rightarrow V_i^*[1]+V_i[1]=2V_{i\,re}[1]=\left|V_i^{sp}\right|^2-1 \tag{4.30}$$

$$V_i[0]V_i^*[2]+V_i[1]V_i^*[1]+V_i[2]V_i^*[0]=0$$
$$\Rightarrow V_i^*[2]+V_i[2]=2V_{i\,re}[2]=-V_i[1]V_i^*[1]$$

$$V_i[0]V_i^*[3]+V_i[1]V_i^*[2]+V_i[2]V_i^*[1]+V_i[3]V_i^*[0]=0$$
$$\Rightarrow V_i^*[3]+V_i[3]=2V_{i\,re}[3]=-\left(V_i[1]V_i^*[2]+V_i[2]V_i^*[1]\right)$$
$$\vdots$$

In (4.30) $V_{i\,re}[n]$ represents the real part of the voltage power series nth coefficient

from the voltage magnitude constraint. The notation δ_{ni} as defined in (4.14) is used to

write a generalized expression to evaluate $V_{i\,re}[n]$. The calculation of $V_{i\,re}[n]$ for an

arbitrary value of n, can be written from (4.30) as,

$$V_{i\,re}[n]=\delta_{n0}+\delta_{n1}\frac{V_i^{sp\,2}-1}{2}-\frac{1}{2}\left(\sum_{k=1}^{n-1}V_i[k]V_i^*[n-k]\right) \tag{4.31}$$

Equations (4.26) and (4.31) represent a consistent system of equations

representing the generator bus model that has a unique solution. However, the

solution of the equations is not trivial in their current form since there are unknowns

on both sides of (4.26). The objective is to rearrange the equations so that the power

series coefficients can be obtained by solving a single linear matrix equation. It is achieved by breaking the complex voltage power series coefficients into real and imaginary parts. While this is necessary for solving the generator bus power series coefficients, it becomes inevitable in the implementation that the load bus power series coefficients are also broken down into real and imaginary components since the system of equations are mutually coupled. Let the entries of the admittance matrix (without shunt elements) be expressed as $Y_{ik\,trans} = G_{ik} + jB_{ik}$. The voltage series coefficients are broken into real and imaginary parts $V_i[n] = V_{i\,re}[n] + jV_{i\,im}[n]$. Thus, the LHS of (4.26) is alternatively expressed for every bus i as follows:

$$
\sum_{k=1}^{N} Y_{ik\,trans} V_k[n] = \sum_{k=1}^{N} \left(G_{ik} + jB_{ik} \right)\left(V_{k\,re}[n] + jV_{k\,im}[n] \right)
$$
$$
= \sum_{k=1}^{N} \left(G_{ik} V_{k\,re}[n] - B_{ik} V_{k\,im}[n] \right) + j\left(B_{ik} V_{k\,re}[n] + G_{ik} V_{k\,im}[n] \right) \quad (4.32)
$$

The holomorphically embedded PV bus equation (4.26) for bus i as broken into real and imaginary components is represented as a matrix equation below. The quantities that can be evaluated on the RHS (involves coefficients up to s^{n-1}) are represented using the term *Rhs_Known* defined in (4.27).

$$
\begin{bmatrix}
G_{i1} & -B_{i1} & \cdots & G_{ii} & -B_{ii} & \cdots & G_{iN} & -B_{iN} \\
B_{i1} & G_{i1} & \cdots & B_{ii} & G_{ii} & \cdots & B_{iN} & G_{iN}
\end{bmatrix}
\begin{bmatrix}
V_{1\,re}[n] \\
V_{1\,im}[n] \\
\vdots \\
V_{i\,re}[n] \\
V_{i\,im}[n] \\
\vdots \\
V_{N\,re}[n] \\
V_{N\,im}[n]
\end{bmatrix}
\tag{4.33}
$$

$$
=
\begin{bmatrix}
\text{Re}(Rhs\_Known[n-1]) \\
\text{Im}(Rhs\_Known[n-1]) - Q_i[n]
\end{bmatrix}
$$

In calculating the nth degree voltage power series coefficients, the quantity $V_{i\,re}[n]$ can be calculated for all voltage buses $i \epsilon p$, from the voltage magnitude constraint (4.31). However, $Q_i[n]$ shown in the RHS of (4.33) is still unknown. This is similar to solving the $Ax=b$ problem with a few of the x's known beforehand but the same number of b's as unknowns. Such problems can be solved by bringing all the unknowns to the LHS and known quantities to the RHS.

To do this, the product of the known $V_{i\,re}[n]$ coefficient and corresponding column vector of the LHS matrix is moved to the RHS. For a PV bus, i, the matrix equation (4.33) thus becomes:

$$
\begin{bmatrix}
G_{i1} & -B_{i1} & \cdots & 0 & -B_{ii} & \cdots & G_{iN} & -B_{iN} \\
B_{i1} & G_{i1} & \cdots & 1 & G_{ii} & \cdots & B_{iN} & G_{iN}
\end{bmatrix}
\begin{bmatrix}
V_{1\,re}[n] \\
V_{1\,im}[n] \\
\vdots \\
Q_i[n] \\
V_{i\,im}[n] \\
\vdots \\
V_{N\,re}[n] \\
V_{N\,im}[n]
\end{bmatrix}
\tag{4.34}
$$

$$
=
\begin{bmatrix}
\text{Re}(Rhs\_Known[n-1]) \\
\text{Im}(Rhs\_Known[n-1])
\end{bmatrix}
-
\begin{bmatrix}
G_{ii} \\
B_{ii}
\end{bmatrix}
V_{i\,re}[n]
$$

Equation (4.34) represents the recurrence relation for one generator bus i. When the PBE's for a N bus system are listed, the coefficients of the LHS matrix and RHS vector for the remaining buses have to be altered, to account for moving unknown variables to LHS and known variables to RHS. To demonstrate this, a sample three-bus system with a PV bus is chosen; the recurrence relation with unknowns on both sides of the equation is shown first. Subsequently, the alteration in the matrix and RHS vector entries is shown. The concept can be generalized for a N-bus system.

Figure 4.1 shows a sample three-bus problem where bus 1 is the slack bus; bus 2 is the generator bus and bus 3 is the load bus.
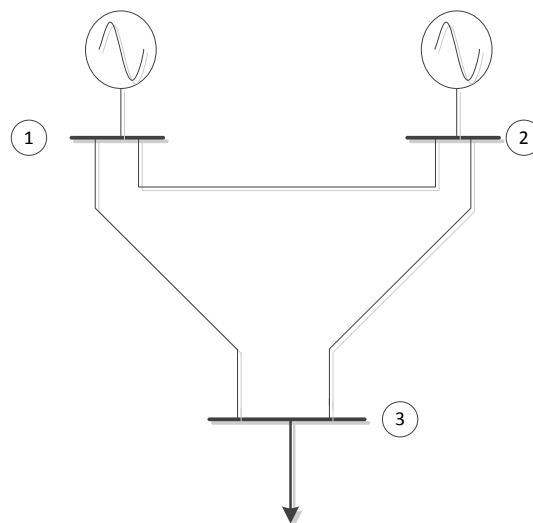
Figure 4.1 Sample Three-bus Test System

In order to write the recurrence relation, as a matrix equation, (4.13), (4.15), (4.31) and (4.33) are to be referred to and combined appropriately. The definition for each entry in the matrix equation is available in the nomenclature. The matrix equation for

different bus types combined is shown in (4.35); for PV bus 2, unknowns $V_{i\,im}[n]$ and $Q_i[n]$ exist on both sides of the equation.

$$\begin{bmatrix} 1 & & & & & \\ & 1 & & & & \\ G_{21} & -B_{21} & G_{22} & -B_{22} & G_{23} & -B_{23} \\ B_{21} & G_{21} & B_{22} & G_{22} & B_{23} & G_{23} \\ G_{31} & -B_{31} & G_{32} & -B_{32} & G_{33} & -B_{33} \\ B_{31} & G_{31} & B_{32} & G_{32} & B_{33} & G_{33} \end{bmatrix} \begin{bmatrix} V_{1\,re}[n] \\ V_{1\,im}[n] \\ V_{2\,re}[n] \\ V_{2\,im}[n] \\ V_{3\,re}[n] \\ V_{3\,im}[n] \end{bmatrix} = \begin{bmatrix} \delta_{n0} + \delta_{n1}(V_{Slack}-1) \\ 0 \\ \mathrm{Re}(Rhs\_Known\ [n-1]) \\ (\mathrm{Im}(Rhs\_Known\ [n-1]))-Q_2[n] \\ \mathrm{Re}(S_3^*W_3^*[n-1]-Y_{3\,shunt}V_3[n-1]) \\ \mathrm{Im}(S_3^*W_3^*[n-1]-Y_{3\,shunt}V_3[n-1]) \end{bmatrix} \quad (4.35)$$

$$V_{2\,re}[n] = \delta_{n0} + \delta_{n1}\frac{V_2^{sp2}-1}{2} - \frac{1}{2}\sum_{k=1}^{n-1} V_2[k]V_2^*[n-k]$$

In (4.35), the value of $V_{2\,re}[n]$ can be calculated from the voltage magnitude constraint. The vector resulting from the product of column 3 (the column corresponding to entry $V_{2\,re}[n]$) and the known value of $V_{2\,re}[n]$ is moved to the RHS. The unknown $Q_2[n]$ is moved to the LHS unknown vector, in place of $V_{2\,re}[n]$; the LHS matrix entries are altered by zeroing the coefficients corresponding to $Q_2[n]$ in all equations, except equation 4 (equation (4.34)). The equations from (4.35) are altered as:

$$\begin{bmatrix} 1 & & & & & \\ & 1 & & & & \\ G_{21} & -B_{21} & 0 & -B_{22} & G_{23} & -B_{23} \\ B_{21} & G_{21} & 1 & G_{22} & B_{23} & G_{23} \\ G_{31} & -B_{31} & 0 & -B_{32} & G_{33} & -B_{33} \\ B_{31} & G_{31} & 0 & G_{32} & B_{33} & G_{33} \end{bmatrix} \begin{bmatrix} V_{1\,re}[n] \\ V_{1\,im}[n] \\ Q_2[n] \\ V_{2\,im}[n] \\ V_{3\,re}[n] \\ V_{3\,im}[n] \end{bmatrix} = \begin{bmatrix} \delta_{n0} + \delta_{n1}(V_{Slack}-1) \\ 0 \\ \mathrm{Re}(Rhs\_Known\ [n-1]) \\ \mathrm{Im}(Rhs\_Known\ [n-1]) \\ \mathrm{Re}(S_3^*W_3^*[n-1]-Y_{3\,shunt}V_3[n-1]) \\ \mathrm{Im}(S_3^*W_3^*[n-1]-Y_{3\,shunt}V_3[n-1]) \end{bmatrix} - \begin{bmatrix} 0 \\ 0 \\ G_{22} \\ B_{22} \\ G_{32} \\ B_{32} \end{bmatrix} V_{2\,re}[n] \quad (4.36)$$

$$V_{2\,re}[n] = \delta_{n0} + \delta_{n1}\frac{V_2^{sp2}-1}{2} - \frac{1}{2}\sum_{k=1}^{n-1} V_2[k]V_2^*[n-k]$$

The matrix on the LHS of (4.36) is constructed by breaking the $Y_{ik\,trans}$ matrix into real and imaginary components and correcting the coefficients corresponding to slack bus and PV buses; from here on, the matrix will be referred as iteration matrix. From

69

(4.36), it can be observed that the iteration matrix is not incident symmetric; also it loses the property of diagonal dominance. Hence, a LU factorization technique with pivoting has been used to solve the linear matrix problem and obtain the power series coefficients; however, no attempt has been made to determine whether there is an ordering to the equations where pivoting is not needed.

These equations from (3.46), for different RHS n indices are solved repeatedly until the desired number of terms in the power series is calculated. The analytic continuation of the voltage power series from the calculated coefficients is evaluated using Padé approximants. A numerical example demonstrating the implementation of generator bus model I is presented in Section 4.5.

4.3 GENERATOR BUS MODEL II USING HE

In the above PV bus formulation, the reactive power term was expressed as a holomorphic function in the s parameter. Another way of representing the generator bus model is eliminating the reactive power term by summing the complex power and its conjugate as shown in [51].

The traditional defining equations for a PV bus, i, are shown in (4.16) and (4.17). Unlike the PQ bus where complex equality constraints are used, for the PV bus equality constraints needed are only on the real part of the complex power injection. Real power injection, P_i, from (4.16) can be expressed in terms of complex power, S_i and subsequently in terms of bus voltages, V_i and bus admittance matrix, Y_{ik}, as follows:

$$S_i + S_i^* = 2P_i$$

$$(V_i \sum_{k=1}^{N} Y_{ik}^* V_k^*) + (V_i^* \sum_{k=1}^{N} Y_{ik} V_k) = 2P_i \qquad (4.37)$$

The bus admittance matrix can be separated into its series branch part and shunt admittance component as follows:

$$(V_i \sum_{k=1}^{N} Y_{ik\,trans}^* V_k^*) + (V_i Y_{i\,shunt}^* V_i^*) +$$

$$(V_i^* \sum_{k=1}^{N} Y_{ik\,trans} V_k) + (V_i^* Y_{i\,shunt} V_i) = 2P_i$$

$$(V_i \sum_{k=1}^{N} Y_{ik\,trans}^* V_k^*) + (V_i^* \sum_{k=1}^{N} Y_{ik\,trans} V_k) + V_i^* V_i (Y_{i\,shunt} + Y_{i\,shunt}^*) = 2P_i \qquad (4.38)$$

$$(V_i \sum_{k=1}^{N} Y_{ik\,trans}^* V_k^*) + (V_i^* \sum_{k=1}^{N} Y_{ik\,trans} V_k) + 2\,\mathrm{Re}(Y_{i\,shunt}) V_i^* V_i = 2P_i$$

The network shunt elements from the shunt admittance of transmission lines, transformer taps, shunt reactors and shunt capacitors, which contribute to the diagonal values of the bus admittance matrix, do not affect the real power injection. This is due to the cancellation of the imaginary component in the $Y_{i\,shunt} + Y_{i\,shunt}^*$ term. However, real power is affected by the real component of the $Y_{i\,shunt}$ term; for example by shunt conductance modeling the corona losses. In developing the generator bus model II using HE, for simplicity, the shunt conductance is not accommodated; hence, the $2\mathrm{Re}(Y_{i\,shunt})V_i V_i^*$ term in (4.38) is not modeled. The resulting expression from (4.38) is embedded in the complex parameter s yielding:

$$(V_i(s) \sum_{k=1}^{N} Y_{ik\,trans}^* V_k^*(s^*)) + (V_i^*(s^*) \sum_{k=1}^{N} Y_{ik\,trans} V_k(s)) = 2sP_i \qquad (4.39)$$

The voltage magnitude constraint is holomorphically embedded as:

$$V_i(s) * V_i^*(s^*) = 1 + \left(\left| V_i^{sp} \right|^2 - 1 \right) s, i \in p \qquad (4.40)$$

Solving (4.39) and (4.40) at $s=0$ while expressing the voltage function as a power series (refer to (4.5)), the system of equations for the PV bus, i, reduces to

$$(V_i[0] \sum_{k=1}^{N} Y_{ik\,trans}^{*} V_k^*[0]) + (V_i^*[0] \sum_{k=1}^{N} Y_{ik\,trans} V_k[0]) = 0 \qquad (4.41)$$

$$V_i[0] * V_i^*[0] = 1$$

To obtain the germ solution when using this PV bus model, the $s=0$ equations representing the load bus and slack bus have to be solved with (4.41) simultaneously. From equation (4.24) the equations representing the load bus and slack bus at $s=0$ are:

$$\sum_{k=1}^{N} Y_{ik\,trans} V_k[0] = 0 \; , \; i \in m \qquad (4.42)$$

$$V_i[0] = 1, i \in slack$$

If the germ solution for all bus voltages, (i.e. $V_i[0]$) is $1\angle 0^o$, the terms $\sum_{k=1}^{N} Y_{ik\,trans}^{*} V_k^*[0]$, $\sum_{k=1}^{N} Y_{ik\,trans} V_k[0]$ in equation (4.41) evaluate to be zero; the reason being the diagonal element in $Y_{ik\,trans}$ matrix is the negative sum of the off-diagonal elements. Also, the voltage magnitude constraint is satisfied at $s=0$. It has been established from Section 4.2.1 that the germ solution of bus voltages equal to $1\angle 0^o$ satisfies (4.42). Thus, the unique germ solution for the voltage function for this holomorphic embedding with generator bus model II must be $1\angle 0^o$ for all buses.

72

4.3.1 EVALUATING THE VOLTAGE SERIES COEFFICIENTS FOR GENERATOR BUS MODEL II

A recurrence relation that expresses the nth degree coefficients of the voltage series as a function of $(n\text{-}1)$ coefficients is next established for this PV bus model, along with the PQ bus model describe earlier. First, the voltage function is represented with a power series truncated up to s^n terms. Next, the voltage series and admittance bus entries are broken into real and imaginary components. The entries of the admittance matrix (without shunt elements) are expressed as $Y_{ik\,trans} = G_{ik} + jB_{ik}$. The voltage series coefficients are broken into real and imaginary parts $V_i[n] = V_{i\,re}[n] + jV_{i\,im}[n]$.

The equations resulting from the expansion of the terms $(V_i(s)\sum\limits_{k=1}^{N} Y_{ik\,trans}{}^* V_k{}^*(s^*))$ and $(V_i{}^*(s^*)\sum\limits_{k=1}^{N} Y_{ik\,trans}V_k(s))$ are shown in equations (4.43)-(4.52). For a PV bus i, the latter term is expanded as:

$$
\begin{aligned}
V_i^*(s^*)&\sum_{k=1}^{N} Y_{ik\,trans}V_k(s)\\
&= \left(V_i^*[0]+V_i^*[1]s+\dots V_i^*[n]s^n\right)\times\left(\sum_{k=1}^{N} Y_{ik\,trans}\left(V_k[0]+V_k[1]s+\dots V_k[n]s^n\right)\right)\\
&= \left(\left(V_{i\,re}[0]-jV_{i\,im}[0]\right)+\left(V_{i\,re}[1]-jV_{i\,im}[1]\right)s+\dots\left(V_{i\,re}[n]-jV_{i\,im}[n]\right)s^n\right)\times\\
&\quad\left(\sum_{k=1}^{N}(G_{ik}+jB_{ik})\left(\left(V_{k\,re}[0]+jV_{k\,im}[0]\right)+\dots\left(V_{k\,re}[n]+jV_{k\,im}[n]\right)s^n\right)\right)
\end{aligned}
\tag{4.43}
$$

Since there is a product of two power series in (4.43), the coefficient of s^n is the sum of the products of the coefficients whose powers of s add up to n. To illustrate the

above statement, consider two series $a(s)$, $b(s)$ and their product $c(s)$ defined as follows:

$$a(s) = \sum_{n=0}^{\infty} a[n]s^n, \, b(s) = \sum_{n=0}^{\infty} b[n]s^n$$

$$c(s) = a(s) * b(s) = \sum_{n=0}^{\infty} c[n]s^n \tag{4.44}$$

The coefficient of the series $c[n]$ is related to the coefficients $a[n]$, $b[n]$ as:

$$c[n] = \sum_{x+y=n} a[x]b[y], 0 \leq x, y \leq n \tag{4.45}$$

The equation (4.43) involves the product of two power series. Applying the same principle discussed above, the $s^{n\,\text{th}}$ term of the series in (4.43) is:

$$\sum_{x+y=n} \left\{ \left(\left(V_{i\,re}[x] - jV_{i\,im}[x] \right) s^x \right) * \sum_{k=1}^{N} \left(G_{ik} + jB_{ik} \right) \left(V_{k\,re}[y] + jV_{k\,im}[y] \right) s^y \right\} \tag{4.46}$$
$$0 \leq x, y \leq n$$

The coefficient of s^n is then expressed in terms of real variables by carefully performing the complex arithmetic from (4.46). The real and imaginary part of the complex equation derived from (4.46) is:

$$\sum_{x+y=n} \left(V_{i\,re}[x] - jV_{i\,im}[x] \right) \left(\sum_{k=1}^{N} \left[G_{ik} \quad -B_{ik} \right] \begin{bmatrix} V_{k\,re}[y] \\ V_{k\,im}[y] \end{bmatrix} + j \left[B_{ik} \quad G_{ik} \right] \begin{bmatrix} V_{k\,re}[y] \\ V_{k\,im}[y] \end{bmatrix} \right)$$

$$= \sum_{x+y=n} \left\{ \sum_{k=1}^{N} \left[G_{ik}V_{i\,re}[x] + B_{ik}V_{i\,im}[x] \quad -B_{ik}V_{i\,re}[x] + G_{ik}V_{i\,im}[x] \right] \begin{bmatrix} V_{k\,re}[y] \\ V_{k\,im}[y] \end{bmatrix} \right\} \tag{4.47}$$
$$+ j \sum_{x+y=n} \left\{ \sum_{k=1}^{N} \left[B_{ik}V_{i\,re}[x] - G_{ik}V_{i\,im}[x] \quad G_{ik}V_{i\,re}[x] + B_{ik}V_{i\,im}[x] \right] \begin{bmatrix} V_{k\,re}[y] \\ V_{k\,im}[y] \end{bmatrix} \right\}$$

74

Equations (4.43)-(4.47) represent the expansion of the $V_i^*(s^*)\sum_{k=1}^{N} Y_{ik\,trans}V_k(s)$

term in (4.39). The $(V_i(s)\sum_{k=1}^{N} Y_{ik\,trans}^*V_k^*(s^*))$ term can be expanded similarly resulting

in the following term.

$$
\begin{aligned}
&= \sum_{x+y=n}\left\{\sum_{k=1}^{N}\left[G_{ik}V_{i\,re}[x]+B_{ik}V_{i\,im}[x] \quad -B_{ik}V_{i\,re}[x]+G_{ik}V_{i\,im}[x]\right]\begin{bmatrix}V_{k\,re}[y]\\ V_{k\,im}[y]\end{bmatrix}\right\}\\
&+ j\sum_{x+y=n}\left\{\sum_{k=1}^{N}\left[-B_{ik}V_{i\,re}[x]+G_{ik}V_{i\,im}[x] \quad -G_{ik}V_{i\,re}[x]-B_{ik}V_{i\,im}[x]\right]\begin{bmatrix}V_{k\,re}[y]\\ V_{k\,im}[y]\end{bmatrix}\right\}
\end{aligned}
\quad (4.48)
$$

Equations (4.47) and (4.48) are expanded forms of the individual terms present in

LHS of equation (4.39). From equations (4.47) and (4.48) it can be observed that the

coefficients on the real components are the same; the coefficients of the imaginary

components are opposite in sign and add up to zero. The original equation to begin with

was the real power constraint; hence, imaginary coefficients adding up to zero is

expected. Upon adding the coefficients of (4.47) and (4.48), the sum becomes:

$$
\sum_{x+y=n}\left\{\sum_{k=1}^{N} 2\left[G_{ik}V_{i\,re}[x]+B_{ik}V_{i\,im}[x] \quad -B_{ik}V_{i\,re}[x]+G_{ik}V_{i\,im}[x]\right]\begin{bmatrix}V_{k\,re}[y]\\ V_{k\,im}[y]\end{bmatrix}\right\}
\quad (4.49)
$$

The objective now is to express the calculation of power series coefficients of order

n ($V_{i\,re}[n]$ and $V_{i\,im}[n]$), using a linear matrix equation. Hence, the unknown quantities

($V_{i\,re}[n]$ and $V_{i\,im}[n]$) will be retained on the LHS; the known quantities (coefficients

up to degree n-1) will be moved to the RHS. (More about this below in the discussion

regarding calculating the RHS term). Calculating the coefficients of s^n, $n\geq0$ from (4.49),

the unknown coefficients, $V_{k\,re}[n]$ and $V_{k\,im}[n]$, occur only when x=0, y=n and x=n,

$y=0$; In other words, the unknown coefficients occur in only two of the $n+1$ terms that meet the relation $x+y=n, x, y \geq 0$. These are:

$$\left\{\sum_{k=1}^{N} 2\left[G_{ik}V_{i\,re}[0]+B_{ik}V_{i\,im}[0] \quad -B_{ik}V_{i\,re}[0]+G_{ik}V_{i\,im}[0]\right]\begin{bmatrix}V_{k\,re}[n]\\V_{k\,im}[n]\end{bmatrix}\right\}$$
$$+\left\{\sum_{k=1}^{N} 2\left[G_{ik}V_{i\,re}[n]+B_{ik}V_{i\,im}[n] \quad -B_{ik}V_{i\,re}[n]+G_{ik}V_{i\,im}[n]\right]\begin{bmatrix}V_{k\,re}[0]\\V_{k\,im}[0]\end{bmatrix}\right\} \tag{4.50}$$

As a part of expressing the calculation process as a linear matrix equation, (4.50) is to be expressed as a product of a known row vector (which will become part of a larger iteration matrix) and an unknown column vector of voltage series terms, $V_{k\,re}[n]$ and $V_{k\,im}[n]$ $\forall$ values of k. For succinct representation of the iteration matrix entries, the coefficients of the elements $V_{k\,re}[n]$ and $V_{k\,im}[n]$ are denoted by γ_{ik} and β_{ik} respectively where i is the index of the generator bus whose real power balance constraint is being modeled. The coefficients γ_{ik} and β_{ik} for $k \neq i$ can be derived from (4.50) as:

$$\begin{aligned}\gamma_{ik} &= 2\left(G_{ik}V_{i\,re}[0]+B_{ik}V_{i\,im}[0]\right), k \neq i\\\beta_{ik} &= 2\left(-B_{ik}V_{i\,re}[0]+G_{ik}V_{i\,im}[0]\right), k \neq i\end{aligned} \tag{4.51}$$

The coefficients of $V_{i\,re}[n]$, $V_{i\,im}[n]$ for a PV bus, i, aggregated from (4.50) are,

$$\gamma_{ii} = 2\left(G_{ii}V_{i\,re}[0]+B_{ii}V_{i\,im}[0]+\sum_{k=1}^{N}\left(G_{ik}V_{k\,re}[0]-B_{ik}V_{k\,im}[0]\right)\right)$$
$$\beta_{ii} = 2\left(-B_{ii}V_{i\,re}[0]+G_{ii}V_{i\,im}[0]+\sum_{k=1}^{N}\left(B_{ik}V_{k\,re}[0]+G_{ik}V_{k\,im}[0]\right)\right) \tag{4.52}$$

Equations (4.51) and (4.52) represent the coefficients of the unknown power series terms $V_{i\,re}[n]$ and $V_{i\,im}[n]$; they are derived from the real power constraint of

76

generator bus *i*; they constitute the entries of the iteration matrix used to determine the power series coefficients.

The RHS of the real power constraint in the voltage bus model, from (4.39) occurs only for power of *s* raised to one. Hence, the term δ_{n1} (as defined in (4.14)) is multiplied with the real power injection term $2P_i$. Also, recall from (4.48) that only the coefficients of s^n (occurring for $x = 0, x = n \,\&\, y = n - x$) are retained on the LHS. The remaining coefficients ($x = 1, 2, \ldots n - 1 \,\&\, y = n - x$) are known and can be moved to the RHS of the equation corresponding to the real power constraint. Thus, the RHS element corresponding to the real power constraint for a PV bus, *i*, denoted by the term $\zeta_i[n]$, can be expressed for a general value of *n* as:

$$\zeta_i[n] = 2\delta_{n1}P_i + \sum_{x=1}^{n-1}\left\{\sum_{k=1}^{N}\left[G_{ik}V_{i\,re}[x] + B_{ik}V_{i\,im}[x] \quad -B_{ik}V_{i\,re}[x] + G_{ik}V_{i\,im}[x]\right]\begin{bmatrix}V_{k\,re}[n-x]\\V_{k\,im}[n-x]\end{bmatrix}\right\} \tag{4.53}$$

The voltage magnitude constraint for a generator bus remains the same as shown in Section 4.2.2 from equations (4.29)-(4.31). The expression for a real coefficient in the voltage series $V_{i\,re}[n]$ is derived from the embedded voltage magnitude constraint.

$$V_{i\,re}[n] = \delta_{n0} + \delta_{n1}\frac{V_i^{sp2} - 1}{2} - \frac{1}{2}\left(\sum_{k=1}^{n-1}V_i[k]V_i^*[n-k]\right) \tag{4.54}$$

When (4.54) is to be represented in the matrix equation, the entry corresponding to $V_{i\,re}[n]$ is made one; the remaining elements of the particular row in the LHS matrix are zeroed.

To summarize, for every PV bus. i, equations (4.51), (4.52) represent the LHS coefficients that correspond to the real power constraint; equation (4.53) is the RHS term corresponding to the real power constraint; and equation (4.54) corresponds to the voltage magnitude constraint for the PV bus, i. The unknowns are the real and imaginary n^{th} series coefficients of the voltage series. Thus, the HE generator bus model obtained by eliminating the reactive power term, can be represented with a linear system of equations that has a unique solution. The primary difference from the previously described model is the equations used to represent the real power constraint of generator buses. Another difference is that the reactive power generated by PV bus i, Q_{Gi} has to be evaluated from the calculated voltage solution, the network parameters and reactive power loading data.

To compare the difference in the structure of the equations that result from implementing generator bus model I against model II, the three-bus example shown in Figure 4.1 is considered. The slack bus and load bus are represented by HE defined in equations (4.2) and (4.3). The generator bus is represented by the HE presented in equations (4.39) and (4.40). The calculation of the voltage series coefficients for the three-bus problem can be expressed using a linear matrix equation shown below

$$
\begin{bmatrix}
1 & & & & & \\
& 1 & & & & \\
\gamma_{21} & \beta_{21} & \gamma_{22} & \beta_{22} & \gamma_{23} & \beta_{23} \\
& & 1 & & & \\
G_{31} & -B_{31} & G_{32} & -B_{32} & G_{33} & -B_{33} \\
B_{31} & G_{31} & B_{32} & G_{32} & B_{33} & G_{33}
\end{bmatrix}
\begin{bmatrix}
V_{1re}[n] \\
V_{1im}[n] \\
V_{2re}[n] \\
V_{2im}[n] \\
V_{3re}[n] \\
V_{3im}[n]
\end{bmatrix}
=
\begin{bmatrix}
\delta_{n0} + \delta_{n1}(V_{Slack} - 1) \\
0 \\
\zeta_2[n] \\
\delta_{n0} + \delta_{n1}\dfrac{V_2^{sp2} - 1}{2} - \dfrac{1}{2}\sum_{k=1}^{n-1} V_2[k]V_2^*[n-k] \\
\text{Re}(S_3^* W_3^*[n-1] - Y_{3\,shun}V_3[n-1]) \\
\text{Im}(S_3^* W_3^*[n-1] - Y_{3\,shun}V_3[n-1])
\end{bmatrix}
\qquad (4.55)
$$

In (4.55), the equations representing the slack bus (rows 1 and 2) and the load bus (rows 5 and 6) remain unaltered from (4.36). Equations representing generator bus model (rows 3 and 4) are modified based on equations (4.51)-(4.54). The voltage power series coefficients can be obtained by repeatedly solving (4.55). The remaining procedure involved in calculating the bus voltages such as usage of analytic continuation, convergence criteria described in Section 4.2 is still applicable.

4.4   POWER-FLOW SOLUTION USING HE

The above described generator bus models do not incorporate the reactive power limit of generators. A physical limit on equipment introduces discontinuities in the problem. This section describes the handling of reactive power limits on generators, discusses the convergence criteria and presents a flow chart for solving the PF problem using the HE procedure.

4.4.1   HANDLING REACTIVE POWER LIMITS OF GENERATOR

Currently, the reactive power limits of generator are handled in the power flow program as follows. Let $Q_{Gi\ MIN}$, $Q_{Gi\ MAX}$ represent the minimum and maximum reactive power limits on generator at bus i respectively. The germ solution followed by a fixed number of terms (say 5) of the power series coefficients are calculated using the HE procedure. For PV bus model I, the analytic continuation of the reactive power series $Q_i(s)$ gives the reactive power injection required to maintain the voltage to the specified value at bus i. Any reactive power load at bus i is added to obtain the

79

total reactive power generated, Q_{Gi}. For the PV bus model II, the Q_{Gi} value is evaluated from the calculated bus voltages.

If the reactive power limits of the limits are violated ($Q_{Gi} > Q_{Gi\ MAX}$ or $Q_{Gi} < Q_{GiMIN}$), the bus type is changed from PV bus to PQ bus. Depending on the maximum or minimum limit that is violated, the reactive power generation at the buses is chosen to be $Q_{Gi\ MAX}$ or $Q_{Gi\ MIN}$. Now, the reactive power injection at the buses is known and the voltage magnitude becomes a free variable. Hence, the buses are represented using the load bus equations described in Section 4.1. The PF problem is re-solved with the altered bus types. This involves recalculating the iteration matrix and establishing a recurrence relation to evaluate the power series coefficients using the altered bus types. The power series coefficients are calculated up to any desired order. From the analytic continuation of the series thus obtained, i.e., the candidate solution, the violation of generator capability is checked. Any additional violation of the reactive power limits or regaining control of PV buses requires resolving the problem again.

Table 4.2 Listing of Bus Types in the PF Problem

Bus type index	Bus type description	Known variables	Unknown variables
0	PQ	P,Q	$|V|,\theta$
2	PV	$P,|V|$	Q,θ
3	Slack	$|V|,\theta$	P,Q
4	PV on minimum Q limit	P,Q	$|V|,\theta$
5	PV bus on maximum Q limit	P,Q	$|V|,\theta$

Based on whether the maximum or minimum reactive power limit is violated a different bus type is assigned. The list of bus type, the indices used to identify the bus types and the corresponding known and unknown variables are listed in Table 4.2.

4.4.2   CONVERGENCE CRITERIA

In the implementation of the HE method, only a finite number of terms in the voltage series are calculated. The number of terms required in the voltage series to find a converged solution varies from problem to problem. Either of the following conditions can be used to determine convergence and end the calculation of the power series.

1.   The change in the voltage solution is less than a specified tolerance.
2.   The mismatch in the original PBE's is less than a tolerance value

In our implementation of the HE method, the convergence criteria was chosen to be the mismatch in the original defining equations of each bus type, i.e. complex power injection for load buses (4.1), real power injection and voltage magnitude for generator buses (equations(4.16) and (4.17)). The maximum allowable tolerance for the mismatch (ΔP, ΔQ for PQ buses and ΔP, $\Delta |V|$ for PV buses) was taken as 1e-04 p.u.

4.4.3   FLOWCHART

The procedure for solving the PF problem with reactive power limits on generators using the HE procedure is shown in Figure 4.2.
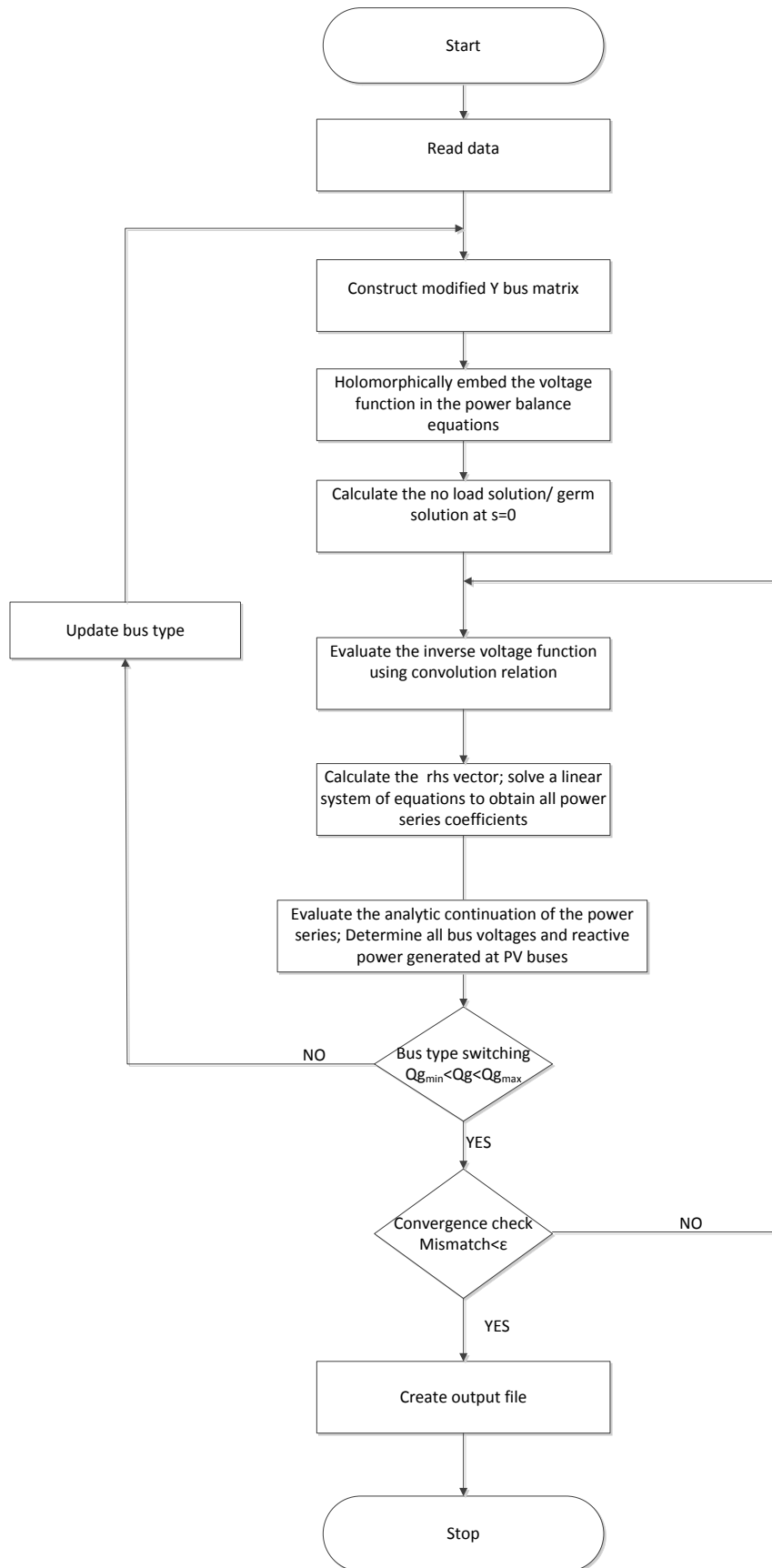
Figure 4.2 Solution Procedure using Holomorphic Embedding

4.5   NUMERICAL ILLUSTRATION

The numerical steps involved in solving the PF problem for a simple four-bus system are presented in detail in this section. The results obtained from tests on IEEE 118 bus test system are also shown.

4.5.1   FOUR BUS EXAMPLE
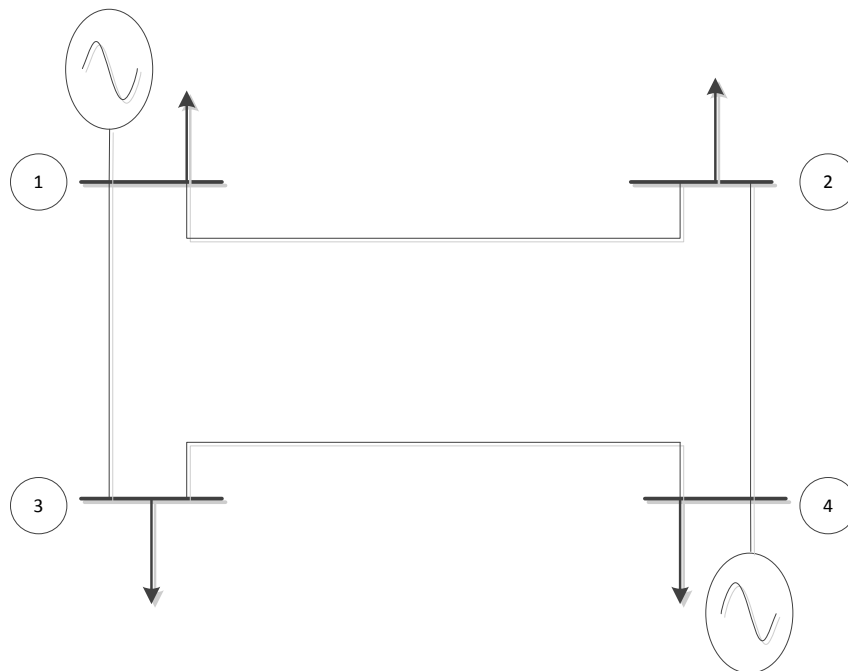
Figure 4.3 One Line Diagram of Sample Four- bus System

Figure 4.3 shows the single line diagram of a four-bus system shown in [53]. The bus and branch data are listed in Table 4.3-Table 4.4. The branch data is listed in p.u. on 100 MVA, 230 kV base. The first step is to construct the admittance bus matrix. Table 4.5 shows the bus admittance matrix calculated in per unit. Bus 1 is taken as slack bus.

Table 4.3 Transmission Line Data for Four- bus Problem

From bus - To bus	Resistance, R (p.u.)	Reactance, X (p.u.)	Shunt admittance, $Y/2$ (p.u.)
1-2	0.01008	0.05040	0.05125
1-3	0.00744	0.03720	0.03875
2-4	0.00744	0.03720	0.03875
3-4	0.01272	0.06360	0.06375

Table 4.4 Bus Data for Four-bus Problem

Bus	Generation		Load		V_{sp} (p.u.)	Bus type
	P_G, MW	Q_G, MVAR	P_L, MW	Q_L, MVAR		
1	-	-	50	30.99	1.00	Slack
2	0	0	170	105.35	-	Load bus
3	0	0	200	123.94	-	Load bus
4	318	-	80	49.58	1.02	Generator bus

Table 4.5 Bus Admittance Matrix for Four-bus Problem

Bus. no	1	2	3	4
1	8.9852-j44.8359	-3.8156+j19.0781	-5.1696+j25.8478	0
2	-3.8156+j19.0781	8.9852-j44.8359	0	-5.1696+j25.8478
3	-5.1696+j25.8478	0	8.1933-j40.8638	-3.0237+j15.1185
4	0	-5.1696+j25.8478	-3.0237+j15.1185	8.1933-j40.8638

The holomorphically embedded system of equations that is to be solved for each bus depends on the bus type. With the generator bus represented using model I presented in Section 4.2, the equations for the 4-bus system under consideration are:

$$V_i(s) = 1 + (V_i^{sp} - 1)s, i = 1$$

$$\sum_{k=1}^{4} Y_{ik\,trans} V_k(s) = \frac{sS_i^*}{V_i^*(s^*)} - sY_{i\,shunt} V_i(s), \ i = 2,3$$

$$\sum_{k=1}^{4} Y_{ik\,trans} V_k(s) = \frac{sP_i - jQ_i(s)}{V_i^*(s^*)} - sY_{i\,shunt} V_i(s), i = 4 \qquad (4.56)$$

$$V_i(s) * V_i^*(s^*) = 1 + \left(\left| V_i^{sp} \right|^2 - 1 \right) s, i = 4$$

The *Y* matrix corresponding to the series elements remains on the LHS. The shunt components are moved to the RHS. Solving (4.56) at *s=0* gives the germ solution. The germ solution has all bus voltages being equal to $1 \angle 0^o$. The next step is to calculate the remaining power series coefficients. The LHS matrix is split into real and imaginary coefficients (4.33). The size of the matrix becomes 8 x 8 for a 4-bus system. The matrix is then modified to correct for the slack bus and generator bus models according the chosen formulation (4.56). The modified matrix constructed from the admittance matrix is shown in Figure 4.4.

$$
\begin{bmatrix}
1 & 0 & 0 & 0 & 0 & 0 & 0 & 0 \\
0 & 1 & 0 & 0 & 0 & 0 & 0 & 0 \\
-3.81 & -19.07 & 8.98 & 44.92 & 0 & 0 & 0 & -25.84 \\
19.07 & -3.81 & -44.92 & 8.98 & 0 & 0 & 0 & -5.16 \\
-5.16 & -25.84 & 0 & 0 & 8.19 & 40.96 & 0 & -15.11 \\
25.84 & -5.16 & 0 & 0 & -40.96 & 8.19 & 0 & -3.02 \\
0 & 0 & -5.16 & -25.84 & -3.02 & -15.11 & 0 & 40.96 \\
0 & 0 & 25.84 & -5.16 & 15.11 & -3.02 & 1 & 8.19
\end{bmatrix}
\begin{bmatrix}
V_{1re}[n] \\ V_{1im}[n] \\ V_{2re}[n] \\ V_{2im}[n] \\ V_{3re}[n] \\ V_{3im}[n] \\ Q_4[n] \\ V_{4im}[n]
\end{bmatrix}
=
\begin{bmatrix}
\delta_{n0} \\
0 \\
\mathrm{Re}(S_2^* W_2^*[n-1] - j0.09V_2[n-1]) \\
\mathrm{Im}(S_2^* W_2^*[n-1] - j0.09V_2[n-1]) \\
\mathrm{Re}(S_3^* W_3^*[n-1] - j0.10V_3[n-1]) \\
\mathrm{Im}(S_3^* W_3^*[n-1] - j0.10V_3[n-1]) \\
\mathrm{Re}(Rhs\_Known[n-1]) \\
\mathrm{Im}(Rhs\_Known[n-1])
\end{bmatrix}
-
\begin{bmatrix}
0 \\ 0 \\ -5.16 \\ 25.84 \\ -3.02 \\ 15.11 \\ 8.19 \\ -40.96
\end{bmatrix}
V_{4re}[n]
$$

$$V_{4re}[n] = \delta_{n0} + 0.0202\delta_{n1} - \frac{1}{2}\sum_{k=1}^{n-1} V_4[k]V_4^*[n-k]$$

Figure 4.4 Recurrence Relation to Calculate Power Series Coefficients for Four-bus

Problem (Generator Bus Model I)

In Figure 4.4, rows 1, 2 of the LHS matrix correspond to real and imaginary components of the slack bus equations. Since the slack bus voltage is assumed fixed, independent of the network, the coefficients corresponding to other bus voltages are zero. Another peculiar point of Figure 4.4 is column 7 of the LHS matrix, where all elements are zero except the last row. This is in accordance with the discussion in Section 4.2.2 regarding the manipulation of the matrix entries to account for the generator bus model. The reactive power series term $Q_4[n]$ occurs only for the reactive power injection equation corresponding to bus 4. Hence, the remaining entries of the column must be zero. The other elements of the matrix are a result of the breaking the admittance matrix into real and imaginary components as shown in (4.32). The calculation of RHS vector in Figure 4.4 for slack bus (rows 1 and 2) and load buses (row 3 to row 6) follows directly from equations (4.13) and (4.15). The calculation of generator bus RHS quantities is shown in (4.34).

To solve for the subsequent power series coefficients, the RHS vector has to be evaluated. For load buses, the RHS vector is a function of the complex power and the inverse voltage series as shown in (4.13). For generator buses, the reactive power series (4.26) and voltage magnitude constraint (4.34) are also involved in the calculation procedure. After evaluating the RHS vector, a linear system of equations is solved to obtain the power series coefficients. The process is repeated and the coefficients evaluated up to five terms are listed in Table 4.6.

Table 4.6 Voltage and Reactive Power Series Coefficients

Degree of s	V_1	V_2	V_3	V_4	Q_4
0	1	1 + j7.636e-18	1 - j4.928e-17	1 - j2.056e-17	-9.297e-15
1	0	-1.628e-02 - j1.597e-02	-2.862e-02 - j3.116e-02	2.021e-02 + j2.832e-02	1.169e+00
2	0	-1.38e-03 - j7.595e-04	-2.69e-03 - j4.834e-04	-6.049e-04 - j1.203e-03	1.449e-01
3	0	-5.854e-05 - j5.103e-06	-1.805e-04 - j1.575e-05	4.63e-05 + j3.439e-06	3.193e-03
4	0	-5.981e-06 - j3.152e-06	-2.114e-05 - j2.256e-06	-1.94e-06 - j5.84e-06	6.384e-04

If the generator bus were to be represented using model II shown in Section 4.3, the real power constraint in (4.56) would need to be modified to:

$$(V_i(s)\sum_{k=1}^{4}Y_{ik\,trans}{}^{*}V_k{}^{*}(s^{*})) + (V_i{}^{*}(s^{*})\sum_{k=1}^{4}Y_{ik\,trans}V_k(s)) = 2sP_i, i = 4 \qquad (4.57)$$

The real coefficient of the PV bus $V_{4\,re}[n]$ is retained on the LHS of the recurrence relation. The reactive power term $Q_4[n]$ is eliminated from the calculation procedure.

The iteration matrix is constructed by breaking $Y_{ik\ trans}$ matrix into real and imaginary parts and including the appropriate coefficients to describe the slack bus and voltage bus formulation; it is shown in Figure 4.5.

$$
\begin{bmatrix}
1 & 0 & 0 & 0 & 0 & 0 & 0 & 0 \\
0 & 1 & 0 & 0 & 0 & 0 & 0 & 0 \\
-3.81 & -19.07 & 8.98 & 44.92 & 0 & 0 & -5.16 & -25.84 \\
19.07 & -3.81 & -44.92 & 8.98 & 0 & 0 & 25.84 & -5.16 \\
-5.16 & -25.84 & 0 & 0 & 8.19 & 40.96 & -3.02 & -15.11 \\
25.84 & -5.16 & 0 & 0 & -40.96 & 8.19 & 15.11 & -3.02 \\
0 & 0 & -10.33 & -51.69 & -6.04 & -30.23 & 16.38 & 81.93 \\
0 & 0 & 0 & 0 & 0 & 0 & 1 & 0
\end{bmatrix}
\begin{bmatrix}
V_{1\,re}[n] \\
V_{1\,im}[n] \\
V_{2\,re}[n] \\
V_{2\,im}[n] \\
V_{3\,re}[n] \\
V_{3\,im}[n] \\
V_{4\,re}[n] \\
V_{4\,im}[n]
\end{bmatrix}
=
\begin{bmatrix}
\delta_{n0} + \delta_{n1}(V_{Slack}-1) \\
0 \\
\mathrm{Re}(S_2^* W_2^*[n-1] - j0.09V_2[n-1]) \\
\mathrm{Im}(S_2^* W_2^*[n-1] - j0.09V_2[n-1]) \\
\mathrm{Re}(S_3^* W_3^*[n-1] - j0.10V_3[n-1]) \\
\mathrm{Im}(S_3^* W_3^*[n-1] - j0.10V_3[n-1]) \\
\zeta_2[n-1] \\
\delta_{n0} + \delta_{n1}\dfrac{V_4^{sp^2}-1}{2} - \tfrac{1}{2}\sum_{k=1}^{n-1}V_4[k]W_4^*[n-k]
\end{bmatrix}
$$

Figure 4.5 Recurrence Relation to Calculate Power Series Coefficients for Four-bus Problem (Generator Bus Model II)

The following are the differences that arise in the linear system of equations when the generator at bus 4, is represented by model II rather than model I (compare Figure 4.4 and Figure 4.5):

1. The unknowns for the PV bus 4 in model II are $V_{4\,re}[n]$, $V_{4\,im}[n]$ as opposed to $Q_4[n]$ and $V_{4\,im}[n]$ in model I. Hence, the entries corresponding to $V_{4\,re}[n]$ in column 7 are non-zero.

2. The equation from row 7 of the matrix equation corresponds to the real power constraint of the PV bus. The coefficients of the matrix equation corresponding to row 7 are calculated from equations (4.51) and (4.52).

3. Row 8 corresponds to the equation derived from the voltage magnitude constraint of the PV bus shown in (4.53).

4. Calculating the RHS vector follows equations (4.52) and (4.53); it does not involve moving the $V_{i\,re}[n]$ term to the RHS like model I.

The power series coefficients thus obtained using generator bus model II were numerically verified to be the same as the results presented in Table 4.6 (obtained from

88

using generator bus model I) up to 16 decimal places. The reasoning behind the two different methods yielding numerically equal results is as follows: Although the generator bus models I and II differ significantly in their implementation details, both models represent accurate holomorphic embedding of the original equations that define the generator bus. The recurrence relation to calculate the power series coefficients, for both models, is derived from the embedded system of equations that are equivalent. The two models essentially represent two different ways of expressing the same equation, in this case the defining equations for the PV bus. Hence, the power series coefficients are evaluated to be the same for this particular problem.

Since the power series coefficients are numerically equal, the subsequent steps involved in calculating the bus voltages remain unaltered irrespective of which generator bus model is chosen. After the calculating the voltage power series coefficients, the next step was to evaluate the actual voltage solution from its series approximation. Using the analytic continuation techniques described in Chapter 3, the maximal analytic continuation of the voltage and reactive power series were evaluated.

The calculation of Padé approximants of the V_2 series using the matrix method described in Section 3.2 is shown below. Other voltages can be calculated similarly. The voltage series $V_2(s)$ described by the entries from Table 4.6 is:

$$
\begin{aligned}
V_2(s) = & \left(1 + j7.636\mathrm{e}\text{-}18\right) + \left(-1.628\mathrm{e}\text{-}02 - j1.597\mathrm{e}\text{-}02\right)s \\
& + \left(-1.38\mathrm{e}\text{-}03 - j7.595\mathrm{e}\text{-}04\right)s^2 + \left(-5.854\mathrm{e}\text{-}05 - j5.103\mathrm{e}\text{-}06\right)s^3 \\
& + \left(-5.981\mathrm{e}\text{-}06 - j3.152\mathrm{e}\text{-}06\right)s^4
\end{aligned}
\tag{4.58}
$$

Using equation (3.11), the denominator polynomial coefficients are found to be:

$$\begin{bmatrix} b_2 \\ b_1 \end{bmatrix} = \begin{bmatrix} 0.0650 + j0.0552 \\ -0.0073 - j0.0008 \end{bmatrix} \tag{4.59}$$

The numerator polynomial coefficients from (3.12)

$$\begin{aligned} a_0 &= 1 + j0 \\ a_1 &= 0.0487 + j0.0393 \\ a_2 &= -0.0089 - j0.0035 \end{aligned} \tag{4.60}$$

The [2/2] Padé approximant evaluated using the matrix method is shown in (4.61).

$$V_2(s) = \frac{1 + (0.0487 + j0.0393)s + (-0.0089 - j0.0035)s^2}{1 + (0.0650 + j0.0552)s + (-0.0073 - j0.0008)s^2} \tag{4.61}$$

$$V_2(1) = 0.9823 - j0.0167 = 0.9824 \angle -0.97°$$

Evaluating (4.60) at $s=1$ yields the required numerical value of V_2. Bus voltages can be evaluated using any other analytic continuation technique presented in Chapter 3. The other bus voltages are calculated similarly and the results are tabulated in Table 4.7. Table 4.7 also lists the mismatch in the original PBE's. The mismatches are used to check for convergence.

Table 4.7 Voltage Solution and Mismatches for the Four-bus System

Bus no	Voltage solution	P mismatch	Q mismatch (PQ bus)/ V mismatch (PV bus)
1	$1\angle 0°$	0	0
2	$0.9824\angle -0.97°$	$-0.1463*10^{-10}$	$-0.1259*10^{-10}$
3	$0.9690\angle -1.87°$	$-0.1499*10^{-10}$	$-0.4717*10^{-10}$
4	$1.0200\angle 1.52°$	$0.0264*10^{-10}$	$0.0011*10^{-10}$

The voltage solution was validated with the solution from [53] and the solution obtained from PowerWorld.

4.5.2 SOLVING IEEE 118 BUS SYSTEM USING HE

The IEEE 118 bus test system in is a portion of the American Electric Power system. The test data available in the IEEE common data format (.cdf) in [54] is used. The power system is robust with many PV buses providing voltage support and converges in five iterations using the Fast Decoupled Load Flow (FDLF) method. Branch data pertaining to parallel transmission lines, fixed transformer taps only alter the bus admittance matrix and not the solution procedure.

Using the PF-solution algorithm described in Figure 4.2 and with a tolerance for the mismatches in the PBE's chosen as 1e-04 p.u., eight terms were required in the voltage power series to find the converged voltage solution for the IEEE 118 bus system. Figure 4.6 is a plot of the maximum value of the absolute error in the real and reactive PBE's against the number of terms in the power series.
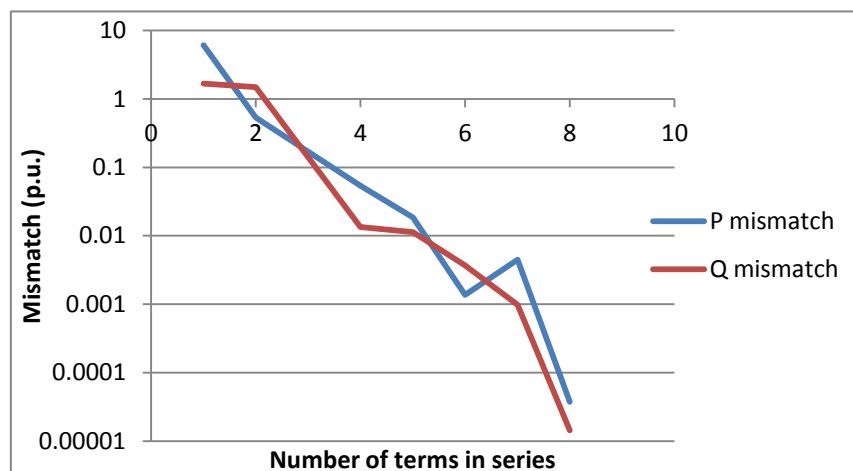
Figure 4.6 Convergence Properties of HE procedure

From Figure 4.6, it can be observed that the mismatch decreases continually as the number of terms increases; with eight terms in the series, the mismatch is less than the specified tolerance. In addition, none of the generator reactive power limits is violated. The solution from the program's text-file output is presented in APPENDIX A. This text file contains the bus voltages, bus type, real and reactive power injection of generators for the 118-bus system. Also, flow on transmission lines and transformers along with transformer taps are listed.

The voltage solution obtained from HE was compared with the solution traditional iterative methods. The IEEE 118 bus test system was solved using the traditional NR method with sparsity programming techniques in [55]. The solution was also calculated using PowerWorld, a commercial power systems analysis software. The HE voltage solution was found to agree with pre-established voltage solutions up to five digits of precision.

Currently, the discontinuities due to var limits are handled by re-solving the problem as described in Figure 4.2. When the HE method was used to solve the 118-bus test system, discontinuities due to bus type switching occurred once. With five terms in the series, the violation in generator limits was checked. The generators that had violated the reactive power limits were made PQ buses and the problem was resolved. With eight terms in the series using the new bus-type assignment, the mismatches in the PBE's were verified to be less than 1e-4 p.u. Generators that had violated the reactive power limits previously did not regain control over voltage. No

additional generators underwent bus type switching. In fact, the list of generators that underwent PV-PQ bus type switching using HE was found to be the same as the list obtained by solving the problem using NR method with PowerWorld.

Table 4.8 Generators Violating Reactive Power Limits- IEEE 118 bus system

Bus no	Bus name	Type	Generation MVAR	Limit (Max/ Min)
19	Lincoln	4	-8.0	Minimum
32	Delaware	4	-14.0	Minimum
34	Rockhill	4	-8.0	Minimum
92	Saltvlle	4	-3.0	Minimum
105	Roanoke	4	-8.0	Minimum
103	Claytor	5	+40.0	Maximum

The HE method was also tested on IEEE 14 bus, 30 bus, 57 bus test systems. The results obtained for other test systems were similar to those reported for the 118 bus system.

4.6 COMPARING THE SOLUTION PROCEDURE OF HE AND NR METHOD

A direct comparison of run times with the NR method was not performed since the HE method was implemented with dense matrix operations in MATLAB. This section compares and contrasts the differences involved in numerical implementation of the two methods and some scope for improvement in computation time for the HE method is presented.

i. SIZE OF MATRIX EQUATION

In implementing the generator bus model using HE, the matrix equation is broken down into real and imaginary components. Hence, the size of the matrix equations to be solved for a N bus system is $2N$. For solving the problem using the NR method,

since the equations are not complex differentiable (non-holomorphic), they are broken down into real equations; this leads to a matrix equation of size $2N$ even in NR method.

ii.   COST OF UPDATING AND RE-FACTORIZING MATRIX

The traditional NR method requires updating and re-factorizing of the Jacobian matrix in each iteration. Thus in the NR method, calculation of a new voltage estimate involves calculating the mismatch vector, updating the Jacobian matrix, LU factorization of the Jacobian matrix, forward and backward substitution. For the HE method, the modified bus admittance matrix needs to be factorized only once. As with the NR method, the RHS vector has to be evaluated, forward and backward substitution must be performed in every step to calculate the power series coefficients. This results in savings in CPU time in the LU factorization routine. However, if bus type switching from PV-PQ buses occurs, the admittance bus matrix is updated and has to be re-factorized.

iii.   CALCULATION OF MISMATCH

Calculation of mismatches in the PBE's is a necessary step in the solution procedure using NR method. With the HE method, a Gauss-Seidel type check, i.e. difference in the voltage solution with one additional term in the power series can be used to determine convergence. While the mismatch tolerance in PBE was used in our PF implementation, the use of voltage change tolerance as the convergence criteria is computationally less expensive. It must be kept in mind that the slow oscillations that

can occur with a load just beyond the BP might fool a voltage-change tolerance test. In the future, exploring whether a voltage-change tolerance works as well is a worthy pursuit.

iv. COMPUTATIONAL EFFORT PER ITERATION

In the NR method, the computational effort involved per iteration is almost identical. However in the HE method, the number of floating point operations increases as the coefficients of the power series increases. This can be attributed to the convolutions involved in the calculation procedure. For instance, in the load bus model, the calculation of the inverse of the voltage series is essential. As the degree of the s increases, the number of floating point operations in calculating this inverse series increases. Similarly, for the voltage bus models, the number of convolutions increases with increasing number of terms in the series.

v. ANALYTIC CONTINUATION

The traditional NR method does not involve the analytic continuation process, which saves CPU time and memory requirements. However, the procedure of analytic continuation, which is unique to the HE procedure, is easily parallelizable since the voltage power series for each bus voltage are independent.

5 ESTIMATING THE BIFURCATION POINT USING HOLOMORPHIC

EMBEDDING

Voltage stability analysis based on the results of PF is crucial information for the system operator. Based on existing iterative methods, various methods have been published for obtaining voltage sensitivity indices and calculating the BP. To perform similar studies using HE, the embedding described in Chapter 4 needs to be modified. With the modified HE, two different methods of estimating the BP of a system with only PQ buses, are developed in this chapter. The theory behind the development of the method along with numerical examples is shown.

5.1 MODIFIED HE FORMULATION

Using the HE procedure, the voltage solution at every bus i can be obtained as rational function of the complex embedding parameter s as follows:

$$V_i(s) = \frac{a_i(s)}{b_i(s)} = \frac{a_i[0] + a_i[1]s + a_i[2]s^2 + \ldots}{b_i[0] + b_i[1]s + b_i[2]s^2 + \ldots} \qquad (5.1)$$

The rational function on the RHS of (5.1) is the Padé approximant, the functions $a_i(s)$, $b_i(s)$ represent the numerator and the denominator polynomials respectively. To obtain the voltage solution, (5.1) is evaluated for one particular value of s, $s=1$. However, the parameter s can also be used to scale the complex power injection at each bus in the original PBE's (4.2). Thus by varying the value of s in (5.1), the voltage solution for different loading conditions can be evaluated. By continually incrementing the s value, the PV, QV curves of the bus can be traced.

In order to trace the PV, QV curves using the HE procedure, the embedding described in Chapter 4 must be modified for the following reason. As claimed previously, the original PBE's can be retrieved from the holomorphically embedded system of equations at $s=1$ from (4.2). However, for values of $s\neq1$, the embedded system of equations do not have any meaningful solution since the $Y_{i\,shunt}$ term is scaled by the value s.

The HE model representing the load bus and slack bus from [20], as described in Section 4.1.2 is:

$$\sum_{k=1}^{N} Y_{ik\,trans} V_k(s) = \frac{sS_i^*}{V_i^*(s^*)} - sY_{i\,shunt}V_i(s) \,, \ i \in m$$

$$V_i(s) = 1 + (V_i^{sp} - 1)s, i \in slack$$

(5.2)

In order to find the accurate voltage solution at no load ($s=0$) conditions, the slack bus and load bus embeddings from (5.2) are written as:

$$\sum_{k=1}^{N} Y_{ik} V_k(s) = \frac{sS_i^*}{V_i^*(s^*)}, \ i \in m$$

$$V_{slack}(s) = V_{sp}$$

(5.3)

In comparing the embeddings of (5.2) and (5.3), the voltage function is holomorphic in both the embeddings. Also, the original PBE's are retrieved from the embeddings at $s=1$. The difference between (5.2) and (5.3) is the germ solution, i.e. solution at $s=0$. Equation (5.2) yields a germ solution of all bus voltages equal to $1\angle0^o$. However, solving (5.3) at $s=0$, the RHS vector goes to zero; hence the following system of linear equations must be solved to obtain the correct germ solution.

$$\sum_{k=1}^{N} Y_{ik} V_k[0] = 0, \ i \in m \qquad (5.4)$$

$$V_{slack}[0] = V_{sp}$$

A practical application of the embedding (5.3) is that the bus voltages obtained as a function of the parameter of s can be reused to evaluate the voltages when the complex power injections in the system are scaled by the quantity s. In other words, the embedding (5.3) can be used to trace what is known as the PV curve of the network by scaling the s parameter. For a system of PQ buses with no shunt components and slack bus voltage equal to 1, the embeddings described in (5.2) and (5.3) are essentially the same.

5.2   ESTIMATING THE BIFURCATION POINT BY EXTRAPOLATING 's'

PARAMETER

Consider a system of PQ buses and one slack bus represented by the embedding shown in (5.3). By solving the PF problem using the HE procedure, coefficients $a_i[n]$, $b_i[n]$ in (5.1) for every bus voltage i can be found. The value of s in (5.1) is increased continually from zero, thereby scaling the complex power injection at every bus. The voltage solution corresponding to the different values of complex power injection can be evaluated varying the value of s parameter in (5.1). The mismatch in the PBE's is found and the process is repeated until the mismatch exceeds a specified tolerance (0.01 p.u.). Since the Padé approximant is the maximal analytic continuation it is

guaranteed to converge to the solution if it exists. The value of s at which, a voltage solution does not exist is taken to be an estimate of the BP.

5.2.1   MERITS AND DEMERITS

The primary advantage of the method is it does not require resolving the PF problem at every point on the PV curve. The PF problem is solved once to obtain the rational approximants. The cost associated with calculating the voltages for a different loading condition is merely reevaluating a polynomial expression as opposed to re-solving the entire PF problem.

For practical purposes, the BP for incrementing the real and reactive load independently at a one or a small set of buses is of interest. A major drawback with the method in its current form is that it does not allow scaling the loads differently at every bus.

5.3   DECIPHERING SINGULARITIES FROM PADÉ APPROXIMANTS

The power series expansion of an analytic function about a point contains all the information about the function. For instance, specific quantitative information about the singularities of the function can be deduced from the rational Padé approximants [44].

For a function with a simple pole, the denominator polynomial of the Padé approximant would have a zero that occurs close to the original pole. This was verified to be true for a simple geometric series described in Section 3.2. For the series,

$f_1(s) = 1 + s + s^2 + \ldots$, the Padé approximant, $\dfrac{1}{1-s}$, indicates the occurrence of a pole

at $s=1$, which is indeed the pole of the original function. For a function with multiple

poles, a higher degree Padé approximant's denominator polynomial will have a cluster

of zeros that approximate the poles of the original function. It is expected that as the

degree of the Padé approximant increases, the poles coalesce together; the original

poles are represented with an increasing degree of accuracy [44].

The function of interest in this case happens to be the PBE's and the point at which

the HE equations become non-holomorphic (or the Jacobian matrix in NR method

becomes singular) is the bifurcation point The PBE's express the complex power

injection as a function of the bus voltage.

$$P + jQ = f_1(V, \theta) \tag{5.5}$$

where f_1 represents the PBE's broken into real and imaginary parts, as shown in (2.1).

However, in the HE solution, the voltage is expressed as a function of the power

injection. In other words, the inverse function is evaluated.

$$V\angle\theta = f_2(P + jQ) \tag{5.6}$$

where f_2 represents the holomorphically embedded system of equations in chapter 4.

While the HE equations express voltage as a function of the complex parameter s, bus

voltages are in essence, expressed as a function of the complex power injection. The

voltage function thus calculated from HE is represented by a rational Padé approximant.

The roots of the numerator and denominator polynomial of the rational approximant

align on what is known as a branch cut of an analytic function [52]. The branch cut is

the region in the complex plane where the function becomes non-holomorphic; Recall, the bifurcation point is the point at which the PBE's become non-holomorphic. As the degree of the Padé approximant increases, the BP is represented with an increasing degree of accuracy [52]. The bifurcation point is taken to be the nearest occurring zero of the numerator polynomial that occurs along the real s axis.

5.3.1 CALCULATION PROCEDURE, MERITS AND DEMERITS

The steps involved in the numerical evaluation of the bifurcation point using Padé approximants are as follows:

1. Obtain the rational approximants to the voltage function by solving the PF problem using the HE procedure using the embedding of (5.3).
2. From the Padé approximant of any one bus voltage, calculate all the roots of the numerator polynomial.
3. The root occurring closest to the origin on or near the real s axis is an estimate of the BP.
4. Compare with estimates of BP obtained from other bus voltages and estimates obtained for a higher degree Padé approximant for reliability.

Instead of re-solving the entire PF problem for different loading conditions, the rational approximant of one bus voltage is sufficient to estimate the BP. Unlike the method of extrapolating s and recalculating the voltages, this method does not require calculating the mismatch in the PBE's. There is a trade-off between choosing a higher degree Padé approximant for accuracy and accumulating round-off errors in the calculation process.

5.4   NUMERICAL EXAMPLE

The numerical implementation of the methods discussed above is shown for a four-bus system.

5.4.1   PROBLEM STATEMENT

Consider the modified four-bus system from Figure 4.3 with the generator at bus 4 removed. The Power Systems Analysis Toolbox (PSAT) [56] software is used to trace the PV curve using the CPF and find the exact value of the BP. If the loading at all buses were incremented uniformly, the value of BP as calculated using PSAT would be 2.4095 times the original loading at all the buses.

5.4.2   RATIONAL APPROXIMANTS TO VOLTAGE USING HE

The original PBE's for the four-bus system is embedded as shown in (5.3) and solved using the HE procedure. A rational approximant of the voltage solution is obtained by constructing an analytic continuation using the matrix method (described in section 3.2). Table 5.1 shows [3/3] Padé approximants for the voltage solution obtained from seven terms in the power series.

Table 5.1 Padé Approximants of Voltage for Four-bus System

Bus no.	Rational approximant
1	1
2	$\dfrac{(1.0072 - j0.0014) + (-0.5127 + j0.0004)s + (0.0565 + j0.0002)s^2 + (0.0003 - j0.0000)s^3}{1 + (-0.4240 + j0.0902)s + (-0.0273 - j0.0305)s^2(0.0014 + j0.0012)s^3}$
3	$\dfrac{(1.0058 - j0.0012) + (-0.4918 + j0.0084)s + (-0.0513 - j0.0025)s^2 + (0.0003 - j0.0001)s^3}{1 + (-0.4152 + j0.0865)s + (0.0261 - j0.0287)s^2 + (0.0013 + j0.0011)s^3}$
4	$\dfrac{(1.0091 - j0.0018) + (-0.5247 + j0.0105)s + (0.0604 + j0.0039)s^2 + (0.0001 - j0.0002)s^3}{1 + (-0.4239 + j0.0910)s + (-0.0273 - j0.0306)s^2(0.0014 + j0.0012)s^3}$

The voltage solution obtained by evaluating the rational approximant at $s=1$ is

$V_1 = 1\angle 0^{\mathrm{o}}$;

$V_2 = 0.9070\angle\text{-}5.85^{\mathrm{o}}$;

$V_3 = 0.9196\angle\text{-}5.00^{\mathrm{o}}$;

$V_4 = 0.8964\angle\text{-}6.71^{\mathrm{o}}$.

The mismatches in the PBE's at the calculated solution are less than 1e-4 p.u. for the specified loading conditions.

5.4.3 ESTIMATION OF BIFURCATION POINT BY EXTRAPOLATING s PARAMETER

In order to trace the PV curve the value of s is incremented from 0 in steps of 0.01. The voltage solution is calculated by reevaluating the rational approximant; this represents the actual solution for the four-bus problem whose complex injections are scaled by the parameter s. If the mismatch in the PBE's is greater than 1e-02 p.u., the

process is terminated; the value of *s* at the termination point is taken as an estimated of the BP. The estimate of the BP obtained from a [3/3] approximant for the four-bus system studied is 2.01 p.u.

The actual value of BP obtained from PSAT is 2.4095 times the original loading. The percentage error in the BP estimate is calculated as 16.58%.

$$\%error\ in\ estimate = \frac{Acutal\ BP - Acutal\ BP}{Acutal\ BP} * 100$$

$$= \left(\frac{2.4095 - 2.01}{2.4095}\right) * 100 = 16.58\%$$

(5.7)

For the voltage solution calculated using a [3/3] Padé approximant, the error in BP is calculated to be 16.58%. While the mismatch of the PBE's at *s=1* is less than 1e-04, it does not faithfully reproduce the PV curve as the value of *s* increases toward the BP. Hence, a higher degree approximant (degree of the Padé approximant is taken as the degree of the numerator or denominator polynomial, whichever is highest) was calculated and the procedure was repeated. Figure 5.1 shows the plot of the percentage error in estimating the BP against the degree of the Padé approximant.
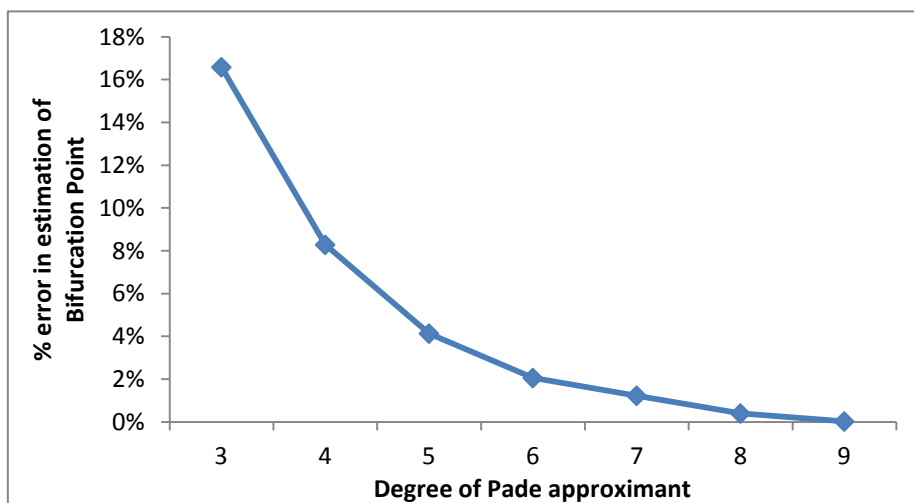
Figure 5.1 Accuracy of Bifurcation Point obtained by Extrapolating *s*

It can be observed that as the degree of Padé approximant increases, the error in the estimate of the BP decreases. A [9/9] approximant calculated with 19 terms in the series gives the estimate of the BP to be 2.41 times the original loading (compare with actual BP of 2.4095). A portion of this error of 0.02% is due to the 0.01 discrete step size in the loading parameter, s. The number of terms required in the power series to obtain a better estimate of the BP, for a general problem is unknown and presents scope for future work.

The variation of the bus voltages with the increase in the complex s parameter, in this case the loading parameter, is shown in Figure 5.2.
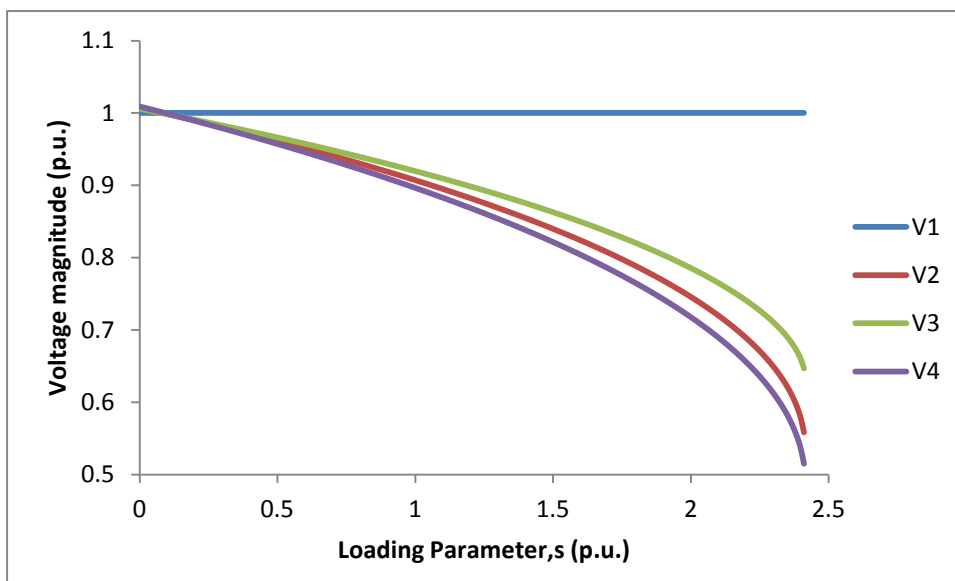
Figure 5.2 Bus Voltages vs. Loading Parameter for Four-bus System

The voltages for Figure 5.2 are calculated using the [9/9] approximant. The voltage solution that corresponds to the lower portion of the PV curve cannot be calculated using the current formulation.

5.4.4 ESTIMATING BIFURCATION POINT USING PADÉ APPROXIMANTS

From the [3/3] Padé approximants of the voltage in Table 5.1, the zeros of the numerator polynomial of the bus voltages are calculated. For bus 2, the roots of the numerator polynomial are calculated as:

$$
\begin{aligned}
&(1.0072 - j0.0014) + (-0.5127 + j0.0004)s \\
&+ (0.0565 + j0.0002)s^2 + (0.0003 - j0.0000)s^3 = 0 \\
&\Rightarrow s = 2.9095 + j0.0013, 5.8895 + j0.0016, -219.75 - j27.35
\end{aligned}
\tag{5.8}
$$

From the previous discussion, it was established that the root of the numerator polynomial that occurs closest to the origin on or near the real s axis is representative of the BP. The roots of the numerator polynomial from (5.8) are complex. However, the value of s by which the loading at each bus has to be scaled before voltage collapse occurs has to be real. Hence, the estimate of the BP is taken to be the real portion of the smallest root of the polynomial along the positive s axis i.e. 2.9095 (20.74% error). The BP estimates can also be obtained from the rational approximants of the other bus voltages. The error in estimate of the voltage collapse point decreases with an increase in the number of terms in the series. For instance, the BP estimates for a [10/10] and [20/20] approximant from V_2 are 2.4709 and 2.4308, with error percentages of 2.54% and 0.88% respectively.

Figure 5.3 and Figure 5.4 show the estimates of the voltage collapse point and the percentage error in the estimate, respectively, as a function of the degree of the Padé approximant.
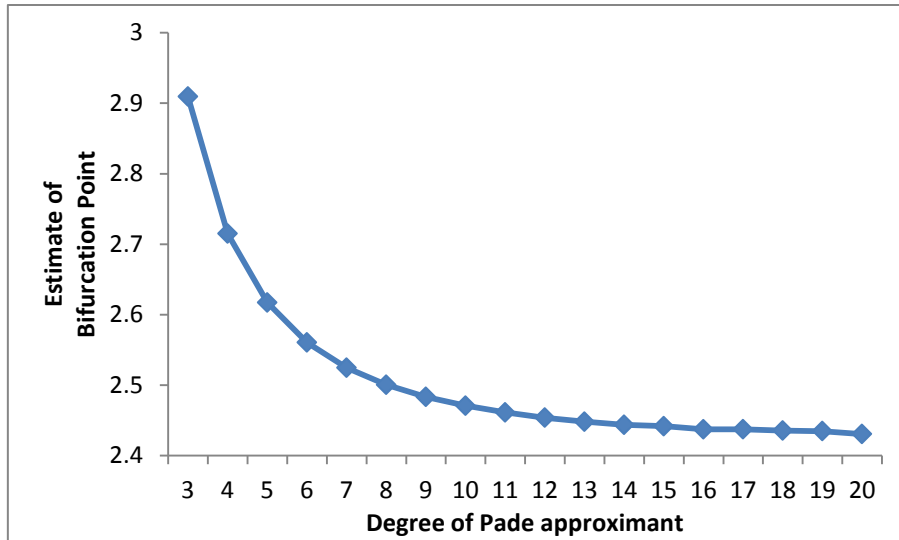
Figure 5.3 Estimate of Bifurcation Point Obtained from Padé Approximant
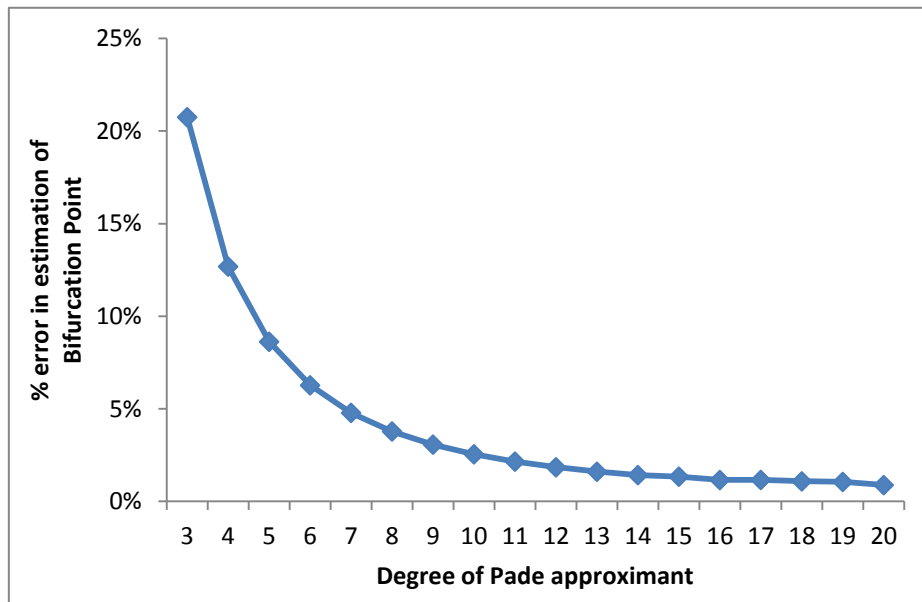
Figure 5.4 Error in Bifurcation Point Obtained from Padé Approximant

5.5   SUMMARY

For a simple four-bus problem with one slack bus and remaining PQ buses, the BP

obtained by uniformly scaling the loads was estimated up to 0.02% accuracy. Tracing

the PV curve was possible by re-evaluating the Padé approximant without resorting to

any CPF technique. Two methods of evaluation of the BP of a system with PQ buses

were presented. The first method involved extrapolating the s parameter; the second

approach calculated the zeros of the numerator polynomial of the Padé approximant. A comparison of the two methods in calculating the bifurcation point is as follows.

To compare the accuracy of the solution, the BP estimates for the four-bus problem described above, are obtained from the two methods with the same number of terms in the series. With 19 terms in the series, the estimate of BP obtained by extrapolating 's' had a percentage error of 0.02%. With the same number of terms in the series, the estimate of BP from the zeros of the Padé approximant had an error of 3.07%. With 41 terms in the series, the former method of extrapolating 's' yields the same estimate of BP. The BP estimate and the error percentage remain unaltered due to the step size chosen (0.01) to increment the s value. With the same 41 terms, using the zeros of the Padé approximant's numerator polynomial, the BP estimate found had an error of 0.88%.

In terms of computational complexity, estimating the BP from the zeros of the Padé approximant requires the calculation of all the roots of a higher degree polynomial. The method of extrapolating s, on the other hand only requires reevaluating the polynomial Padé approximant, but multiple times. In the current implementation, this is not quite a distinguishing feature since calculation of roots of polynomial using software such as MATLAB is fast.

6 CONCLUSION AND FUTURE WORK

6.1   CONCLUSION

The research presented in this document is directed towards implementing a non-iterative solution procedure for solving the ac power-flow problem, by embedding the PBE's as a holomorphic function.

Different techniques for analytic continuation, along with numerical examples were presented in chapter 3. The numerical issues that should to be taken into consideration while evaluating the maximal analytic continuation of an analytic function were demonstrated.

Current literature has an HE model for the load bus. In chapter 4, two different holomorphically embedded models for the generator bus were developed by:

1.   Representing the reactive power injection Q_i as a holomorphic function.
2.   Eliminating the reactive power term by summing the complex power and its conjugate.

The details of implementing the HE method to solve the ac PF problem for a small to medium sized system were presented. The solution procedure was demonstrated in detail for a sample four-bus system. The HE method was tested on several IEEE test cases; results from the 118-bus system were presented. The implementation was done with dense matrix operations in MATLAB. The time taken to solve the 118 bus system was approximately 0.7 sec. However, the run times and storage requirements would be

significantly improved if it were to be programmed in a third generation language (C++, Java, etc.) with sparsity programming techniques.

A modified HE that allows tracing the PV curve and calculating the bifurcation point was developed in chapter 5 above. Using the Padé approximants to the voltage function obtained from HE, it is shown that accurate estimates of the BP can be obtained, at least for the four-bus problem examined. The solution procedure along with the theory involved was discussed in detail with numerical examples.

6.2   FUTURE WORK

The HE approach of solving a PF problem should be quantified, compared with the existing methods on speed of computation, memory requirements and ability to handle ill-conditioned problems among several other factors. Currently, discontinuities occurring due to reactive power limits on generators are handled by performing bus type switching and re-solving the PF problem; a procedure to handle discontinuities without re-solving the problem could be developed. Numerical testing on a larger scale model warrants the inclusion of HVDC lines, phase shifting transformers, remote regulation of buses; in that case, development of a holomorphically embedded model representative of each component's original equation becomes necessary. In order to evaluate the BP using the HE method for a general problem, the generator bus model ought to be modified and included. Also, a formulation that allows varying the loads independently at different buses presents scope for future work.

REFERENCES

[1] J. D. Glover, M. S. Sarma and T. J. Overbye, "Power System Analysis and Design 4th Edition," Cengage Learning, Stamford, 2007.

[2] J. B. Ward and H. W. Hale, "Digital Computer Solution of Power-Flow Problems," Power Apparatus and Systems, Part III, Transactions of the American Institute of Electrical Engineers, Jan. 1956, vol. 75, no. 3, pp. 398-404.

[3] W. Tinney and C. Hart, "Power Flow Solution by Newton's method," IEEE Transactions on Power Apparatus and Systems, Nov. 1967, vol. PAS-86, no. 11, pp. 1449-1460.

[4] W. Tinney and J. Walker, "Direct Solution of Sparse Network Equations by Optimally Ordered Triangular Factorization," Proceedings of the IEEE, Nov. 1967, vol. 55, no.11, pp.1801-1809.

[5] B. Stott and O. Alsac, "Fast Decoupled Load Flow," IEEE Transactions on Power Apparatus and Systems, May 1974, vol. PAS-93, no. 3, pp. 859-869.

[6] B. Stott, "Decoupled Newton Load Flow," IEEE Transactions on Power Apparatus and Systems, Sep. 1972, vol. PAS-91, no. 5, pp. 1955-1959.

[7] S. C. Tripathy, G. D. Prasad, O. P. Malik and G. S. Hope, "Load-Flow Solutions for Ill-Conditioned Power Systems by a Newton-Like Method," IEEE Transactions on Power Apparatus and Systems, Oct. 1982, vol. PAS-101, no.10, pp. 3648-3657.

[8] S. Iwamoto and T. Tamura, "A Load Flow Calculation Method for Ill-Conditioned Power Systems," IEEE Transactions on Power Apparatus and Systems, Apr. 1981, vol. PAS-100, no. 4, pp. 1736-1743.

[9] D. J. Tylavsky, P. E. Crouch, L. F. Jarriel and R. Adapa, "Improved Power Flow Robustness for Personal Computers," Industry Applications Society Annual Meeting, Oct. 1990, vol. 2, no. 7, pp. 1401-1407.

[10] D. J. Tylavsky, P.E. Crouch, L.F. Jarriel, and H. Chen, "Advances in Fast Power Flow Algorithms," Advances in Theory and Applications, Control and Dynamics, Academic Press, 1991, vol. 42, Part 4 of 4, pp. 295-344.

[11] P. Crouch, D. Tylavsky, L. Jarriel and H. Chen, "Critically Coupled Algorithms for Solving the Power Flow Equation," IEEE Transactions on Power Systems, Feb. 1992, vol. 7, no. 1, pp. 451-457.

[12] D. Tylavsky, P. Crouch, L. Jarriel, J. Singh, and R. Adapa, "The Effects of Precision and Small Impedance Branches on Power Flow Robustness," IEEE Transactions on Power Systems, Feb. 1994, vol. 9, no. 1, pp. 6-14.

[13] M. Schaffer and D. Tylavsky, "A Nondiverging Polar-Form Newton-Based Power Flow," IEEE Transactions on Industry Applications, Sep. 1988, vol. 24, no. 5, pp. 870 -877.

[14] D. Tylavsky and M. Schaffer, "Non-Diverging Power Flow Using a Least-Power Type Theorem," IEEE Transactions on Industry Applications, Sep. 1987, vol. IA-23, no. 5, pp. 944-951.

[15] V. Ajjarapu, "Computational Techniques for Voltage Stability Assessment and Control," Springer US, New York, 2006.

[16] C. Taylor, "Power System Voltage Stability," McGraw Hill, New York, 1994.

[17] U.S.-Canada Power System Outage Task Force, "Final Report on the August 14, 2003 Blackout in the United States and Canada: Causes and Recommendations," Apr. 2004 available at:
http://energy.gov/sites/prod/files/oeprod/DocumentsandMedia/BlackoutFinalWeb.pdf.

[18] V. Ajjarapu and C. Christy, "The Continuation Power Flow: A Tool for Steady State Voltage Stability Analysis," IEEE Transactions on Power Systems, Feb. 1992, vol. 7, no. 1, pp. 416–423.

[19] C. Canizares and F. L. Alvarado, "Point of Collapse and Continuation Methods for Large ac/dc Systems," IEEE Transactions on Power Systems, Feb. 1993, vol. 8, no. 1, pp. 1–8.

[20] A. Trias, "The Holomorphic Embedding Load Flow Method," IEEE PES General Meeting, San Diego, CA, July 2012, pp. 1-8.

[21] A. Trias, "System and Method for Monitoring and Managing Electrical Power Transmission and Distribution Networks," US Patents 7,519,506 (2009) and 7,979,239 (2011).

[22] B. Stott, "Review of Load Flow Calculation Methods", Proceedings of IEEE, July 1974, vo1.62, no. 7, pp. 916-929.

[23] M. Laughton and M. Davies, "Numerical Techniques in the Solution of Power System Load Flow Problems," Proceedings of the Institute of Electrical Engineers, Sept. 1964, vol. 111, no. 9, pp. 1575-1588.

[24] G. Huang and W. Ongsakul, "Parallel Implementation of Gauss-Seidel Type Algorithms for Power Flow Analysis on a SEQUENT Parallel Computer," Proceedings of the 20th International Conference of Parallel Processing, 1991, pp. 171 -174.

[25] H. Dommel, W. Tinney and W. Powell, "Further Developments in Newton's Method for Power Systems Applications," IEEE Winter Power Meeting, NewYork, Jan. 1970.

[26] A. Keyhani, A. Abur and S. Hao, "Evaluation of Power Flow Techniques for Personal Computers," IEEE Transactions on Power Systems, May 1989, vol.4, no.2, pp.817-826.

[27] D. Tylavsky, "Lecture notes on Decoupled Power-flow algorithms," Computer Solution of Power Systems, Fall 2012.

[28] P. Sauer, "Explicit Load Flow Series and Functions", IEEE Transactions on Power Apparatus and Systems, 1981, vol. PAS-100, no. 8, pp. 3754-3763.

[29] Y. Wang, L. Silva, W. Xu and Y. Zhang, "Analysis of Ill-Conditioned Power-Flow Problems using Voltage Stability Methodology," IEEE Proceedings Generation, Transmission and Distribution, Sep 2001, vol.148, no.5, pp.384-390.

[30] W. Xu, Y. Liu, J. C. Salmon, T. Le and G. Chang, "Series Load Flow: A Novel Non-Iterative Load Flow Method," IEEE Proceedings Generation, Transmission and Distribution, May 1998, vol. 145, no. 3, pp. 251-256.

[31] L. Shao-Hua and Hsiao-Dong Chiang, "Continuation Power Flow with Multiple Load Variation and Generation Re-Dispatch Patterns," IEEE Power Engineering Society General Meeting, 2006.

[32] X. Zhang, P. Ju and E. Handschin, "Continuation Three-Phase Power Flow: A Tool for Voltage Stability Analysis of Unbalanced Three-Phase Power Systems," Aug. 2005, IEEE Transactions on Power Systems, vol.20, no.3, pp.1320,1329.

[33] F. L. Alvarado and T. H. Jung, "Direct Detection of Voltage Collapse Conditions," Proceedings: Bulk Power System Voltage Phenomena - Voltage Stability and Security, EPRI EL-6183, Project 2473-21, Electric Power Research Institute, Jan. 1989.

[34] F. L. Alvarado, M. Gu and Y. Hu, "Direct Detection of Instability Points using an Augmented Formulation," available at: http://citeseerx.ist.psu.edu/viewdoc/summary?doi=10.1.1.29.5643

[35] D. Irisarri, X. Wang, J. Tong and S. Mokhtari, "Maximum Loadability of Power Systems using Interior Point Nonlinear Optimization Method," IEEE Transactions on Power Systems, Feb. 1997, vol. 12, no. 1, pp. 162–172.

[36] J. Lu, C. W. Liu and J. S. Thorp, "New Methods for Computing a Saddle-Node Bifurcation Point for Voltage Stability Analysis," IEEE Transactions on Power Systems, May 1995, vol. 10, no. 2, pp. 978–985.

[37] C. Vournas, M. Karystianos and N. Maratos, "Bifurcation Points and Loadability Limits as Solutions of Constrained Optimization Problems," IEEE Power Engineering Society Summer Meeting, 2000, vol.3, pp.1883-1888.

[38] A. Yang, "Notes on Functions of a Complex Variable," available at: http://www.math.dartmouth.edu/~m43s12/.

[39] Y. Feng, "Solving for the Low-Voltage Power-Flow Solutions by using a Holomorphic Embedded Formulation," April 2014, Ph.D. Qualifying exam, School of Electrical, Computer and Energy Engineering, Arizona State University, pp. 38-41.

[40] R.C.Gunning and H.Rosi, "Analytic Functions of Several Complex Variables," American Mathematical Society, 1965, pp.317.

[41] A. Bulthell, "Division Algorithms for Continued Fractions and the Padé Table," Journal of Computational and Applied Mathematics, 1980, vol. 6, Issue 4, pp. 259-266.

[42] H. Stahl, "On the Convergence of Generalized Padé Approximants," Constructive Approximation, 1989, vol. 5, pp. 221–240.

[43] H. Stahl "The Convergence of Padé Approximants to Functions with Branch Points," Journal of Approximation Theory, 1997, vol. 91, no. 2, pp. 139–204.

[44] G. Baker and P. Graves-Morris, "Padé approximants," Series: Encyclopaedia of Mathematics and its applications, Cambridge University Press, New York, 1996.

[45] C. G. Small, "Expansions and Asymptotics for Statistics," Chapman and Hall/CRC Publications, May 2010, pp. 85-88.

[46] D. Tylavsky, "Lecture Notes on Padé approximants and Nonlinear equations," Computer Solution of Power Systems, Spring 2014.

[47] D. Shanks, "Nonlinear Transformations of Divergent and Slowly Convergent Sequences," Journal of Mathematical Physics, 1955, vol. 34, pp. 1-42.

[48] P. Wynn, "Upon Systems of Recursion which obtain among Quotients of the Padé Table," Journal of Computational and Applied Mathematics, 1966, vol. 5, Issue 4, pp. 264-269.

[49] W.E. Weisstein "Gregory Series," From MathWorld-A Wolfram Web Resource available at: http://mathworld.wolfram.com/GregorySeries.html.

[50] E. Cheney and D. Kincaid, "Numerical Mathematics and Computing," Cengage Learning, Stamford, August 2007.

[51] M. Subramanian, Y. Feng and D. Tylavsky, "PV Bus Modeling in a Holomorphically Embedded Power-Flow Formulation," North American Power Symposium, Sep. 2013, pp. 1-6.

[52] A. Trias, Personal communication, February 2014.

[53] J.J. Grainger and W.D. Stevenson, "Power Systems Analysis," McGraw-Hill, New York, Jan. 1994.

[54] R. Christie, "118 Bus Power Flow Test Case," May 1993, available at: http://www.ee.washington.edu/research/pstca/pf118/pg_tca118bus.htm.

[55] M. Subramanian, "Computer Solution of Power Systems-Final project report," Arizona State University, Dec. 2012.

[56] F. Milano, "Power Systems Analysis Toolbox," available at: http://faraday1.ucd.ie/software.html.

APPENDIX A

VOLTAGE SOLUTION FOR IEEE-118 BUS SYSTEM

```
-----------------------------------------------------------------

              Converged Bus Voltages

-----------------------------------------------------------------

| Bus |Bus      |Type  |V      |Angle    |Generation      |
| No  |name     |      |pu     |Degree   |MW     |Mvar    |

  -----------------------------------------------------------------

      1   Riversde    2    0.9550    -19.0177    0.00        -3.10

      2    Pokagon    0    0.9714    -18.4777    0.00         0.00

      3   HickryCk    0    0.9677    -18.1344    0.00         0.00

      4   NwCarlsl    2    0.9980    -14.4169    -9.00      -15.01

      5      Olive    0    1.0020    -13.9719    0.00         0.00

      6   Kankakee    2    0.9900    -16.6987    0.00        15.93

      7   JacksnRd    0    0.9893    -17.1431    0.00         0.00

      8      Olive    2    1.0150     -8.9514   -28.00       62.76

      9    Bequine    0    1.0429     -1.6973    0.00         0.00

     10      Breed    2    1.0500      5.8837   450.00      -51.04

     11   SouthBnd    0    0.9851    -16.9845    0.00         0.00

     12   TwinBrch    2    0.9900    -17.5012   85.00        91.27

     13    Concord    0    0.9683    -18.3594    0.00         0.00

     14   GoshenJt    0    0.9836    -18.2174    0.00         0.00

     15    FtWayne    2    0.9700    -18.5111    0.00         3.06

     16       N.E.    0    0.9839    -17.8028    0.00         0.00

     17   Sorenson    0    0.9951    -15.9949    0.00         0.00

     18   McKinley    2    0.9730    -18.2086    0.00        25.53

     19    Lincoln    4    0.9634    -18.6932    0.00        -8.00

     20      Adams    0    0.9581    -17.8133    0.00         0.00

     21        Jay    0    0.9586    -16.2254    0.00         0.00

     22   Randolph    0    0.9696    -13.6709    0.00         0.00

     23    CollCrnr    0   0.9997     -8.7502    0.00         0.00

     24    Trenton    2    0.9920     -8.8825   -13.00      -15.28

     25   TannrsCk    2    1.0500     -1.8161   220.00       49.80

     26   TannrsCk    2    1.0150     -0.0356   314.00        9.90

     27    Madison    2    0.9680    -14.3879    -9.00        2.83

     28     Mullin    0    0.9616    -16.1125    0.00         0.00

     29      Grant    0    0.9632    -17.1049    0.00         0.00

     30   Sorenson    0    0.9855    -10.9604    0.00         0.00

     31    DeerCrk    2    0.9670    -16.9880    7.00        31.98

     32   Delaware    4    0.9636    -14.9405    0.00       -14.00

     33   Haviland    0    0.9716    -19.1361    0.00         0.00

     34   Rockhill    4    0.9859    -18.4941    0.00        -8.00

     35   WestLima    0    0.9807    -18.9213    0.00         0.00

     36   Sterling    2    0.9800    -18.9168    0.00        -1.25
```

```
----------------------------------------------------------------
           Converged Bus Voltages
----------------------------------------------------------------
|  Bus |Bus       |Type  |V       |Angle     |Generation       |
|  No  |name      |      |pu      |Degree    |MW      |Mvar    |
       ----------------------------------------------------------------
    37   EastLima    0    0.9920   -18.0303   0.00      0.00
    38   EastLima    0    0.9620   -12.8934   0.00      0.00
    39   NwLibrty    0    0.9705   -21.4028   0.00      0.00
    40   WestEnd     2    0.9700   -22.4766  -46.00     26.89
    41   S.Tiffin    0    0.9668   -22.9227   0.00      0.00
    42   Howard      2    0.9850   -21.3271  -59.00     41.00
    43   S.Kenton    0    0.9785   -18.5401   0.00      0.00
    44   WMVernon    0    0.9850   -16.0545   0.00      0.00
    45   N.Newark    0    0.9867   -14.2238   0.00      0.00
    46   W.Lancst    2    1.0050   -11.4178   19.00     -5.23
    47   Crooksvl    0    1.0171    -9.1954   0.00      0.00
    48   Zanesvll    0    1.0206    -9.9752   0.00      0.00
    49   Philo       2    1.0250    -8.9721   204.00    115.65
    50   WCambrdg    0    1.0011   -11.0112   0.00      0.00
    51   Newcmrst    0    0.9669   -13.6302   0.00      0.00
    52   SCoshoct    0    0.9568   -14.5837   0.00      0.00
    53   Wooster     0    0.9460   -15.5586   0.00      0.00
    54   Torrey      2    0.9550   -14.6469   48.00     3.90
    55   Wagenhls    2    0.9520   -14.9369   0.00      4.66
    56   Sunnysde    2    0.9540   -14.7502   0.00      -2.29
    57   WNwPhil1    0    0.9706   -13.5454   0.00      0.00
    58   WNwPhil2    0    0.9590   -14.4022   0.00      0.00
    59   Tidd        2    0.9850   -10.5476   155.00    76.83
    60   SWKammer    0    0.9932    -6.7663   0.00      0.00
    61   W.Kammer    2    0.9950    -5.8750   160.00   -40.39
    62   Natrium     2    0.9980    -6.4915   0.00      1.26
    63   Tidd        0    0.9687    -7.1691   0.00      0.00
    64   Kammer      0    0.9837    -5.4034   0.00      0.00
    65   Muskngum    2    1.0050    -2.2783   391.00    80.81
    66   Muskngum    2    1.0500    -2.4372   392.00    -1.95
    67   Summerfl    0    1.0197    -5.0771   0.00      0.00
    68   Sporn       0    1.0032    -2.3994   0.00      0.00
    69   Sporn       3    1.0350     0.0000   516.40    0.00
    70   Portsmth    2    0.9840    -7.3800   0.00      9.66
    71   NPortsmt    0    0.9868    -7.7909   0.00      0.00
    72   Hillsbro    2    0.9800    -8.8885  -12.00    -11.13
```

118

```
-----------------------------------------------------------------

                 Converged Bus Voltages

-----------------------------------------------------------------

|  Bus |Bus       |Type  |V      |Angle      |Generation      |
|  No  |name      |      |pu     |Degree     |MW      |Mvar   |

  -----------------------------------------------------------------

    73    Sargents    2    0.9910    -8.0024    -6.00      9.65

    74    Bellefnt    2    0.9580    -8.3288     0.00     -5.63

    75    SthPoint    0    0.9673    -7.0670     0.00      0.00

    76     Darrah     2    0.9430    -8.1970     0.00      5.27

    77     Turner     2    1.0060    -3.2431     0.00     11.94

    78    Chemical    0    1.0034    -3.5470     0.00      0.00

    79    CapitlHl    0    1.0092    -3.2478     0.00      0.00

    80    CabinCrk    2    1.0400    -1.0023   477.00    105.04

    81    Kanawha     0    0.9968    -1.8505     0.00      0.00

    82     Logan      0    0.9887    -2.7227     0.00      0.00

    83     Sprigg     0    0.9845    -1.5326     0.00      0.00

    84    BetsyLne    0    0.9798     1.0008     0.00      0.00

    85    BeaverCk    2    0.9850     2.5549     0.00     -5.77

    86     Hazard     0    0.9867     1.1854     0.00      0.00

    87    Pinevlle    2    1.0150     1.4447     4.00     11.02

    88    Fremont     0    0.9875     5.6859     0.00      0.00

    89    ClinchRv    2    1.0050     9.7414   607.00    -11.79

    90    Holston     2    0.9850     3.3365   -85.00     59.30

    91    HolstonT    2    0.9800     3.3555   -10.00    -14.85

    92    Saltvlle    4    0.9923     3.8545     0.00     -3.00

    93    Tazewell    0    0.9869     0.8434     0.00      0.00

    94    Switchbk    0    0.9906    -1.3105     0.00      0.00

    95    Caldwell    0    0.9809    -2.2823     0.00      0.00

    96    Baileysv    0    0.9927    -2.4496     0.00      0.00

    97    Sundial     0    1.0114    -2.0764     0.00      0.00

    98    Bradley     0    1.0235    -2.5539     0.00      0.00

    99     Hinton     2    1.0100    -2.9157   -42.00    -17.54

   100    GlenLyn     2    1.0170    -1.9196   252.00    110.08

   101     Wythe      0    0.9924    -0.3468     0.00      0.00

   102     Smythe     0    0.9910     2.3511     0.00      0.00

   103    Claytor     5    1.0007    -5.5146    40.00     40.00

   104    Hancock     2    0.9710    -8.2595     0.00      5.65

   105    Roanoke     4    0.9660    -9.3816     0.00     -8.00

   106    Cloverdl    0    0.9618    -9.6295     0.00      0.00

   107    Reusens     2    0.9520   -12.4196   -22.00      5.70

   108     Blaine     0    0.9668   -10.5725     0.00      0.00
```

119

```
-----------------------------------------------------------------
           Converged Bus Voltages
-----------------------------------------------------------------
|  Bus |Bus      |Type |V     |Angle      |Generation      |
|  No  |name     |     |pu    |Degree     |MW     |Mvar    |

   -----------------------------------------------------------------
    109   Franklin     0    0.9675    -11.0218    0.00       0.00
    110    Fieldale    2    0.9730    -11.8606    0.00       4.86
    111    DanRiver    2    0.9800    -10.2155   36.00      -1.84
    112    Danville    2    0.9750    -14.9598  -43.00      41.51
    113    DeerCrk     2    0.9930    -15.9969   -6.00       6.32
    114   WMedford     0    0.9604    -15.2708    0.00       0.00
    115    Medford     0    0.9603    -15.2784    0.00       0.00
    116   KygerCrk     2    1.0050     -2.8344 -184.00      51.32
    117      Corey     0    0.9738    -19.0422    0.00       0.00
    118   WHuntngd     0    0.9494     -8.0547    0.00       0.00
```

```
----------------------------------------------------------------
                   Line flows in branches and Tap ratios
----------------------------------------------------------------
Branch  |Tap   |Z    |Tap   |From bus injection|To bus injection  |
        |Bus   |Bus  |Ratio |P(M.W.)  |Q(MVar)|P(M.W.)  |Q(MVar)|
 ----------------------------------------------------------------
1       1      2      0.000  -12.36    -13.04  12.45     11.01
2       1      3      0.000  -38.64    -17.06  38.89     16.89
3       4      5      0.000  -103.21   -26.79  103.41    27.49
4       3      5      0.000  -68.10    -14.49  69.34     17.28
5       5      6      0.000  88.46     4.11    -87.53    -1.30
6       6      7      0.000  35.53     -4.77   -35.47    4.50
7       8      9      0.000  -440.64   -89.73  445.25    24.43
8       8      5      0.985  338.42    124.72  -338.42   -92.01
9       9      10     0.000  -445.25   -24.43  450.00    -51.04
10      4      11     0.000  64.21     -0.21   -63.35    1.34
11      5      11     0.000  77.21     2.97    -76.00    -0.63
12      11     12     0.000  34.28     -35.13  -34.14    35.13
13      2      12     0.000  -32.45    -20.01  32.74     19.42
14      3      12     0.000  -9.79     -12.39  9.90      8.86
15      7      12     0.000  16.47     -6.50   -16.44    5.75
16      11     13     0.000  35.06     11.41   -34.74    -12.16
17      12     14     0.000  18.29     2.63    -18.21    -4.15
18      13     15     0.000  0.74      -3.84   -0.74     -2.05
19      14     15     0.000  4.21      3.15    -4.18     -7.84
20      12     16     0.000  7.50      4.29    -7.49     -6.30
21      15     17     0.000  -103.72   -24.41  105.30    25.36
22      16     17     0.000  -17.51    -3.70   17.66     -0.29
23      17     18     0.000  80.27     24.85   -79.39    -22.49
24      18     19     0.000  19.39     14.02   -19.32    -14.79
25      19     20     0.000  -10.65    5.42    10.69     -7.97
26      15     19     0.000  11.41     12.25   -11.37    -13.07
27      20     21     0.000  -28.69    4.97    28.86     -6.16
28      21     22     0.000  -42.86    -1.84   43.28     1.49
29      22     23     0.000  -53.28    -6.49   54.32     7.41
30      23     24     0.000  8.30      10.80   -8.26     -15.61
31      23     25     0.000  -162.61   -25.92  166.81    38.38
32      26     25     0.960  90.30     21.58   -90.30    -18.64
33      25     27     0.000  143.49    30.06   -137.09   -15.27
34      27     28     0.000  32.86     -0.59   -32.64    -0.44
35      28     29     0.000  15.64     -6.56   -15.57    4.64
36      30     17     0.960  231.06    93.37   -231.06   -70.51
```

```
----------------------------------------------------------------
              Line flows in branches and Tap ratios
----------------------------------------------------------------
Branch  |Tap   |Z     |Tap    |From bus injection|To bus injection   |
        |Bus   |Bus   |Ratio  |P(M.W.)  |Q(MVar)|P(M.W.)  |Q(MVar)|
    ----------------------------------------------------------------
37      8     30    0.000   74.22     27.77   -73.87    -75.07
38      26    30    0.000   223.70    -11.68  -219.72   -36.38
39      17    31    0.000   14.77     11.55   -14.58    -14.76
40      29    31    0.000   -8.43     -8.64   8.45      7.92
41      23    32    0.000   92.99     4.71    -90.21    -5.91
42      31    32    0.000   -29.87    11.82   30.21     -13.04
43      27    32    0.000   12.50     1.02    -12.46    -2.69
44      15    33    0.000   7.23      -4.88   -7.20     1.96
45      19    34    0.000   -3.66     -10.57  3.72      4.75
46      35    36    0.000   0.67      6.25    -0.67     -6.50
47      35    37    0.000   -33.67    -15.25  33.82     14.66
48      33    37    0.000   -15.80    -10.96  15.94     7.93
49      34    36    0.000   30.43     11.50   -30.33    -11.75
50      34    37    0.000   -94.58    -38.57  94.86     38.61
51      38    37    0.935   243.68    112.11  -243.68   -86.62
52      37    39    0.000   54.96     3.75    -53.97    -3.07
53      37    40    0.000   44.10     -2.93   -42.93    2.21
54      30    38    0.000   62.53     18.08   -62.28    -55.10
55      39    40    0.000   26.97     -7.93   -26.82    6.97
56      40    41    0.000   15.51     1.17    -15.48    -2.19
57      40    42    0.000   -11.77    -6.47   11.86     2.32
58      41    42    0.000   -21.52    -7.81   21.74     5.26
59      43    44    0.000   -16.57    -1.03   16.75     -4.10
60      34    43    0.000   1.44      1.92    -1.43     -5.97
61      44    45    0.000   -32.75    5.81    33.00     -6.94
62      45    46    0.000   -36.32    -3.38   36.86     1.92
63      46    47    0.000   -31.10    -1.22   31.46     -0.79
64      46    48    0.000   -14.76    -5.83   14.90     1.42
65      47    49    0.000   -9.55     -10.83  9.59      9.27
66      42    49    0.000   -64.80    5.21    67.96     0.37
67      42    49    0.000   -64.80    5.21    67.96     0.37
68      45    49    0.000   -49.69    -1.95   51.42     2.17
69      48    49    0.000   -34.90    3.21    35.11     -3.92
70      49    50    0.000   53.67     13.43   -52.88    -13.14
71      49    51    0.000   66.64     20.44   -64.35    -17.40
72      51    52    0.000   28.56     6.24    -28.37    -6.99
```

```
----------------------------------------------------------------
              Line flows in branches and Tap ratios
----------------------------------------------------------------
Branch  |Tap    |Z     |Tap    |From bus injection|To bus injection    |
        |Bus    |Bus   |Ratio  |P(M.W.)  |Q(MVar)|P(M.W.) |Q(MVar)|
   ----------------------------------------------------------------
73      52     53     0.000    10.37      1.99    -10.32    -5.45
74      53     54     0.000   -12.68     -5.55     12.73     2.99
75      49     54     0.000    37.77     13.07    -36.58   -15.60
76      49     54     0.000    37.75     11.20    -36.39   -13.79
77      54     55     0.000     7.08      1.46     -7.07    -3.25
78      54     56     0.000    18.53      4.34    -18.52    -4.97
79      55     56     0.000   -21.43     -5.82     21.45     5.56
80      56     57     0.000   -22.99     -9.10     23.22     7.49
81      50     57     0.000    35.88      9.14    -35.22   -10.49
82      56     58     0.000    -6.67     -3.69      6.69     1.53
83      51     58     0.000    18.79      3.16    -18.69    -4.53
84      54     59     0.000   -30.38     -7.51     30.90     4.26
85      56     59     0.000   -27.96     -4.18     28.67     0.99
86      56     59     0.000   -29.31     -3.91     30.07     1.13
87      55     59     0.000   -34.51     -8.26     35.15     5.88
88      59     60     0.000   -43.31      3.57     43.94    -4.40
89      59     61     0.000   -51.71      5.03     52.63    -4.63
90      60     61     0.000  -112.06      8.52    112.40    -8.23
91      60     62     0.000    -9.87     -7.11      9.89     5.74
92      61     62     0.000    25.49    -13.86    -25.42    13.20
93      63     59     0.960   151.75     67.48   -151.75   -57.03
94      63     64     0.000  -151.75    -67.48    152.23    52.51
95      64     61     0.985    30.52     13.99    -30.52   -13.69
96      38     65     0.000  -181.41    -57.01    184.62    -9.07
97      64     65     0.000  -182.76    -66.49    183.75    40.06
98      49     66     0.000  -132.18      4.31    135.18     8.33
99      49     66     0.000  -132.18      4.31    135.18     8.33
100     62     66     0.000   -37.17    -17.26     37.93    14.68
101     62     67     0.000   -24.31    -14.41     24.50    12.15
102     65     66     0.935     8.46     72.25     -8.46   -70.55
103     66     67     0.000    53.16     19.27    -52.50   -19.15
104     65     68     0.000    14.17    -22.43    -14.16   -41.85
105     47     69     0.000   -55.91     11.62     58.65   -10.06
106     49     69     0.000   -46.51     10.63     48.75   -12.05
107     68     69     0.935  -125.66    112.81    125.66  -103.65
108     69     70     0.000   108.35     16.08   -104.92   -13.99
```

123

```
----------------------------------------------------------------
                  Line flows in branches and Tap ratios
----------------------------------------------------------------
Branch |Tap   |Z    |Tap   |From bus injection|To bus injection   |
       |Bus   |Bus  |Ratio |P(M.W.)  |Q(MVar)|P(M.W.) |Q(MVar)|
 ----------------------------------------------------------------
109    24     70    0.000  -6.21     -2.97   6.21     -6.80
110    70     71    0.000  16.65     -12.38  -16.61   11.68
111    24     72    0.000  1.47      3.31    -1.46    -7.98
112    71     72    0.000  10.60     -0.94   -10.54   -3.15
113    71     73    0.000  6.01      -10.74  -6.00    9.65
114    70     74    0.000  16.20     12.89   -16.01   -15.42
115    70     75    0.000  -0.14     9.94    0.20     -13.17
116    69     75    0.000  109.97    20.49   -105.12  -18.32
117    74     75    0.000  -51.99    -6.19   52.36    6.44
118    76     77    0.000  -61.17    -21.03  63.23    24.39
119    69     77    0.000  62.10     6.81    -60.95   -13.84
120    75     77    0.000  -34.63    -9.54   35.44    7.37
121    77     78    0.000  45.37     6.62    -45.29   -7.63
122    78     79    0.000  -25.71    -18.37  25.76    17.95
123    77     80    0.000  -96.62    -37.40  98.39    37.52
124    77     80    0.000  -44.39    -20.54  45.07    20.59
125    79     80    0.000  -64.76    -29.58  65.53    31.08
126    68     81    0.000  -44.30    -4.61   44.36    -75.55
127    81     80    0.935  -44.36    75.55   44.36    -73.05
128    77     82    0.000  -3.09     17.34   3.23     -25.08
129    82     83    0.000  -47.11    24.51   47.44    -27.11
130    83     84    0.000  -24.73    14.73   25.29    -16.04
131    83     85    0.000  -42.71    12.07   43.60    -12.37
132    84     85    0.000  -36.29    9.04    36.74    -9.29
133    85     86    0.000  17.17     -7.35   -17.05   5.09
134    86     87    0.000  -3.95     -15.09  4.00     11.02
135    85     88    0.000  -50.33    7.58    50.87    -7.52
136    85     89    0.000  -71.18    0.66    72.43    3.73
137    88     89    0.000  -98.87    -2.48   100.27   7.70
138    89     90    0.000  58.17     -4.72   -56.44   5.80
139    89     90    0.000  110.74    -5.43   -107.85  7.04
140    90     91    0.000  1.29      4.46    -1.28    -6.50
141    89     92    0.000  201.79    -6.59   -197.80  21.49
142    89     92    0.000  63.60     -6.49   -62.02   8.72
143    91     92    0.000  -8.72     -8.35   8.77     5.33
144    92     93    0.000  57.71     -10.75  -56.82   11.57
```

124

145	92	94	0.000	52.26	-14.31	-50.85	14.95
146	93	94	0.000	44.82	-18.57	-44.29	18.48
147	94	95	0.000	40.98	9.34	-40.74	-9.63
148	80	96	0.000	18.93	20.85	-18.63	-24.42
149	82	96	0.000	-10.12	-6.87	10.14	1.60
150	94	96	0.000	19.91	-9.46	-19.79	7.61
151	80	97	0.000	26.38	25.54	-26.14	-26.98
152	80	98	0.000	28.86	8.33	-28.66	-10.45
153	80	99	0.000	19.48	8.18	-19.27	-12.96
154	92	100	0.000	31.45	-15.81	-30.68	14.56
155	94	100	0.000	4.24	-49.30	-3.85	44.49
156	95	96	0.000	-1.26	-21.37	1.34	20.18
157	96	97	0.000	-11.06	-19.97	11.14	17.98
158	98	100	0.000	-5.34	2.45	5.36	-7.31
159	99	100	0.000	-22.73	-4.57	22.83	2.78
160	100	101	0.000	-16.73	22.07	16.96	-24.35
161	92	102	0.000	44.62	-7.67	-44.37	7.39
162	101	102	0.000	-38.96	9.35	39.37	-10.39
163	100	103	0.000	121.08	-4.30	-118.82	6.29
164	100	104	0.000	56.42	10.62	-54.95	-9.34
165	103	104	0.000	32.31	7.93	-31.78	-10.08
166	103	105	0.000	42.95	6.55	-41.92	-7.39
167	100	106	0.000	60.57	9.17	-58.34	-6.78
168	104	105	0.000	48.73	0.07	-48.48	-0.04
169	105	106	0.000	8.68	4.55	-8.67	-5.82
170	105	107	0.000	26.73	-1.85	-26.33	-1.09
171	105	108	0.000	23.99	-10.61	-23.80	9.39
172	106	107	0.000	24.00	-3.40	-23.67	0.22
173	108	109	0.000	21.80	-10.39	-21.74	9.86
174	103	110	0.000	60.56	3.23	-59.11	-1.03
175	109	110	0.000	13.74	-12.86	-13.64	11.23
176	110	111	0.000	-35.70	0.96	36.00	-1.84
177	110	112	0.000	69.46	-30.61	-68.00	28.51
178	17	113	0.000	2.06	6.04	-2.06	-6.79
179	32	113	0.000	4.11	-17.53	-3.94	13.11
180	32	114	0.000	9.36	2.17	-9.35	-3.61
181	27	115	0.000	20.73	4.67	-20.65	-6.13
182	114	115	0.000	1.35	0.61	-1.35	-0.87
183	68	116	0.000	184.13	-66.36	-184.00	51.32
184	12	117	0.000	20.15	5.20	-20.00	-8.00
185	75	118	0.000	40.19	23.59	-39.85	-23.56
186	76	118	0.000	-6.83	-9.70	6.85	8.56